Fusaric acid dampens the Nrf2-mediated Stress Response in Human Embryonic Kidney cells

By

Melissa Govender

211509049

B.Sc., B.Med.Sc. (Hons), (UKZN)

Submitted in the fulfilment of the requirements for the degree M.Med.Sc. in the

Discipline of Medical Biochemistry and Chemical Pathology

School of Laboratory Medicine and Medical Sciences

College of Health Sciences

University of Kwa-Zulu Natal

Durban

2016

Declaration

This dissertation contains the original work by the author and has not been submitted in any form to another university. The use of work by others has been duly acknowledged in the text.

The research described in this study was carried out in the division of Medical Biochemistry and Chemical Pathology, School of Laboratory Medicine and Medical Science, Faculty of Health Sciences, University of Kwa-Zulu Natal, Durban, under the supervision of Prof. A. A. Chuturgoon and Dr S. Nagiah.

Melissa Govender

Acknowledgements

I would like to express my sincere gratitude and heartfelt appreciation to the following people for their assistance and support in making this study possible:

Prof. A. A. Chuturgoon

Your love and passion for science has truly been inspirational to me. Thank you for affording me the opportunity of joining your department, it has been an educational journey that has evoked a desire to fulfil a greater purpose not only in terms of research but in discovery of one's spiritual self. The example you set is one that I endeavour to follow. Your encouragement and faith in me has been invaluable.

Dr Savania Nagiah

I am highly indebted to you for your unselfish dedication to ensuring the smooth running of the lab. Thank you for your time, patience, advice and feedback on all aspects of my work. You have surpassed the expectations of a supervisor and without your guidance and constant assistance, this study would not have been possible. I feel extremely blessed to have encountered you in my academic journey and your achievements and hunger for knowledge has and will continue to inspire me.

Miss Yashodani Pillay

Thank you for the guidance, mentorship and expertise, which has allowed me to improve my skills in the laboratory. Your assistance in troubleshooting problems I encountered in my lab work as well as the constructive criticism provided in the process of writing has been instrumental to my growth as a scientist.

Miss Shanel Raghubeer

I am truly grateful for your generosity in offering your time to supervise my work and your willingness to share your knowledge and expertise. Thank you for the technical assistance as well, I am now able to skilfully use Graphpad and Endnote.

My Parents

Thank you for your unconditional love and support throughout my academic career. Your sacrifices have not gone unnoticed and I am eternally grateful for all that you have done that has allowed for

me to chase my dreams. It is your belief in me that has enabled me to always keep my head up and persevere.

My Brother

Thank you for all your emotional support, your advice and encouragement. Despite being younger, you are wise beyond your years and you inspire me to always do my best.

My Fellow Colleagues at the Discipline of Medical Biochemistry

Thank you for your companionship and friendship. It has certainly been an eventful journey and I wish that each and every one of you realize your academic aspirations.

National Research Foundation

Thank you to the financial support that gave me the opportunity to pursue my dreams.

UKZN - College of Health Science

Thank you for the financial assistance provided for running expenses during the course of my Masters.

Presentations

The Biochemical Effects of Fusaric acid on Human Kidney (HEK293) Cells.

Govender M., Nagiah S., Pillay Y. and Chuturgoon A.A.

UKZN College of Health Science Research Symposium 2015 (10-11 September 2015), K-RITH tower building, Durban, South Africa.

Abstract

Fusaric acid (FA), a common contaminant of maize and other cereal grains, is produced by several species of the *Fusarium* genus. The mechanism by which FA elicits its toxicity include chelation of divalent cations, disruption of mitochondrial function, promoting Reactive Oxygen Species (ROS) generation and activating cell death. The antioxidant response is regulated by the transcription factor, Nuclear erythroid 2-related factor 2 (Nrf2), which facilitates the transcription of numerous antioxidant and cytoprotective genes. Oxidative stress, a condition defined by insufficient antioxidant response, can result in damage to macromolecules which promotes cell death. We investigated the effects of FA on endogenous antioxidant and DNA repair pathways in human embryonic kidney cells (HEK293).

Cell viability was determined using the MTT assay, following a 24 hour incubation with a range of FA concentrations (0-500µg/ml). Intracellular ATP concentrations, glutathione levels and caspase activity were evaluated using luminometry. The oxidative status was assessed by quantifying MDA levels using the TBARS assay. Protein expression of total Nrf2, phosphorylated Nrf2, p53 and PARP-1 was determined by western blotting. The mRNA levels of *GPx, CAT* and *OGG1* were measured using qPCR. DNA damage was assessed by utilizing the comet assay. Necrosis was determined by quantifying LDH levels.

FA caused a dose-dependent decrease in cell viability (IC_{50} = 137.9µg/ml) with an increase in lipid peroxidation ($p < 0.005$) and a reduction in GSH ($p < 0.05$) and ATP ($p < 0.005$) levels. FA dampened the antioxidant response as evidenced by decreased total Nrf2 protein expression ($p < 0.05$), however a significant increase in phosphorylated-Nrf2 ($p < 0.05$) was also noted. Down-stream antioxidant genes were decreased (GPx ($p < 0.05$) and CAT ($p < 0.0001$)). FA induced DNA damage ($p < 0.0001$) with a concomitant decrease in p53 ($p < 0.05$) and Parp-1 ($p < 0.005$) protein expression and *OGG1* ($p < 0.005$) gene expression. Caspase activity (caspase 8 and 9; $p < 0.05$, caspase 3/7; $p < 0.005$) and LDH levels ($p < 0.001$) were increased in FA-exposed cells, indicative of cell death. These results suggest that FA induces cytotoxicity in HEK293 cells by down-regulating the Nrf2-mediated antioxidant response, compromising genomic integrity and inducing cell death.

List of figures

List of tables

List of abbreviations

β	Beta
ADP	Adenosine diphosphate
AP site	Apurinic/ apyrimidinic site
Apaf-1	Apoptotic protease activating factor-1
APS	Ammonium persulphate
ARE	Antioxidant response element
ATP	Adenosine triphosphate
BCA	Bicinchoninic acid
BER	Base excision repair
BHT	Butylated hydroxytoluene
Bis	N,N'-methylene bisacrylamide
BSA	Bovine serum albumin
bZip	Basic region leucine zipper
°C	Degree Celsius
C2H2	Cys-Cys-His-His motif
CAT	Catalase
cDNA	Complementary DNA
CO_2	Carbon dioxide
Cu^{+}/ Cu^{2+}	Copper (Cuprous ion/ Cupric ion)
Cul3-E3 ligase	Cullin 3- Rbx1-E3 ubiquitin ligase
Cyt c	Cytochrome c
dATP	deoxyadenosine triphosphate
DBH	Dopamine β hydroxylase
dCTP	deoxycytidine triphosphate
DISC	Death inducing signaling complex
DMEM	Dulbucco's minimum essential medium
DMSO	Dimethyl sulphoxide
DNA	Deoxyribonucleic acid
dNTP	Deoxynucleotide triphosphates
DON	Deoxynivalenol

Ds	Double stranded
ECL	Enhanced chemiluminescence
EDTA	Ethylenediaminetetraacetic acid
ETC	Electron transport chain
FA	Fusaric acid
FAD	Flavin adenine dinucleotide
FAO	Food and Agriculture Organisation of the United Nations
FapyG	2,6-diamino-4-oxo-5-formamidopyrimidine
FB1	Fumonisin B1
Fe^{2+}/Fe^{3+}	Iron (Ferrous ion/ Ferric ion)
G	Gravitational force
G6PD	Glucose-6-phosphate dehydrogenase
GCL	Glutamate cysteine ligase
GCLC	Glutamate cysteine ligase- catalytic subunit
GCLM	Glutamate cysteine ligase- modifier subunit
GPx	Glutathione peroxidase
GR	Glutathione reductase
GSH	Glutathione
GSSG	Glutathione disulphide
GST	Glutathione-S- Transferase
GTP	Guanosine triphosphate
4-HNE	4-hydroxy-2-nonenal
H^+	Hydrogen ion
H_2O_2	Hydrogen peroxide
H_3PO_4	Phosphoric acid
HCl	Hydrochloric acid
HEK293	Human embryonic kidney 293 cell line
HEPES	4-(2-hydroxyethyl)-1-piperazineethanesulphonic acid
HO-1	Heme oxygenase-1
HRP	Horseradish peroxidase
IC_{50}	Half maximal inhibitory concentration
IgG	Immunoglobulin G

INT	Iodonitrotetrazolium
Keap1	Kelch-like ECH-associated protein 1
LDH	Lactate dehydrogenase
LMPA	Low melting point agarose
MDA	Malondialdehyde
Mg^{2+}	Magnesium
Mn^{2+}	Manganese
MPTP	Mitochondrial permeability transition pore
mRNA	Messenger RNA
MTT	3-(4,5-Dimethyl-2-thiazolyl)-2,5-diphenyl-2H-tetrazolium bromide
NA	Nicotinic acid
Na_2EDTA	Disodium ethylenediaminetetraacetic acid
NaCl	Sodium chloride
NAD/NADH	Nicotinamide adenine dinucleotide
NADP/NADPH	Nicotinamide adenine dinucleotide phosphate
NaOH	Sodium hydroxide
NO•	Nitric oxide
NQO1	NADPH Quinone Oxidoreductase-1
Nrf2	Nuclear erythroid 2-related factor 2
8-oxoA	7, 8-dihydroxy—8-oxo-2'-deoxyadenine
8-oxoG	8-oxoguanine
$\cdot O_2^-$	Superoxide anion radicals
OD	Optical density
OGG1	8-oxoguanine glycosylase-1
OH^-	Hydroxyl radicals
$ONOO^-$	Peroxynitrite
OTA	Ochratoxin A
p53	Tumour suppressor 53
PA	Picolinic acid
PAGE	Polyacrylamide gel electrophoresis
PARP1	Poly-ADP-ribose-Polymerase-1
PAT	Patulin

PBS	Phosphate buffered saline
PCR	Polymerase chain reaction
PKC	Protein Kinase C
ppm	Parts per million
PUFA	Polyunsaturated fatty acids
qPCR	Quantitative polymerase chain reaction
RBD	Relative band density
RLU	Relative light units
RNA	Ribonucleic acid
ROS	Reactive oxygen species
SDS	Sodium dodecyl sulphate
Ser40	Serine 40
SIRTs	Silent mating type information regulation 2 homolog
SOD	Superoxide dismutase
ss	Single stranded
Taq	*Thermus aquaticus*
TBA	Thiobarbituric acid
TBARS	Thiobarbituric acid reactive substances
TCA	Tricarboxylic Acid
TEMED	N,N,N',N'-Tetramethylethylenediamine
TNF	Tumour necrosis factor
TTBS	Tween 20-Tris buffered saline
ZEN	Zearolenone
Zn^{2+}	Zinc

Table of Contents

Chapter 1

1.1. Introduction

Fusaric acid (FA) is a common contaminant of various cereal grains used for livestock feed and other agricultural commodities. It is ubiquitously produced by fungal species of the Fusarium genus [1]. Rural populations in developing countries are at particular risk, as grain (maize, wheat and barley) forms a staple part of their diet. Many of these communities lack proper storage facilities for harvested crops, which leads to increased fungal contamination and exposure to FA [2].

Fusaric acid is predominantly found in corn-based foods, wheat, barley, other cereal grains and animal feeds worldwide [3, 4]. A recent study found that FA was the most prevalent and in the highest concentration of mycotoxins produced in corn [5]. However, FA is often overlooked with respect to research, in favour of more potent mycotoxins [6]. As a result, FA is not monitored or regulated in food intended for human and animal consumption and the exact mechanism of toxicity remains poorly understood.

Metabolism of FA showed that there is significant retention of this fusariotoxin in the plasma as albumin conjugates, as well as kidney and liver [7]. The kidney is highly susceptible to damage by environmental toxins, due to the increased toxin uptake and the concentrating ability of the kidney which results in increased toxin exposure [8, 9]. As a vital excretory organ, the kidney is rich in mitochondria to ensure a constant supply of ATP for efficient removal of toxic compounds [10]. These highly metabolic processes increase vulnerability to toxic insult through mitochondrial dysfunction and altered oxidative status [9-11].

A consequence of normal cellular metabolism is the production of reactive oxygen species (ROS) formed by the partial reduction of molecular oxygen. The main cellular source of ROS is the mitochondrial respiratory chain [12]. Under physiological conditions, these oxidants are produced in a controlled manner and play a role in intracellular signaling. Reactive oxidants are

counterbalanced by intricate antioxidant defense systems which maintain the redox homeostasis in the cell. Environmental stresses, such as exposure to certain toxins can promote uncontrolled production of ROS, disturbing redox homeostasis [13].

Oxidative stress is a condition of imbalance between enhanced ROS production and / or reduced cellular antioxidant capacity. The induction of oxidative stress has previously been implicated as a contributing factor in FA-mediated toxicity [14, 15]. Under oxidative conditions, cellular macromolecules such as lipids, proteins and DNA are prone to oxidative modification which alter their structure and function. This can facilitate activation of cell death pathways such as apoptosis and necrosis [16].

The body possesses innate survival mechanisms, which counterbalance cellular stressors and restore homeostasis. One of the fundamental adaptive stress responses that combats oxidative stress is the activation of the Kelch like-ECH associated protein 1(Keap1)/ Nuclear erythroid 2-related factor 2 (Nrf2)/ Antioxidant response element (ARE) pathway [13, 17]. This mechanism facilitates the transcriptional induction of an entire array of cytoprotective proteins (known as phase 2 antioxidant enzymes). Nrf2 is an important stress response transcription factor that is activated in response to reactive oxygen and electrophilic species [17].

Nrf2 levels are regulated by its cytosolic repressor - Keap1, which when bound promotes Nrf2 degradation by the ubiquitin proteasome pathway. The Nrf2/Keap1 complex senses oxidative stress when excess free radicals disrupt critical cysteine residues in Keap1, resulting in Nrf2 being freed from the complex [18]. Unbound Nrf2 then translocates into the nucleus, where it heterodimerizes with a small Maf protein, which possess a leucine zipper domain that is required for complex formation thereby facilitating binding to the ARE in the upstream promoter region of many anti-oxidative genes, where it initiates their transcription [18, 19].

When cellular ROS production overwhelms the antioxidant detoxifying capacity, then the resulting damage to macromolecules leads to chromosome instability, genetic mutation, and/or aberrant cell

growth that may result in cancer [20]. The cellular stress responses act by upregulating repair mechanisms to restore molecular function or activate cell death for efficient removal [21]. The DNA damage response is robust and sophisticated, involving several systems that detect DNA damage, signal its presence and mediate its repair [22]. The base excision repair (BER) pathway is of greatest significance to the repair of single base aberrations. In BER, a damaged base is often recognized by a DNA glycosylase enzyme that mediates base removal before nuclease, polymerase and ligase enzymes complete the repair [22, 23]. Efficient repair of damaged DNA is integral to maintaining genomic stability and preventing carcinogenesis.

Failure of attempts to repair damage and restore homeostasis can promote cell death [16]. Apoptosis is an energy-dependent process that uses caspases, a group of cysteine aspartic proteases, as the driving force to execute this form of programmed cell death. The alternative to apoptosis is necrosis, characterised by disorganised and passive cellular disintegration. Several studies have demonstrated FA's ability to induce cell death in various cell models [24-26]. In plants, FA has demonstrated potential to exhibit apoptotic and necrotic cell death [24, 26], whereas in human cell cancer lines fusaric acid has induced apoptosis [15, 25, 27].

Fusaric acid has been found to alter mitochondrial integrity and redox status as well as promote genetic instability. However the exact mechanism of FA-induced cytotoxicity is relatively unknown. We investigated the effects of FA on the antioxidant response and the DNA damage stress response in HEK293 cells after acute exposure (24 hours).

Aims and objectives

Aim: To determine the effect of FA exposure on cellular stress response pathways in human embryonic kidney (HEK293) cells.

Objectives:

This study was conducted to determine the following:

- The effect of Fusaric acid on HEK293 cell viability.
- The oxidative status in HEK293 cells exposed to FA.
- The effects of FA on antioxidant response signaling in HEK293 cells.
- The effect of FA on genomic integrity in HEK293 cells by assessing DNA damage and associated repair mechanisms.
- The cell death pathways activated in HEK293 cells when treated with FA.

1.2. Literature review

1.2.1. Mycotoxins

Mycotoxins are low molecular weight, secondary metabolites produced by fungi. Mycotoxins are a group of naturally occurring chemical compounds that exhibit varied toxicological and chemical effects. These compounds have no involvement in primary metabolic processes, however they are capable of causing adverse effects in plants, animals and humans [28, 29]. Mycotoxins that exhibit phytotoxic abilities possess a variety of biological activities and cause morphological, physiological and metabolic effects, including necrosis, chlorosis, growth inhibition, wilting and inhibition of seed germination. Whereas, mycotoxins affect human and animal health by acting as carcinogenic agent, causing immune suppression, hindering normal developmental processes, altering metabolism and function of vital organs systems and in severe cases resulting in death.

Exposure to mycotoxins occurs via fungal infection of crops mainly cereal grains (corn, wheat, barley, oats, sorghum, etc.) that are consumed directly or used as livestock feed. Other food items that are contaminated by mycotoxins include spices, peanuts, fruit, coffee, and even meat and animal products (milk and eggs) obtained from animals that have consumed contaminated feed [30].

The term mycotoxin was coined in 1962 following an incident of a mass death of approximately 100 000 turkey poults in England caused by what was called turkey X disease [31]; it was later discovered that the toxigenic agent was aflatoxin which contaminated the groundnut meal that was fed to the turkey poults [32].

This was the first discovery of a multitude of other mycotoxins, which exhibited a variety of biological effects and were produced by a vast number of different fungal species [33]. Presently, there are more than 400 different mycotoxin documented, with new ones still being identified [33].

The disease condition associated with a fungal toxin is termed mycotoxicosis. Mycotoxicosis occurs globally, but is more prevalent in developing countries. Incidences of mycotoxicosis increase when

environmental, social and economic conditions combine with climatological conditions (humidity, temperature) to favour the growth of moulds [28, 34]. These factors coupled with poor agricultural practices, improper storage, handling and shipping of crops promote the growth of mould [30].

According to the Food and Agriculture Organization of the United Nations (FAO), it is estimated that approximately 25% of the world's crop is contaminated with mycotoxins, thus emphasizing the need to implement strict food safety regulations to protect consumers from the harmful effects of these mycotoxins [35]. The mycotoxins that have regulatory limits and are of greatest concern from a public health and agro-economical perspective include aflatoxins (AFT), trichothecenes such as deoxynivalenol (DON), fumonisins, ergot alkaloids, ochratoxin A (OTA), patulin (PAT) and zearolenone (ZEN)[30] (Figure.1.1).

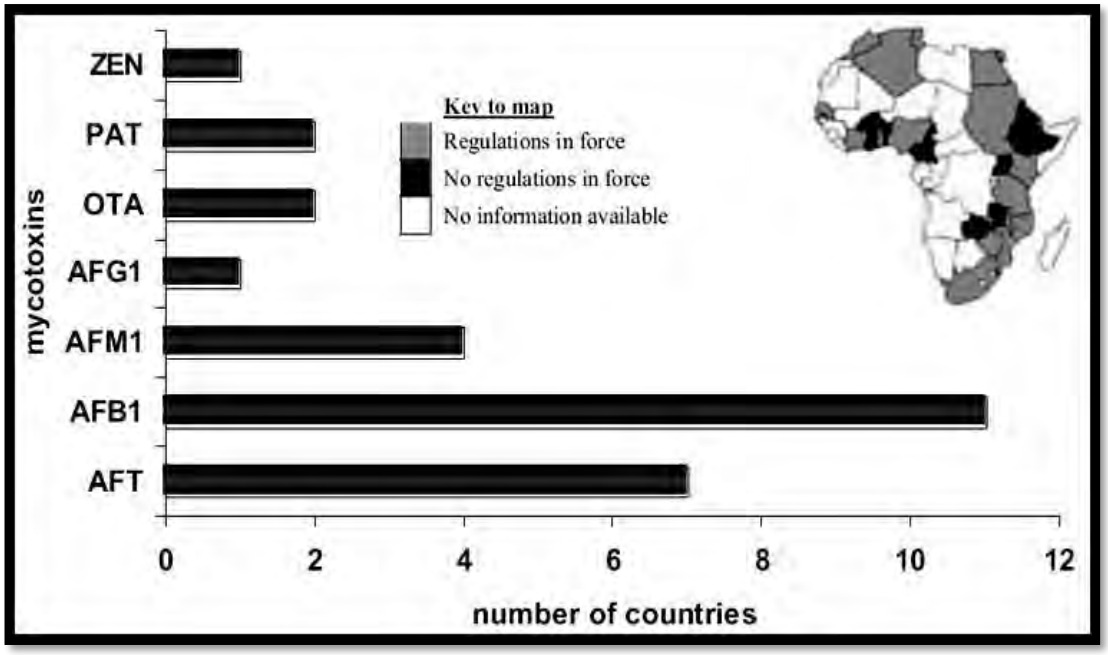

Figure 1.1: Mycotoxins that have regulatory standards in food in Africa (Taken from Worldwide regulations of mycotoxins in food and feed in 2003 from FAO.org [35]). (Note: ZEN- Zearolenone, PAT- Patulin, OTA- Ochratoxin A, AFG1- Aflatoxin G1, AFM1- Aflatoxin M1, AFB1- Aflatoxin B1 and AFT- Aflatoxin).

1.2.1.1. Mycotoxin Toxicity

Toxicity varies among individual mycotoxins based on various factors, including, target organ/s, absorption, dose and time period of exposure. The chemical and structural attributes of the different mycotoxins significantly affect toxicity. Within the cell, the interaction of the mycotoxin with cellular components alter structure and function of macromolecules, metabolic pathways and induce cell death activity [36].

The exposure period to the toxin greatly impacts the negative effects seen in human health. Acute exposure results in a rapid onset and an obvious toxic response following a single exposure to the toxin, whereas chronic exposure is characterised by several low dose exposures over a long time period causing irreversible adverse effects. The greatest threat to human and veterinary health is thought to be related to chronic exposure resulting in cancer, kidney-toxicity and immune suppression. However, the best known mycotoxin incidences have arose following acute exposure, such as human ergotism, turkey X disease and stachybotryotoxiscosis [30]. Moreover, the effect on each person or animal varies as well depending on the individual's immune system [36, 37].

1.2.1.2. Fusaric acid

Fusaric acid is a host non-specific mycotoxin, produced by various Fusarium species such as *F. moniliforme* and *F. oxysporum* [1]. Numerous surveys of several types of cereal grain, mixed livestock and poultry feed indicated that FA is a natural contaminant of these food and feed grains [38]. This was validated by a study carried out by Smith and Sousadias, 1993 [3], where it was shown that approximately 79-100% of grain and animal feed samples on farms were contaminated with FA. The most common route of exposure is through oral consumption of contaminated foods [33, 39].

The IUPAC name for FA is 5-butylpyridine-2-carboxylic acid and it has a molecular weight of 179.2157g/mol. FA is one of the oldest known mycotoxins and was first identified by Yabuta *et al.,* (1934) during the lab culture of *Fusarium heterosporum* Nees which was found to exhibit phytotoxic effects on rice seedlings [40].

Fusaric acid was found to be the most prevalent and in the highest concentration of mycotoxins produced in corn [5]. It is often neglected and overlooked with regards to research in favour of more potent mycotoxins [6]. As a result, the exact mechanism of toxicity of FA is poorly understood and its threat to food security is underestimated. This is validated by the fact that FA is not regulated by health or safety standards in food and animal feed [3, 41].

1.2.1.2.1. Structural and chemical properties of fusaric acid

Fusaric acid is a picolinic acid (PA) derivative [42] (Figure.1.2). Picolinic acid is a powerful bidentate chelating agent [43]. Additionally, it is a membrane permeating weak acid that acts as a proton conductor within the electron transport chain (ETC) causing loss of the mitochondrial electrochemical gradient [44]. The structure of FA is similar to that of its parent molecule with the addition of a butyl side chain, therefore the properties of PA are conserved [44].

The butyl tail on FA increases the lipophilicity of the compound and facilitates entry into the cellular interior [44]. The structure consists of a pyridine ring linked to a carboxylic acid moiety (Figure.1.2). The chelating effect of FA on divalent cations is attributed to the two adjacent atoms in the 2-pyridinecarboxylic acid moiety namely, the nitrogen atom in the pyridine ring and the oxygen atom in the carboxylic group [45, 46].

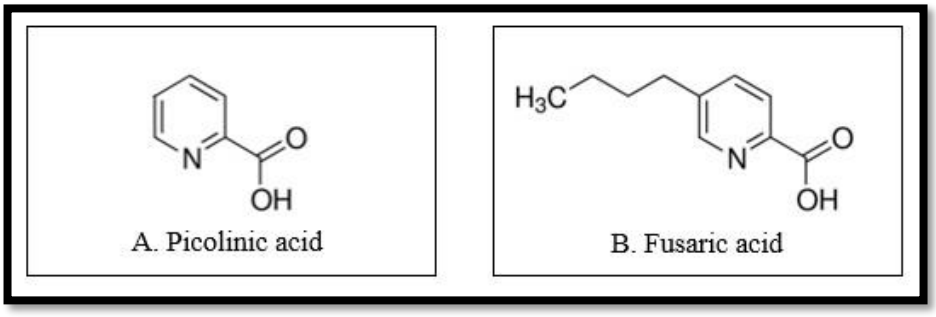

Figure 1.2: The chemical structure of picolinic acid ($C_6H_5NO_2$) (A) and its derivative, fusaric acid ($C_{10}H_{13}NO_2$) (B).

1.2.1.2.2. Toxicity of fusaric acid

Fusaric acid is considered to be low to moderately toxic to animals and humans [1, 38]. Fusaric acid is however, produced in conjunction with numerous other mycotoxins that are associated with higher levels of toxicity and these synergistic interactions are likely to increase toxicity [1, 6]. A study conducted by Bacon *et al.*, (1995) in the chicken egg, showed co-administration of equal concentration of Fumonisin B_1 (FB_1) and FA (5µg/egg) resulted in enhanced toxicity compared to the individually treated eggs with FB_1 or FA [42]. Similarly, DON and FA (0 or 200mg) demonstrated a synergistic toxicity in immature swine that were fed grain containing a combination of DON and FA and each mycotoxin separately. It was found that the combined effect of both mycotoxins resulted in a significant decrease in growth and feed consumption [47]. These observations were made following sacrifice of the animals at 4.5, 9, 18 and 36 hour intervals. It was also shown that a synergistic relationship exists with FA and trichothecene [48, 49].

On the contrary, some studies have shown that no synergistic effect exists between FA and other co-occurring Fusarium mycotoxins. Studies carried out using FA (0-400mg FA/kg of feed) and T-2 toxin, a trichothecene mycotoxin, co-administration in broiler chicks and turkey poults showed no synergism in toxicity [50]. Another study, using FA (0-400ppm) and FB_1 (3.4-437ppm) individually and a combination of both, illustrated similar results in rats [51]. The kidney and liver were removed for analysis and effects observed in these organs were consistent with FB_1 toxicity. It was concluded that FA exerted no synergistic, additive or antagonistic effects *in vivo* with FB_1. Therefore, the role of FA in toxic responses *in vivo* appears to produce unpredictable results.

1.2.1.2.2.1. Phytotoxic effects - a wilt toxin

Fusaric acid was one of the first mycotoxins implicated in plant pathogenesis [52]. Fusaric acid was found to be the causative agent of wilt disease in many plants [53]. Fusaric acid mediates its toxicity by altering cell membrane permeability and subsequently modifying mitochondrial membrane potential, increasing electrolyte leakage, inhibiting mitochondrial activity and oxygen uptake, decreasing ATP production and inhibiting root growth in several plant species. It was also shown that FA induced apoptotic and necrotic cell death in certain plants [26, 54, 55].

1.2.1.2.2.2. Cytotoxicity of fusaric acid in cultured cells

Fusaric acid has demonstrates potent cytotoxic activity *in vitro*. The effects of FA on the growth and viability of various human cancer cell lines have demonstrated the potent anti-cancer activity *in vitro*. Fusaric acid has been shown to arrest cell proliferation and inhibit DNA synthesis, with a consequential reduction in tumour growth in head and neck squamous cell carcinomas and adenocarcinoma cells [56-58]. The concentration of FA at which these effects were observed ranged between 1.4-500mM. Additionally, FA is actively involved in DNA damage and prevention of DNA repair by interfering with the catalytic DNA-associated metalloproteins. Therefore FA facilitates cytotoxicity seen in these cells that prime them for cell death [46].

Fusaric acid is commonly recommended as a therapeutic intervention in various cancers. This is evidenced by studies that have demonstrated FA is beneficial in the treatment of head and neck squamous carcinomas (0.1-0.5mM- *in vitro* model, 1.395mM- *in vivo* model), colorectal and mammary adenocarcinomas and phaeochromocytomas [25, 46, 56, 57, 59, 60].

Conversely, FA is also cytotoxic to normal cells, as illustrated by Fernandez- Pol *et al*., (1993) using human WI-38 fibroblasts. FA (500mM) caused a cytostatic effect in these cells, however an increased sensitivity to the toxin was seen in cancerous cells lines [56]. The information available with respect to the effect of FA in non-cancer cell lines is limited.

1.2.1.2.2.3. Effects in animals and humans

FA has been associated with moderate toxicity in animals [4, 61]. Fusaric acid is a pharmacologically active compound that biochemically inhibits the enzymatic action of dopamine β hydroxylase (DBH) *in vivo* and *in vitro* [3, 38, 62]. Dopamine β hydroxylase is a regulatory enzyme in the biosynthesis of norepinephrine from dopamine. Norepinephrine is an endogenous catecholamine and the body's primary adrenergic neurotransmitter. Norepinephrine is also required for the synthesis of epinephrine, therefore FA acts to lower the levels of both endogenous hormones in the brain, heart, spleen and adrenal gland. This inhibitory effect on DBH has allowed for FA to

be used as a hypotensive agent, as a decrease in norepinephrine results in a decrease in blood pressure [63]. Studies conducted in rats and dogs demonstrated a decline in blood pressure following administration of FA [38]. Similarly, the effects of a calcium salt of FA was tested in elderly hypertensive Japanese patients, which found that there was a reduction in the systolic and the diastolic blood pressures [38]. Furthermore, neurochemical alterations occurred in the brain and pineal gland due to dysregulation of hormones affected by FA, namely serotonin, tyrosine, 5-hydroxyindoleacetic acid and dopamine, resulting in neurotoxic effects in mammals [61, 64].

The study conducted by Smith and MacDonald (1991), also showed that FA enhanced vomiting and feed refusal in pigs administered with trichothecenes [64]. FA is also associated with developmental changes, such as a reduction in weight gain observed in immature swine and rats being fed FA contaminated feed. The absence of the egg pip in chicken eggs incubated with FA, further highlights developmental abnormalities elicited by FA [38]. A more recent study has demonstrated that FA exposure causes notochord malformation as seen in zebrafish [41].

1.2.1.2.3. Mechanism of action of fusaric acid

1.2.1.2.3.1. Oxidative stress

Like many other mycotoxins, FA employs the mechanism of excessive ROS generation in mediating its cytotoxicity [36]. ROS is a collective term used to describe an array of free radicals derived from molecular oxygen that are chemically reactive in nature. In aerobic cells, ROS is produced as a by-product of oxidative metabolism, where it is plays an integral role in signaling pathways to maintain cellular homeostasis [36].

Under normal cellular conditions, basal levels of ROS levels are maintained by endogenous antioxidant defence mechanisms which work efficiently to detoxify potentially harmful radicals and ensure maintenance of the redox homeostasis [65]. A disruption to redox homeostasis favouring a pro-oxidant environment, due to either an increased generation of free radicals and/or a reduced detoxifying capacity of the antioxidant systems, is known as oxidative stress [66].

Oxidative stress promotes cellular damage, due to the interaction of ROS with intracellular targets such as lipids, DNA and proteins, that affect their structure and function. These alterations lead to loss of structural integrity of the cell (lipid peroxidation of membrane), genetic mutations, protein malfunction, and even complete enzyme inactivation that affect overall cell signaling processes. The ROS mediated modifications compromise cell viability, which can have potentially detrimental effects on the cell [66].

Approximately 90% of total oxygen uptake in cells is processed by the ETC. The ETC is localised in the inner mitochondrial membrane and consists of protein complexes (complex I-V) [67]. The ETC comprises of two synchronized processes; 1) the passage of electrons through the complexes into the intermembrane space of the mitochondria to generate an electrochemical proton gradient and 2) the phosphorylation of ADP via ATP synthase as protons are channelled back into the mitochondrial matrix through complex V (Figure.1.3). The end product of the ETC and oxidative phosphorylation is cellular energy in the form of ATP [68].

Under normal cellular function, molecular oxygen is reduced to water via a 4 electron mechanism (Figure.1.3). However, about 1-3% of the oxygen consumed is leaked from the system, mostly at complex I and III after undergoing incomplete reduction, therefore producing superoxide anion radicals ($\bullet O_2^-$) [67]. Studies have shown that FA altered mitochondrial function by suppressing the ETC and subsequently reducing activity of the ATPase complex [69, 70].

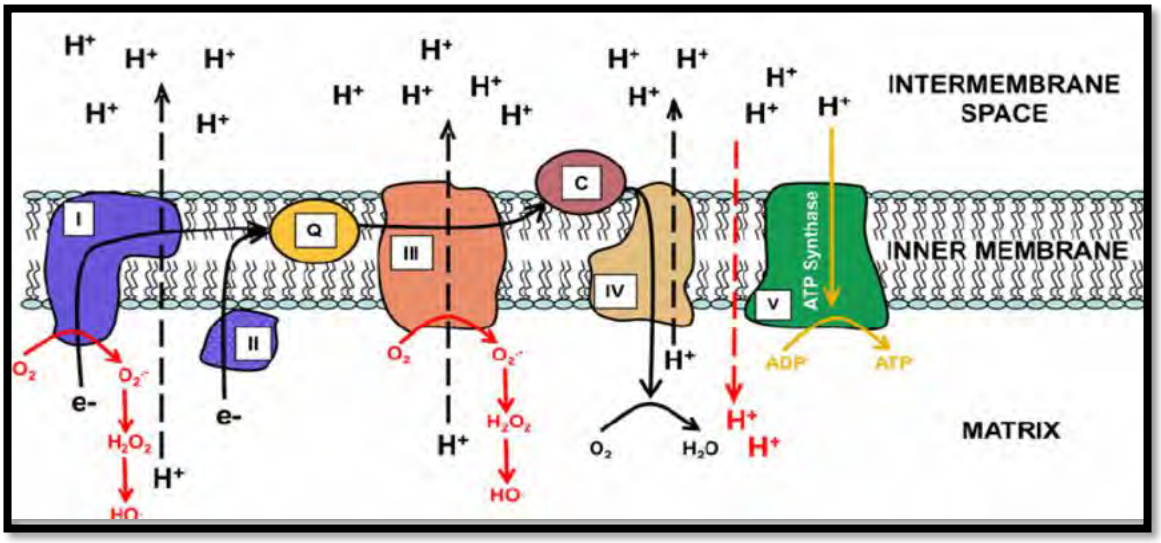

Figure 1.3: Production of superoxide radicals in the electron transport chain, located on the inner mitochondrial membrane (Taken from McEwan *et al*., (2011) [71]).

The $\bullet O_2^-$ radicals act as precursors for the formation of other forms of ROS. The dismutation of $\bullet O_2^-$ by superoxide dismutases (SODs) results in hydrogen peroxide (H_2O_2) production. Subsequent processing of the H_2O_2 in the Fenton reaction (in the presence of Fe^{2+}) produces hydroxyl radicals (OH^-). Fusaric acid involvement in Fenton reactions has also been documented; it is thought that chelation of the iron ion enhances the progression of Fenton reactions (Figure.1.4), fundamentally increasing the overall generation of ROS [45].

Figure 1.4: Production of hydroxyl radicals by the Fenton reaction [72].

1.2.1.2.3.2. Chelation

Fusaric acid has been identified as a chelating agent with specificity for divalent cations. Chelation of the essential metal ions (Zn^{2+}, Cu^{2+}, Fe^{2+}, Mn^{2+}, etc.) rob metalloproteins of their catalytic core. This changes their three dimensional structure and therefore impairs or disables their functional activity and facilitates the activation of cell death mechanisms [46].

Fusaric acid has the ability to chelate Zn^{2+}, Fe^{2+}, Cu^{2+} and Mn^{2+} ions, which affects important structural and functional components in numerous proteins associated with cell proliferation, differentiation, and protection against free radicals such as the transcriptionally active zinc finger proteins, heme-containing (Fe^{2+} ion at its core) complexes and the Zn^{2+}/Cu^{2+} and Mn^{2+} containing superoxide dismutase (SOD) enzymes [44, 46].

A study conducted by Fernandez-Pol *et al*. (1993) implicated FA in the inhibition of ribonucleotide reductase (zinc-,copper-and iron-requiring enzyme) activity, a rate limiting enzyme in DNA synthesis, due to chelation of metal ion cofactors [56]. Another study showed FA induced copper chelation hindered the function of (copper dependent) lysyl oxidase, leading to malformation of notochords in zebrafish [41].

1.2.1.2.3.3. Fusaric acid as a nicotinic acid derivative

Fusaric acid and its parent compound, PA are derivatives of Nicotinic acid (NA). Nicotinic acid, also known as vitamin B_3 (niacin), is a water-soluble vitamin. Nicotinamide is the derivative of niacin and is used by the body as building blocks in the synthesis of the coenzymes nicotinamide adenine dinucleotide (NAD^+) and nicotinamide adenine dinucleotide phosphate (NADP) [73]. Catabolic processing of macronutrients utilises NAD^+ in various energy-producing reactions. Nicotinamide adenine dinucleotide is of great importance in redox reactions, especially within the mitochondria, where it acts as a carrier of electrons with reducing potential that is required for function of the Krebs cycle and the electron transport system. Non-redox reactions also require NAD, were it is utilised as a cofactor for catalytic activity of enzymes. Sirtuins (silent mating type information regulation 2 homolog - SIRTs) are a NAD^+-dependent class of enzymes, which act as deacetylases or mono- ADP ribosyl transferases involved in post-translational modification of proteins that alter their activity [74]. Another group of enzymes that require NAD^+ are Poly-ADP-Ribose Polymerases (PARP), which catalyse the transfer of polymers of ADP from NAD^+ to acceptor proteins. PARPs are involved in DNA repair and stress responses, thus NAD^+ is critical for genome stability. Nicotinamide, which is a NAD^+ precursor, often has an inhibitory effect on NAD^+ requiring enzymes. The structural similarity of FA with nicotinamide could affect reactions that require NAD^+ through competitive inhibition [15].

Previous studies conducted by Telles-Pupulin *et al.,* (1996 & 1998) [69, 70], demonstrated that FA treatment resulted in inhibition of α-ketoglutarate dehydrogenase and succinate dehydrogenase in the Krebs cycle. These enzymes utilise NAD and produce NADH, which are used as reducing equivalents in the ETC. Therefore, FA alters the metabolic function of the energy-producing reactions and facilitates mitochondrial dysfunction as a mechanism of toxicity.

1.2.2. Cellular stress responses

Cells are often exposed to a vast array of mutagens, potential carcinogens, environmental and man-made toxicants all of which cause adverse health effects in humans and animals. Evolutionary development of the eukaryotic cell has allowed for the acquisition of several defence mechanisms which aid in counteracting and adapting to stressful stimuli [16], which is referred to as the cellular stress response. The cellular stress response is a reaction to fluctuations in extracellular conditions, which cause damage to the structure and function of macromolecules [75]. However, exposure to certain stressors can result in irreversible damage to the cell, thus triggering cell death mechanisms [16].

1.2.2.1. The Nrf2-antioxidant response element signaling pathway

Nuclear erythroid 2- related factor 2 (Nrf2) is a member of the Cap' n' Collar subfamily of basic region leucine zipper (bZip) transcription factors. Nrf2 is considered to be the master switch that regulates redox homeostasis [18], as it modulates the expression of over 600 gene targets, where the protein products are antioxidants and xenobiotic metabolizing enzymes. Induction of these detoxifying enzymes lead to neutralization of potential oxidative damage caused by reactive oxygen and/or nitrogen species to cellular components that are sensitive to redox change [17].

Under normal unstressed conditions, Nrf2 interacts with the cytosolic- actin bound Kelch-like ECH-associated protein 1 (Keap1). Keap1, a negative regulator of Nrf2, sequesters Nrf2 in the cytoplasm where it acts as a substrate adapter protein for the Cullin 3- Rbx1-E3 ubiquitin ligase (Cul3-E3 ligase), which is a multiprotein complex that recognises and targets substrates for ubiquitin-dependent degradation. The interaction between Nrf2 and Keap1 targets Nrf2 for ubiquitination and subsequent degradation via the 26s proteasome [76], thus maintaining low basal levels of Nrf2 [17]. Keap1 acts as a sensor of oxidative stress, as the cysteine-rich residues in the amino acid sequence undergo modification when intracellular ROS levels increase. Subsequently, the Cul3-E3 ligase complex is inhibited, facilitating the efficient up-regulation of Nrf2 to enable an adaptive antioxidant response to counteract the ROS and maintain homeostasis [13]. Nrf2 is stabilized and translocates to the nucleus where it accumulates and dimerizes with small Maf proteins, which then bind to the ARE leading to the transcriptional activation of protective genes (Figure.1.5) [17, 18].

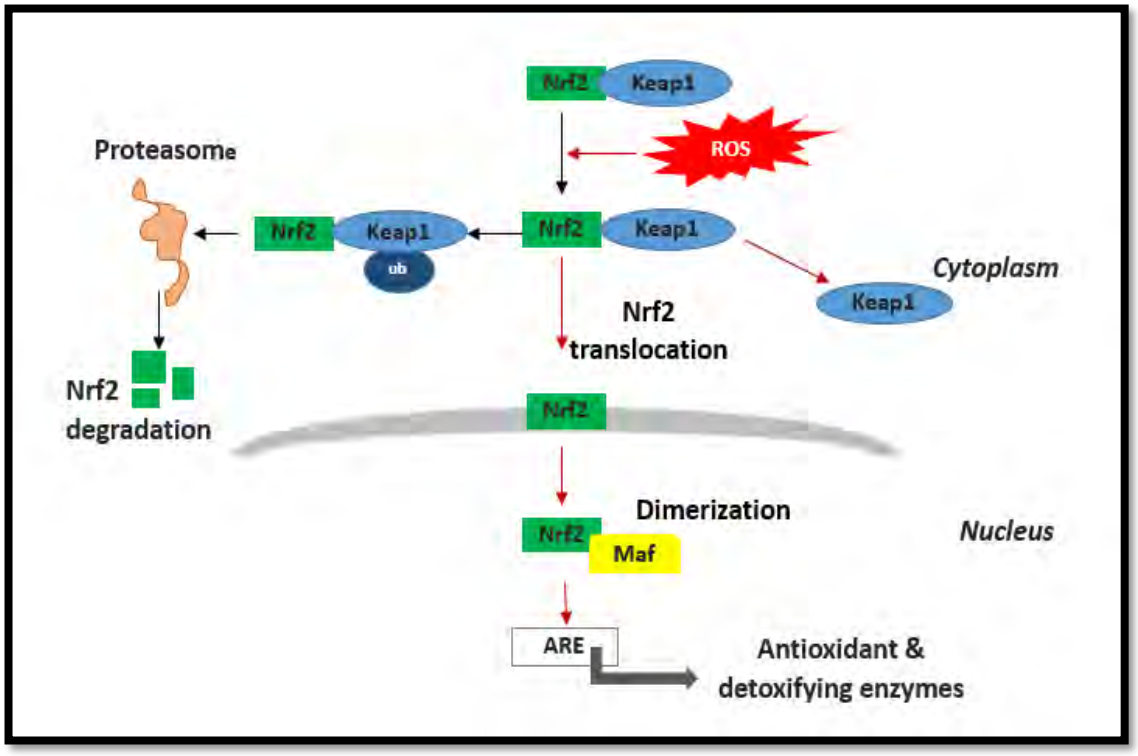

Figure 1.5: Schematic representation of the regulatory pathway of Nrf2 mediated by ROS (Adapted from Espinosa-Diez *et al*., (2015) [77]).

1.2.2.2. The antioxidant defence system

The antioxidant defence system is initiated by the ARE upon activation by Nrf2. The association of Nrf2 with the ARE within the nucleus facilitates the transcription of genes that encode phase II detoxifying enzymes and antioxidant enzymes, such as Glutamate-cysteine ligase-catalytic (GCLC), Glutamate-Cysteine ligase-modifier (GCLM), NAD(P)H Quinone Oxidoreductase 1 (NQO1), Heme Oxygenase-1 (HO-1), Glutathione Peroxidase (GPx), and glutathione S-transferases (GST), that serve to protect the cell from oxidative insult. Prolonged exposure to oxidants alters cell signaling outcomes resulting in mutation, carcinogenesis and even cell death due to ROS interaction with biological molecules. Maintaining a balance between the pro-oxidants and antioxidants is integral to cell survival. Therefore despite the constant generation of ROS by various processes in the body, the endogenous antioxidant defence systems work efficiently to counterbalance oxidising agents. Antioxidants perform their function by scavenging free radicals, decomposing peroxides, donating electrons and hydrogen and/or binding pro-oxidant metal ions [78].

The antioxidant enzymes that are necessary to maintain cellular health are superoxide dismutase, catalase and glutathione peroxidase, which function cohesively for optimum detoxification of ROS and maintenance of redox state (Figure.1.6) [65].

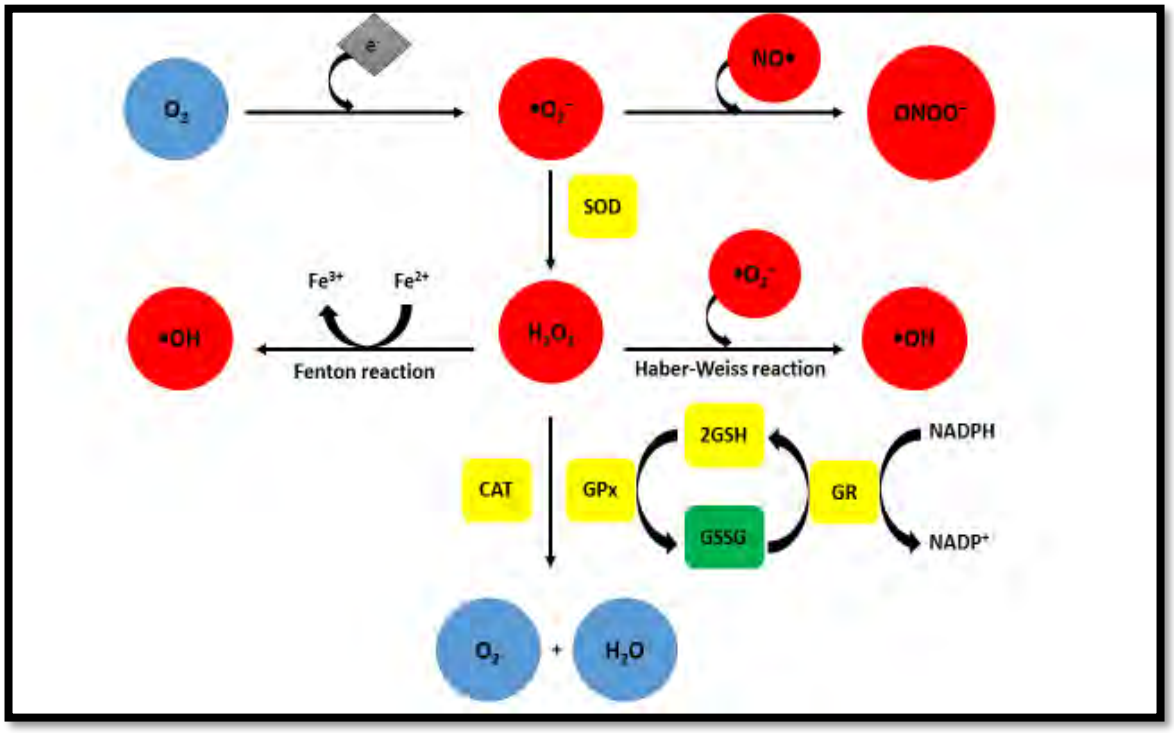

Figure 1.6: The network of antioxidants that act to detoxify ROS (Adapted from Hermes-Lima, (2004) [79]) (Note: NO•- nitric oxide, $\bullet O_2^-$superoxide radicals, ONOO⁻peroxynitrite, •OH-hydroxyl radicals, H_2O_2- hydrogen peroxide, CAT- catalase, SOD- superoxide dismutase, GSH-reduced glutathione, GSSG- glutathione disulphide, GR- glutathione reductase, GPx- glutathione peroxidase).

1.2.2.2.1. Superoxide dismutases

Superoxide dismutases are a closely related class of metalloenzymes which catalyse the conversion of superoxide anion radicals ($\bullet O_2^-$) to molecular oxygen and hydrogen peroxide. Superoxide dismutases exist in several isoforms, which differ in the metal/s present in their active site, amino acid composition, cofactors and localisation within the cell [66].

In humans, there are 3 known isoforms of SOD. SOD1 (Cu, Zn-SOD) is located in the cytoplasm and exists as a dimer whereby each of the subunits contain a dinuclear metal cluster made up of copper and zinc at the active site. SOD2 is found in the mitochondrial matrix and is a homotetramer that contains one manganese atom per subunit. SOD3 is located extracellularly as a tetramer that also requires copper and zinc ions in its reactive centre. In mammals, SOD3 is regulated by cytokine levels and has little influence on the adaptive response to oxidative stress [68].

Cu, Zn-SOD and Mn-SOD are thought to act as bulk scavengers of $\bullet O_2^-$ radicals. The product of the SOD reaction is hydrogen peroxide which is also potentially toxic and therefore requires efficient removal [72]. In mammalians cells, there are 2 enzyme families which act to carry out the detoxification of hydrogen peroxide namely, GPx and CAT [66].

1.2.2.2.2. Catalase

Catalase is a ubiquitous heme-containing peroxisomal enzyme that is present in aerobic cells. The function of catalase is to catalyse the decomposition of hydrogen peroxide into water and gaseous oxygen. Catalase is a tetramer of four polypeptide chains, with a porphyrin heme (iron) present in each subunit, which facilitates the reactivity of the enzyme with hydrogen peroxide, thereby mitigating its toxic effects [72].

1.2.2.2.3. The glutathione network

The glutathione system constitutes several enzymes which include glutathione (non-enzymatic thiol) (GSH), GPx, glutathione reductase (GR) and GST that work in conjunction with each other to detoxify and eliminate toxic electrophilic metabolites and xenobiotics [78].

Glutathione peroxidases are a family of tetrameric selenium-requiring enzymes which uses GSH as the reducing equivalent to catalyse the conversion of hydrogen peroxide or hydroperoxides to water and alcohol while simultaneously oxidizing GSH [68].

Glutathione S-transferases is a family of cytosolic multifunctional enzymes. They catalyse the conjugation of GSH with a variety of reactive electrophilic compounds, thereby neutralizing their active electrophilic sites and subsequently making the parent compound more water-soluble [78].

Glutathione, is a major non-enzymatic thiol in living organisms, which plays an essential role in coordinating the body's antioxidant defence processes in response to oxidative stress [72]. This ubiquitous intracellular tripeptide is made up of glutamate, cysteine and glycine which is responsible for the maintenance of cellular redox state [68]. Glutathione is synthesised in the cell by 2 ATP-requiring enzymes, γ -glutamylcysteine synthetase (also called glutamate cysteine ligase-GCL) and glutathione synthetase [80]. The GCL catalysed reaction results in the formation of γ-glutamylcysteine and is the rate limiting step in *de novo* glutathione synthesis. Glutathione is implicated in a feedback loop to inhibit GCL and in doing so, regulates cellular concentrations of GSH [81]. The next step is the addition of glycine to the C-terminal of γ-glutamylcysteine, catalysed by glutathione synthethase. The cysteine residue is the rate limiting factor and the sulfhydryl group of cysteine acts as a proton donor; therefore cysteine is responsible for the biological activity of GSH. Glutathione exerts its antioxidant effects by directly scavenging radicals or by participating in reactions catalysed by enzymes that use GSH as an electron donor (GPx and GST) [80].

Glutathione reductase is a ubiquitous flavoenzyme that exists as a homodimer, containing 1 flavin adenine dinucleotide (FAD) and NADPH binding site per subunit that catalyses the reduction of oxidised glutathione (GSSG) to GSH that is essential for the continuation of the glutathione redox cycle by regenerating reduced form of GSH that has antioxidant capacity [82]. The GSH/GSSG ratio is a major determinant of oxidative stress. In healthy cells, the glutathione pool consists of approximately 98% of GSH. However, exposure to oxidative stress causes an accumulation of GSSG, decreasing the ratio of reduced to oxidised glutathione [83]. These enzymes function to prevent ROS-induced damage in the cell, nonetheless, in times of excessive stress these mechanisms are inadequate and oxidative damage occurs [81].

1.2.2.3. Macromolecular damage

When macromolecules are subjected to oxidative modification due to failure of the antioxidant system, the function and structure are altered, ultimately affecting cellular processes and even viability. Oxidative stress can induce radical-mediated damage to cellular membranes resulting in lipid peroxidation, which converts unsaturated lipids into polar lipid hydroperoxides. Lipid peroxidation was the first type of oxidative damage to be investigated [66] and is particularly damaging to the cell due to its facile propagation of free radical reactions [65].

Lipid peroxidation results in the formation of a variety of oxidised products including reactive electrophiles such as epoxides and aldehydes, which are capable of modifying DNA, protein and other macromolecules. Malondialdehyde (MDA) and 4-hydroxy-2-nonenal (4-HNE) are examples of such, whereby MDA can react with nucleic acid bases and form adducts, that are mutagenic. These lipid peroxidation products are commonly used as indirect measures of oxidative stress [84]. Oxidative damage to lipids may compromise cell function by increasing membrane permeability and inactivating membrane bound receptors and enzymes [72].

Oxidative damage to proteins can significantly affect cellular homeostasis by altering cell signalling, cell structure, and enzymatic processes [84]. Protein oxidation is regarded as covalent modifications made to a protein by ROS directly or by secondary products of oxidative damage. The effect that ROS has on proteins include: oxidation of amino acid side chains that result in fragmentation of peptide chains, alterations to physical properties of the protein such as electrical charge and formation of protein-protein or protein-DNA crosslinks [85]. All amino acids are subject to oxidation, however cysteine and methionine are most vulnerable to ROS-mediated modification due to the high reaction susceptibility of the sulphur groups within these amino acids [85].

DNA is also prone to oxidative modifications, which can lead to genomic instability. Oxidative damage to DNA causes alteration to bases, single- (ss) or double-stranded (ds) DNA breaks, purine, pyrimidine or sugar-bound modifications, mutations, deletions or translocations, and cross-linking with proteins [72]. Guanine is the most susceptible DNA base because of its low oxidation

potential, thereby producing 8-oxoguanine (8-oxoG), which is the most abundant, stable and well documented DNA oxidation product [84]. It is often utilised as a biomarker of oxidative stress. These lesions are strongly promutagenic, as it promotes the mismatched incorporation of dATP instead of dCTP opposite the lesion during replication, leading to a guanine: cytosine to thymine: adenine transversion [86].

1.2.2.4. Cellular repair pathways

Cells are not defenseless against oxidative damage, as they can adapt to either overcome damage by initiating various sophisticated repair mechanisms or induce cellular death if damage is too extensive [66].

The major fate of most oxidised proteins is degradation by proteasome or lysosomal pathways where they undergo complete catabolism to form its constitutive amino acids. Thereafter new replacement protein molecules are synthesised *de novo* using recycled amino acids [87].

The primary repair mechanism for oxidative base lesions including 8-oxoG, is base excision repair (BER). Base excision repair is responsible for recognition and repair of oxidised bases, abasic (AP) sites, DNA ss-breaks, alkylated bases, deaminated bases, and base mismatches [84]. The repair process begins with the identification and subsequent removal of the damaged or incorrect base by the DNA glycosylase. This results in the formation of an AP site, which are cleaved by AP endonucleases. The gap that remains in the DNA backbone is filled in by the action of a DNA deoxyribose phosphodiesterase, a DNA polymerase and a DNA ligase [23, 66].

The major glycosylase employed in carrying out the first step of the BER process in mammals, is 8 – oxoguanine glycosylase 1 (OGG1). Human OGG1 also recognises and excises several other oxidative lesions, including 2,6-diamino-4-oxo-5-formamidopyrimidine (FapyG) and 7,8-dihydroxy-8-oxo-2'-deoxyadenine (8-oxoA) [84]. OGG1 is ubiquitously expressed and exists in 2 isoforms due to the alternative splicing of the single mRNA gene product, whereby α-OGG1

(OGG1 type 1a) is located in the nucleus and β- OGG1 (type 2a) is found in the mitochondria. OGG1 contains critical thiol moieties that are essential for catalytic activity. OGG1 protein contains 2 distinct DNA-binding motifs namely, a helix-hairpin-helix domain and a Cys-Cys-His-His (C_2H_2) classical zinc finger domain [88].

It has been shown that diminished OGG1 reduces the DNA repair capacity leading to an increase in base mutations [86, 88]. As the 8-oxoG lesions have mutagenic potential, OGG1 activity is crucial in preventing mutations that propagate carcinogenesis [86].

Another repair protein integral to the BER process is PARP-1, which is a chromatin-associated enzyme that catalyses the post-translational modification of proteins [73]. Poly ADP-Ribose Polymerase-1 activity is regulated by interaction with DNA strand breaks and is involved in other cellular processes in addition to DNA repair, which include cell cycle control, transcriptional regulation and apoptotic cell signalling [21, 89].

Poly ADP-Ribose Polymerase-1 acts downstream of OGG1 and binds to the ss-DNA breaks through its zinc finger motif, where it modifies it and other proteins by long branched polymers of ADP-ribose, which in turn recruit downstream DNA repair proteins and chromatin remodelling factors to complete the DNA repair process [90]. High levels of DNA damage saturates cellular repair capacity, therefore genomic integrity is compromised, resulting in apoptosis. It has been shown that the tumour suppressor, p53 is an important regulator of the cellular response to ROS-induced DNA damage [84]. The p53 protein is a homotetrameric transcription factor that is located in the nucleus and induces transcription of target genes involved in cell cycle arrest, DNA repair and apoptosis. Oxidative stress acts as a potent inducer of p53 activity [91]. Exposure to low levels of oxidative stress cause p53 to exhibit antioxidant properties to ensure cell survival. However, in response to high levels of oxidative stress, p53 acts as a pro-oxidant to further increase ROS, leading to cell death [92].

Studies have shown the involvement of p53 in detecting oxidative DNA damage and subsequently modulating the BER function in response to oxidative stress [93]. Under conditions of oxidative

stress, high levels of DNA damage cause an ongoing cycle of p53 activation and accumulation that mediates the initiation of apoptosis in damaged cells, thereby maintaining genetic integrity. The functional activity of p53 being integral in the prevention of cancer is well documented. Therefore, it has been shown that decreased repair will result in elevated lesions and an increased risk of disease. Hence the DNA repair capacity of a cellular system, is seen as potential marker for cancer susceptibility [86].

1.2.2.5. Cell death

The adaptive capacity of a cell ultimately determines its fate. Therefore, when cellular defence mechanisms and pro-survival strategies are unsuccessful, cell death programs are activated to eliminate these damaged cells from the organism. The energy status plays a pivotal role in dictating the manner in which a cell dies [94]. The two major mechanisms of cell death are apoptosis and necrosis (Figure.1.7).

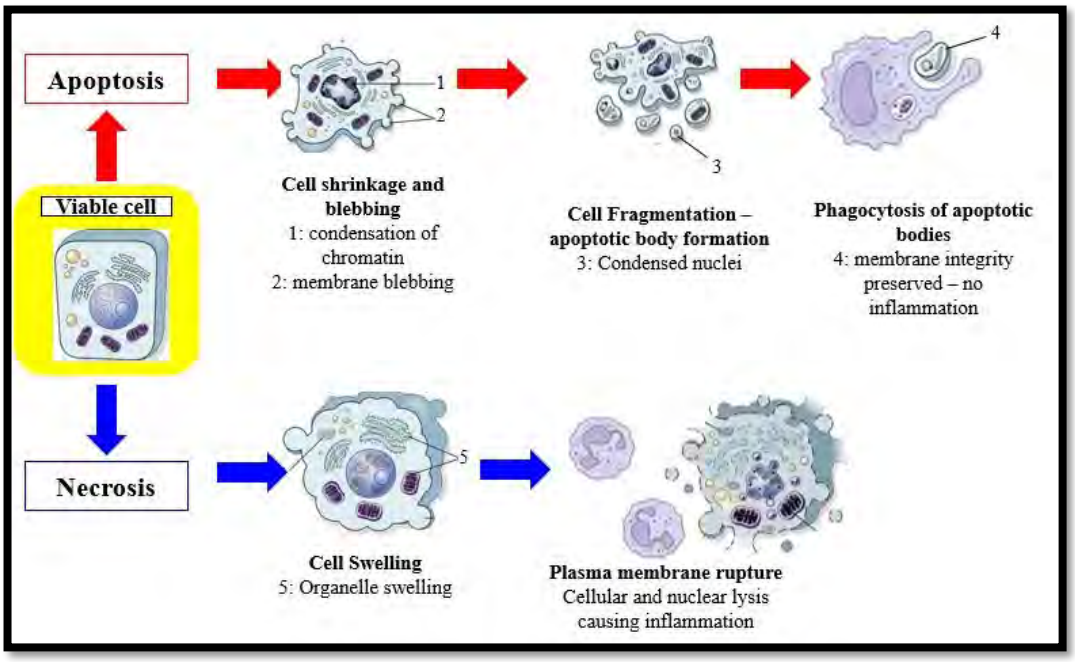

Figure 1.7: The main morphological changes seen in apoptotic and necrotic cell death (Adapted from Van Cruchten and Van Den Broeck, (2002) [95]).

Apoptosis, a form of programmed cell death, is vital for both developmental processes and maintenance of cellular homeostasis. Apoptosis is characterised by distinct morphological changes that involve a series of highly regulated energy-dependent biochemical mechanisms that leads to cell destruction and disintegration [96]. The core component of the apoptotic machinery is a proteolytic system involving a group of aspartate-specific cysteinyl proteases referred to as caspases. Caspases are widely expressed as inactive zymogens in most cells and once activated can often activate other procaspases, allowing initiation of a protease cascade [97]. All caspases contain a cysteine residue at their active site and cleave their target proteins at specific aspartic acids [98]. Caspases involved in apoptosis have been classified by their mechanism of action and are either initiator caspases (caspase-8 and -9) or executioner caspases (caspase-3, -6, and -7) [97]. The morphological changes seen in cells undergoing apoptosis include cell shrinkage, hypercondensation of chromatin, chromosomal cleavage into nucleosomal fragments, blebbing of plasma membrane and packaging of cellular contents into apoptotic bodies-membrane enclosed vesicles (Figure.1.7.) [96, 99].

There are two major apoptotic pathways that exist in mammalian cells: the extrinsic death receptor-mediated and intrinsic mitochondria-mediated pathways [100]. Both pathways are tightly regulated and controlled by a host of regulatory molecules, which will be highlighted further on. The extrinsic pathway of apoptosis, also called the death receptor pathway, is triggered by ligation of death receptors belonging to the tumour necrosis factor (TNF) family [16]. They are characterised by cysteine rich extracellular subdomains which allow highly specific ligand recognition, subsequent trimerization, and activation of the death receptor [21]. TNF receptors contain an intracellular death domain, which interacts with adapter molecules within the cytoplasm to form the death inducing signalling complex (DISC), that facilitates the recruitment of procaspase-8 to the DISC [96]. This results in the accumulation of procaspase-8 at the DISC that leads to autocatalytic activation and subsequent release of active caspase-8 which activates effector caspases 3, 6 and 7 resulting in cell death (Figure.1.8) [96, 100].

The intrinsic, or the mitochondrial, pathway is activated by developmental cues upon cellular stresses such as reduced oxygen levels, increased levels of ROS and DNA damage. This pathway is regulated by the Bcl2 family of proteins which comprise of both anti-apoptotic family members, for

example, Bcl-2, Bcl-XL, and Mcl-1, and pro-apoptotic molecules such as Bax, Bak, and BH3 domain only molecules [101]. Accumulation of pro-apoptotic (Bax and Bak) proteins on the mitochondrial outer membrane results in oligomerization which allows for pore formation and initiates the permeabilisation of the outer mitochondrial membrane [100]. This facilitates the release of proteins located in the intermembrane space such as Cytochrome c (Cyt c). Cytochrome c binds Apaf-1 (Apoptotic protease activating factor-1), and couples with procaspase 9 to form the apoptosome [101]. The oligomerization of procaspase-9 in apoptosome formation facilitates the activation of caspase-9 which in turn cause proteolytic activation of the effector procaspases-3, -6, and -7, resulting in the execution of cell death (Figure.1.8) [96, 100].

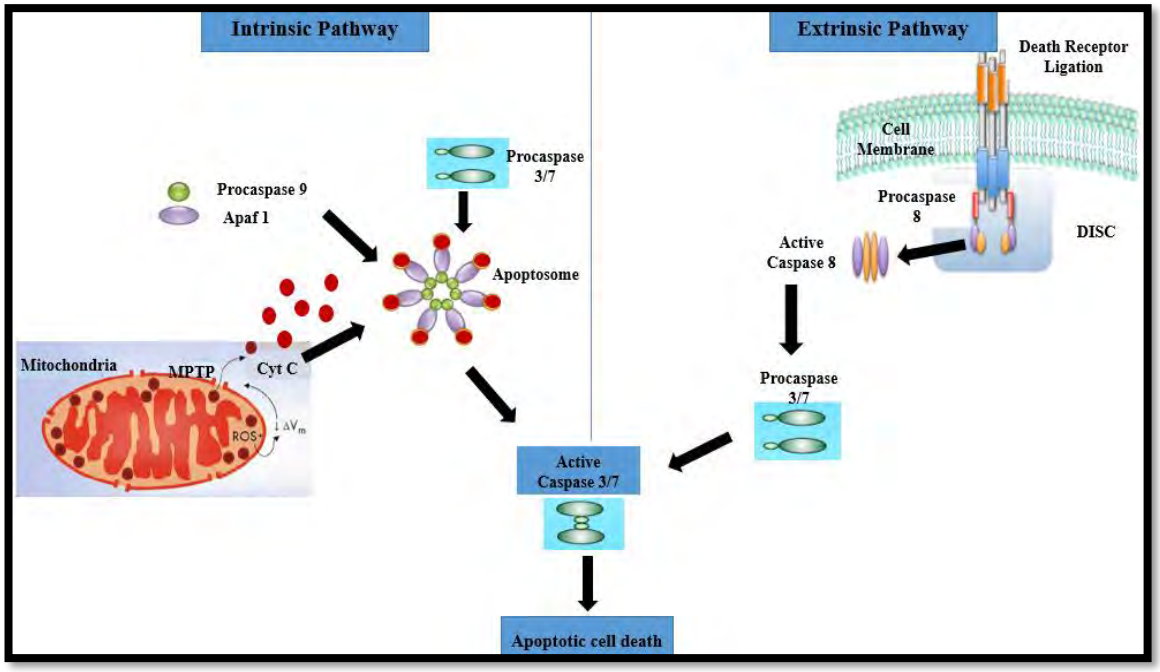

Figure 1.8: The sequence of events leading to the activation of the intrinsic and extrinsic apoptotic pathway (prepared by author).

The alternative to apoptotic cell death is necrosis, whereby cellular injury results in an energy-independent mode of death caused by environmental perturbations such as toxins, heat and reduced oxygen. Some of the major morphological changes seen in cells undergoing necrosis include

cellular swelling, aggregation of DNA, distended endoplasmic reticulum, formation of cytoplasmic blebs; swelling of mitochondria, disrupted organelle membranes; swollen and ruptured lysosomes; and eventually disruption of plasma membrane integrity which are characteristics that are recapitulated by ATP depletion (Figure.1.7) [96].

This loss of cell membrane integrity results in the release of the cytoplasmic contents into the surrounding environment and therefore mediates inflammation. However, apoptotic cells do not release their cellular constituents into the surrounding environment and are quickly phagocytosed by macrophages or adjacent normal cells, thus there is essentially no inflammatory reaction [96].

Chapter 2

Materials and methods

2.1. Materials

The Human Embryonic Kidney 293 cell line (HEK293) was purchased from Highveld Biologicals (Johannesburg, South Africa). Cell culture reagents were purchased from Lonza Biowhittaker (Basel, Switzerland). Fusaric acid (FA), phosphate buffered saline (PBS) tablets and bicinchoninic acid (BCA) reagents were purchased from Sigma Aldrich (St Louis, Missouri, United States). Luminometry Kits and reagents (CellTitre-Glo™, GSH-Glo™ Glutathione and Caspase-Glo® assay kits) were purchased from Promega (Madison, Wisconsin, United States). Reagents for western blot and quantitative-PCR (qPCR) were purchased from Bio-Rad (Hercules, California, United States). Quantitative-PCR primer sequences were obtained from Inqaba Biotechnologies (Pretoria, South Africa). Antibodies for western blots were purchased from Santa Cruz Biotechnologies (Dallas, Texas, United States), Cell Signalling Technology (Beverly, Massachusetts, United States) and Abcam (Cambridge, United Kingdom). All other reagents and consumables were purchased from Merck (Darmstadt, Germany), unless otherwise specified.

2.2. Cell culture

The HEK293 cell line is derived from primary human embryonic kidney cells obtained from a healthy aborted foetus. The HEK293 cell line is thought to be of epithelial origin. HEK293 cells are an adherent cell line that has been transformed with sheared adenovirus 5 DNA [102]. The HEK293 cell line is one of the most used lines, second to HeLa cells in cell biology studies. Its highly metabolic nature, in addition to its quick and easy reproduction and maintenance make it a popular choice. Due to its popularity, it provides a means for complementary biochemical/cell biological evaluation of expressed proteins to be performed in concert with functional analyses to establish detailed profiles for the action of various compounds.

The HEK293 cells were cultured using Dulbecco's Modified Eagle's Medium (DMEM), supplemented with 1% L-glutamine (an energy source for highly metabolic cells, supports synthesis of proteins and nucleic acids by acting as a nitrogen source), 1% Penicillin/Streptomycin/Fungizone

(antibiotic/anti-fungal), 10% foetal bovine serum (delivers growth factors, nutrients, essential minerals and trace elements, transport and attachment proteins to the cells) and 2.5% 4-(2-hydroxyethyl)-1-piperazineethanesulphonic acid (HEPES) buffer (zwitterionic buffer to maintain physiological pH). The cultures were maintained at 37°C in a humidified incubator supplied with 5% CO_2.

Cells were cultured in 25cm^3 flasks and washed regularly using 0.1M PBS. Cells were grown to 90% confluency prior to treatment. Cells were removed from flasks by agitating flasks to dislodge cells. Cell counting was carried out using the Trypan blue exclusion method. Trypan blue is a vital dye used to determine number of viable cells in a cell suspension. The principle of the method is based on the ability of living cells to exclude the dye, whereas non-viable cells allow the dye to permeate its cell membrane. Therefore light microscopic examination of cells suspended in culture media containing trypan blue can be used to determine, viable cells (unstained) from non-viable cells (appear blue) [103]. Viable cells were counted and cell numbers adjusted according to the assay requirement.

2.3. Preparation of fusaric acid treatment

Fusaric acid, produced by *Gibberella fujikuroi*, was supplied as a white powder (Product no. F6513; Sigma Aldrich, St Louis, Missouri, United States). A stock solution (1mg/ml) was prepared in 0.1M PBS. Cells were treated with a range of concentrations of FA (0-500µg/ml) to obtain a half maximal inhibitory concentration (IC_{50}) following a 24 hour incubation.

2.4. Cell viability

2.4.1. **3-(4, 5-Dimethyl-2-thiazolyl)-2, 5-diphenyl-2H-tetrazolium bromide (MTT) assay**

2.4.1.1. Principle

The MTT assay is a colorimetric assay used to assess cell viability and cytotoxicity. MTT is a water-soluble, yellow tetrazolium salt that is reduced to insoluble purple formazan crystals in the mitochondria of metabolically active cells [104]. Tetrazolium salts accept electrons from oxidised substrates (NADH and NADPH) and suitable enzymes (NAD (P)-dependent oxidoreductases).

MTT is specifically reduced at the site of ubiquinone and Cytochrome b and c of the electron transport chain and is the result of succinate dehydrogenase enzyme activity [105].

An organic solvent, dimethyl sulphoxide (DMSO), is used to solubilize the insoluble formazan product, which can then be measured spectrophotometrically (Figure 2.1). The intensity of the resulting coloured solution is proportional to the cell viability [106]. This calculation was carried out by equating the mean OD for each concentration to the mean OD treatment blank (no FA added) to determine percentage viability.

2.4.1.2. Protocol

For the MTT assay, approximately 10000 cells/well were seeded into a 96-well microtitre plate and allowed to attach overnight. The following day, the cells were incubated with a range of FA concentrations (0-500µg/ml) in triplicate (300µl/well) for 24 hours (37˚C, 5% CO_2). After the incubation period, cells were rinsed twice with 0.1M PBS, followed by the addition of 20µl MTT (5mg/ml in 0.1M PBS) and 100µl complete culture media (120µl/well). The plate was incubated for a further 4 hours (37˚C, 5% CO_2). Thereafter, the supernatant was removed and 100µl DMSO was added to each well and incubated for 1 hour (37˚C, 5% CO_2). The optical density (OD) of the formazan product was measured at 570nm with a reference wavelength of 690nm using a spectrophotometer (Bio-Tek µQuant; Winooski, Vermont, United States) (Appendix A).

The percentage cell viability for each concentration of FA was calculated and used to determine an IC_{50} value by plotting a concentration response curve using GraphPad Prism V5.0 statistical software (GraphPad Software Inc., San Diego, California, United States). The experimental cells in all subsequent assays were treated using the IC_{50} concentration.

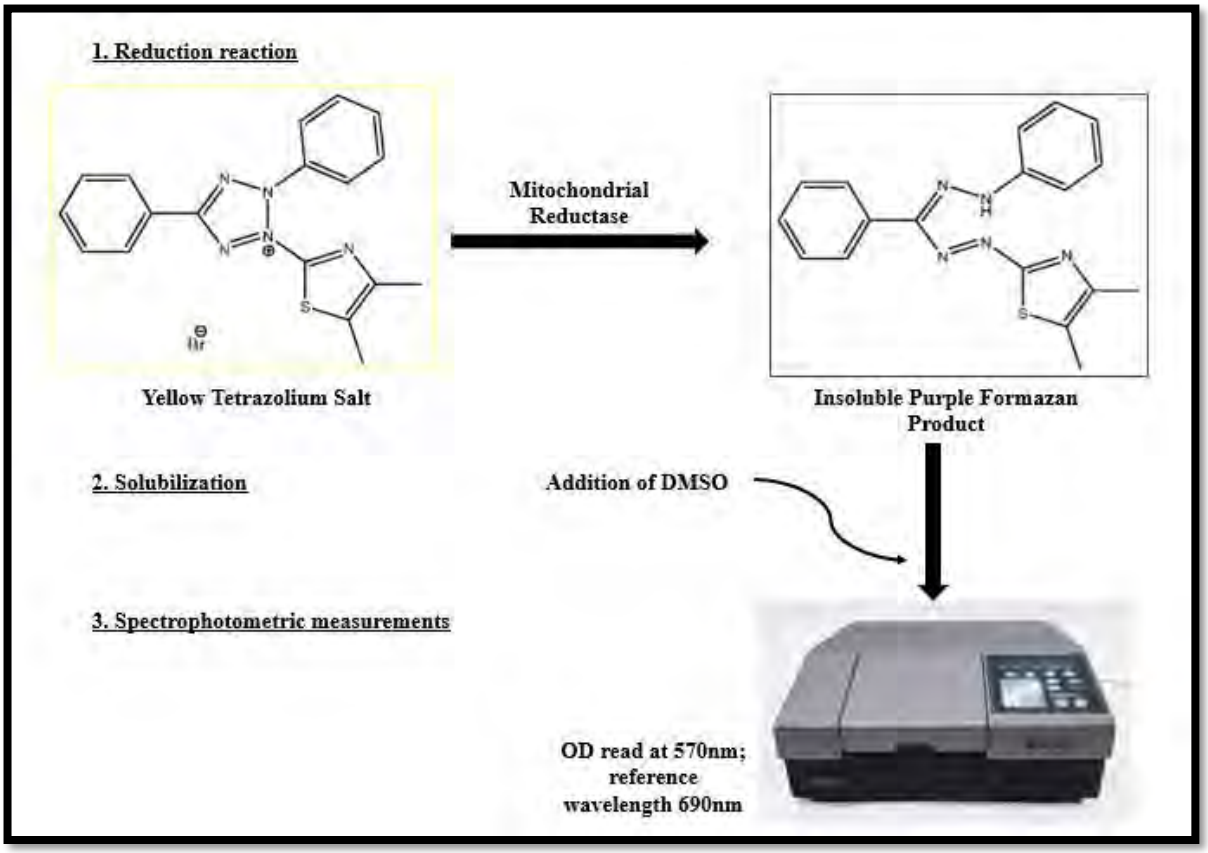

Figure 2.1: The process of MTT salt reduction and subsequent quantification steps (Adapted from Barahuie et al.,(2014)[107]).

2.4.2. **ATP quantification assay**

2.4.2.1. Principle

Luminometry is an analytical technique used to measure chemiluminescent and bioluminescent reactions. Chemiluminescence occurs when an exothermic chemical reaction releases energy to generate electromagnetic radiation in the visible light spectrum. Bioluminescence is a type of chemiluminescence which is based on the production and emission of light by living organisms. Fireflies exhibit bioluminescence and possess the biomolecule luciferase, which is exploited for scientific purposes. The light-producing reaction is catalysed by luciferase, using ATP, Mg^{2+} and oxygen as cofactors in the presence of its substrate, luciferin. The mono-oxygenation of luciferin produces oxyluciferin in an unstable electron excited state. Excited oxyluciferin releases its energy in the form of photons of light producing a glow. When all energy has been released, it returns to a

ground state and becomes inactive [108]. The principle of the CellTitre Glo™assay is based on the use of ATP as a cofactor in the reaction. Therefore, the intensity of the light emitted is proportional to the intracellular ATP concentration (Figure 2.2).

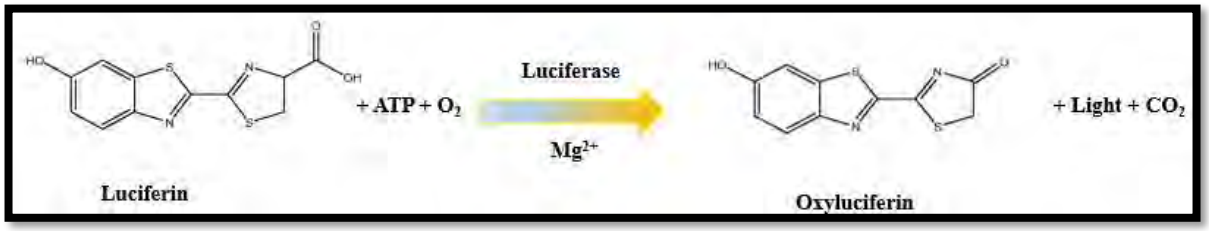

Figure 2.2: Luciferase catalyses ATP-dependent oxidation of D-luciferin to produce light (Adapted from Held, (2006)[109]).

2.4.2.2. Protocol

To determine ATP concentrations, the CellTitre Glo™ assay (Promega; Madison, Wisconsin, United States) was carried out as per manufacturer's guideline. Cells (20000 cells in 50µl PBS/well) were aliquoted in an opaque 96-well microtitre plate to which the ATP CellTitre Glo™ reagent (50µl) was added and allowed to react in the dark (30 minutes, room temperature). Following incubation, the luminescent signal produced was detected with a Modulus™ microplate luminometer (Turner Biosystems; Sunnyvale, California, United States). Results were expressed as mean relative light units (RLU).

2.5. Oxidative status

2.5.1. Glutathione assay

2.5.1.1. Principle

Reduced glutathione (GSH) is considered one of the most abundant endogenous antioxidants. GSH acts as a free radical scavenger by donating an electron to free radicals, thereby detoxifying ROS. This results in two electron donating GSH molecules forming oxidised GSSG. ROS has the capacity to deplete GSH stores by oxidation or reactivity with the thiol group [77]. Additionally, exacerbated production of ROS by toxigenic agents can cause increased demand for GSH, which exceeds GSH

replenishing mechanisms that can further reduce GSH availability. GSH is tightly regulated by a number of enzymes governing its production and functioning. Glutathione-S-transferase and GPx are enzymes that use GSH to catalyse detoxification reactions of electrophilic compounds. GSH is recycled by the action of glutathione reductase (GR) using NADPH as a reducing equivalent [77]. Glucose-6-phosphate dehydrogenase (G6PD) maintains the level of NADPH, which maintains the level of GSH in cells (Figure.2.3).

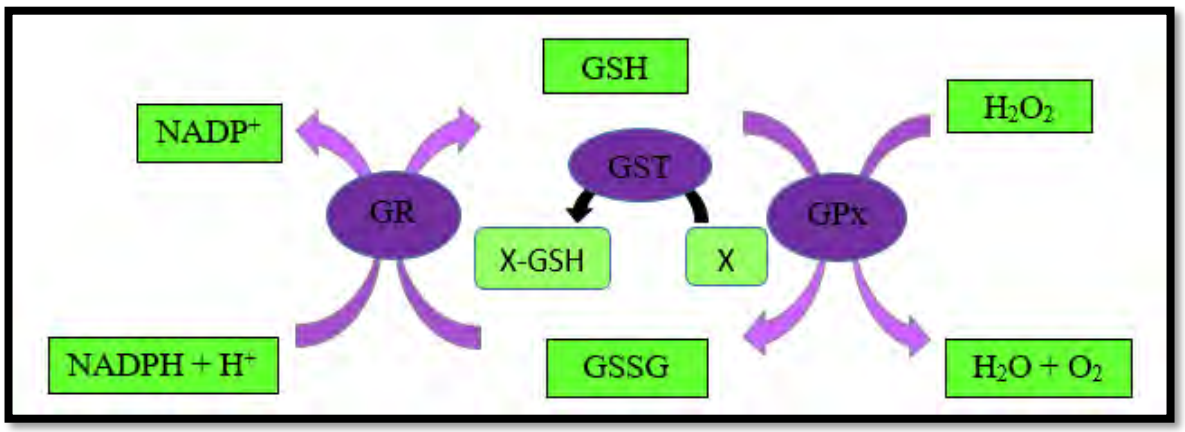

Figure 2.3: The glutathione network of detoxifying enzymes (Adapted from Weydert et al., (2010) [110].

Therefore, a change in GSH levels is important in determining toxicological responses in cells and is often used an indicator of oxidative stress. The GSH-Glo™ Assay was used to quantify intracellular GSH levels in the cell. This assay is based on the conversion of the luciferin derivative in the presence of GSH, which is catalysed by a GST enzyme. The luciferin formed is detected in a coupled reaction utilizing the Ultra-Glo™ Recombinant Luciferase. The resulting luminescence is proportional to the amount of GSH present in the cell.

2.5.1.2. Protocol

The Glutathione-GloTMAssay (Promega, Madison, Wisconsin, United States) was carried out as outlined in the manufacturer's guidelines in order to quantify cellular GSH content. After removing cells from treatment, the cells were counted (20000 cells in 50µl PBS/well) and plated in triplicate in a white 96-well microtitre plate. GSH standards ranging 0-50µM were prepared from a 5mM stock solution, which was serially diluted (two fold) using de-ionised water. Thereafter GSH

standards were plated in triplicate (50µl/well). The GSH-Glo™ reagent (1µl Luciferin-NT, 1µl Glutathione-S-transferase, 48µl GSH-Glo™ Reaction buffer) was added to all wells (50µl/well) and incubated in the dark for 30 minutes at room temperature. Reconstituted Luciferin Detection Reagent (50µl) was added to each well and incubated for a further 15 minutes at room temperature. Luminescence was measured using a Modulus™microplate luminometer (Turner Biosystems; Sunnyvale, California, United States). A standard curve was constructed using the GSH standards and GSH concentration in the samples were extrapolated and reported as µM concentrations (Appendix B).

2.5.2. Lipid peroxidation –MDA quantification

2.5.2.1. Principle

Reactive oxygen species have a relatively short half-life, making direct quantification difficult. A common method employed to quantify redox status is the measurement of oxidised macromolecules, which can be used to indirectly quantify ROS. Lipid peroxides, by-products of lipid interaction with ROS, are often used as biomarkers of oxidative stress [111].

Lipid peroxidation occurs when unsaturated fats are oxidised by ROS which give rise to additional free radicals as well as other toxic byproducts in a chain reaction mechanism. Polyunsaturated fatty acids (PUFA) are most prone to oxidative damage due to the presence of double bonds between adjacent carbon atoms, which have the ability to react and form lipid peroxides [111].

The chain reaction mechanism of lipid peroxidation is initiated by oxidizing free radicals abstracting hydrogen (H^+) atoms from methylene groups in the PUFA. This results in the formation of unstable fatty acid radicals which react with molecular oxygen and form peroxyl radicals. These peroxyl radical intermediates are also unstable and react with adjacent lipid molecules abstracting a H^+ atom and forming another fatty acid radical and hydroperoxide, thus creating a chain reaction (Figure 2.4) [111]. The hydroperoxides are further reduced to form reactive aldehydes such as MDA, 4-hydroxynonenal (4-HNE) and isoprostanes by-products. This process is terminated when 2 radicals react forming non-radicals or with the addition of antioxidants which act as hydrogen donors. MDA levels are routinely measured as a biomarker of oxidative stress [112].

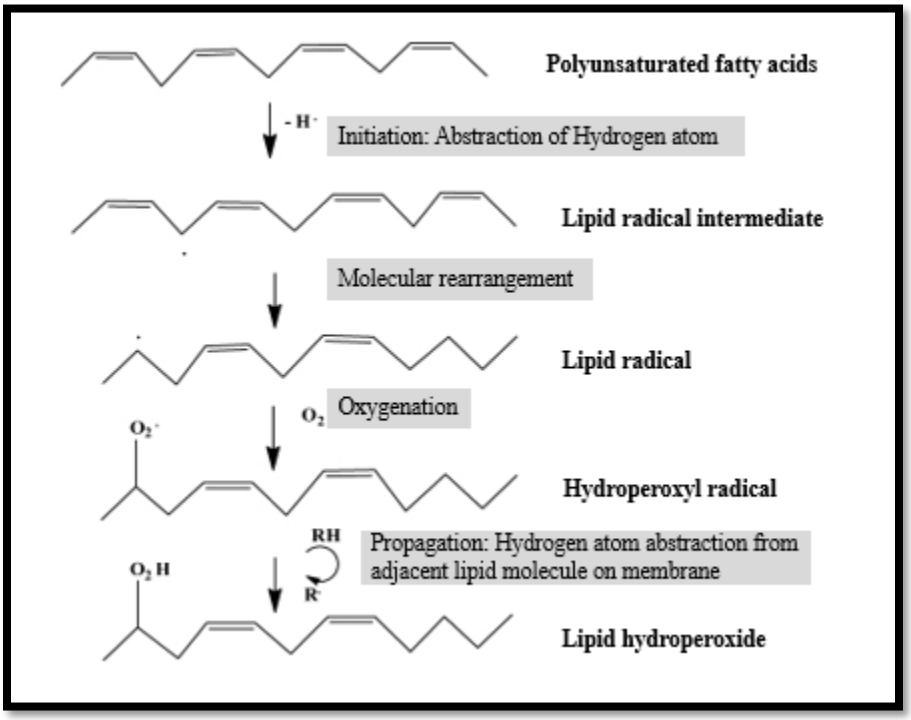

Figure 2.4: The mechanism of lipid peroxidation (Adapted from Basu,(2007) [113]).

Malondialdehyde levels were measured using the thiobarbituric acid reactive substances (TBARS) assay. The TBARS assay is a colorimetric assay that is based on the quantification of the MDA-thiobarbituric acid (TBA) adduct. This adduct is formed by MDA reacting with TBA molecules in a 1:2 ratio under acidic conditions at a high temperature (100°C). The resulting chromophoric complex absorbs maximally at 532nm, and therefore can be measured using a spectrophotometer (Figure 2.5) [114].

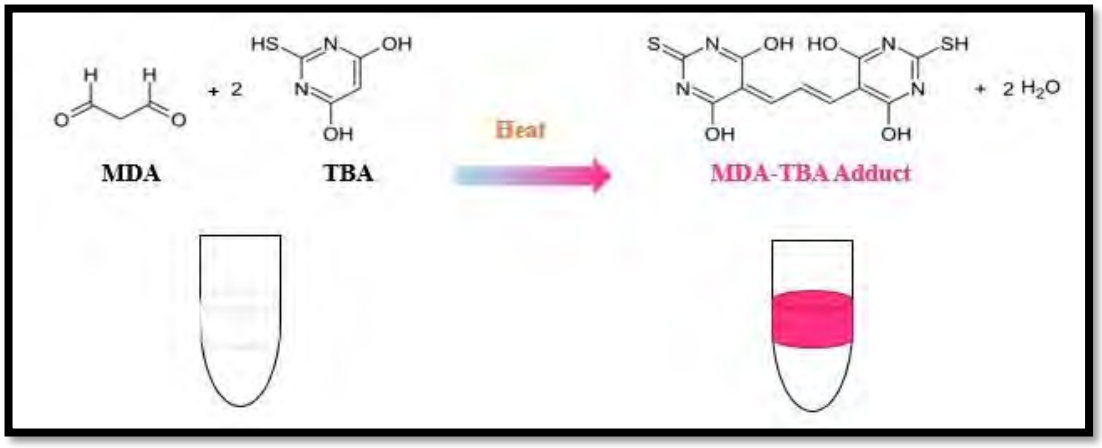

Figure 2.5: The reactivity of MDA with TBA producing a pink coloured product (Adapted from Janero,(1980) [114]).

2.5.2.2. Protocol

The thiobarbituric reactive substances (TBARS) assay was used to measure extracellular MDA levels. The TBARS assay was conducted as per the method described by Abdul *et al*., (2016) [15]. Extracellular MDA was quantified using the supernatant from the FA-treated cells and the untreated control. In addition to the treatment samples, a blank (3mM HCl) and positive control (1µl MDA), both containing no cells were also prepared (Appendix D). The sample blank was included to account for any background interference that may affect the sample measurement. The positive control contained MDA, as it is known to produce an effect, to which experimental treatments can be compared and in doing so also assesses the reactivity of the reagents.

Briefly each of the following was added to clean glass test tubes in addition to 400µl of supernatant: 200µl 2% phosphoric acid (H_3PO_4), 200µl 7% H_3PO_4, 400µl TBA/ butylated hydroxytoluene (BHT) and 200µl 1M HCl. The blank contained all the above mentioned reagents except the TBA/BHT indicator.

All test tubes were then vortexed and placed in a water bath pre-set at 100°C for 15 minutes. Samples were allowed to cool and 1.5ml butanol was added to each test tube, vortexed for 10 seconds and left to separate into two distinct phases. Thereafter 100µl of the upper butanol phase

was transferred to a 96-well microtitre plate in triplicate. The OD was measured using a spectrophotometer (Bio-Tek μQuant; Winooski, Vermont, United States) at 532nm/ reference 600nm. Concentrations of MDA (μM) were determined by calculating the mean OD of replicates per treatment and subtracting the mean blank OD from each. This value was then divided by the extinction coefficient ($156mM^{-1}$) and results were expressed as μM concentrations.

2.6. DNA damage - comet assay

2.6.1. Principle

The Comet Assay, also known as Single Cell Gel Electrophoresis, is a simple technique used to quantify and analyse DNA strand breaks at the level of the individual cell. This method was first described by Östling and Johanson (1984) [115], and was later modified by Singh *et al.,* (1988) [116]. These modifications involved treatment of cells embedded in agarose on a microscope slide, with a hypertonic lysis solution and non-ionic detergent under alkaline conditions. The comet assay is based upon the movement of nuclear DNA through an agarose gel when an electric current is applied. The theory is that undamaged DNA exists in the nucleus in a highly organised form in association with matrix proteins, referred to as DNA supercoils. However, when DNA is damaged the integrity of this level of organization is disrupted [117].

During electrophoresis, the strands of damaged DNA unwind and are drawn out of the nucleus into the agarose suspension. This occurs due to the attraction of the DNA, which carries a negative charge conferred by its phosphate backbone, towards the positively charged anode. The DNA that has maintained its structural integrity does not migrate, and remains within the nucleus [117]. Conversely, damaged DNA migrates out of the nucleus, resulting in the formation of a DNA tail. Collectively, the DNA tail and the undamaged DNA resemble a comet [117]. The longer and brighter comet tails are indicative of more extensive DNA damage.

2.6.2. Protocol

The assay was carried out as per the method used by Raghubeer *et al*., (2014) [118]. Following treatment of cells in a 6-well cell culture plate, cells were washed twice with 0.1M PBS. Thereafter the plate was agitated to dislodge and remove cells, which were subsequently counted. The cells in suspension were adjusted to 10000 cells per 25µl 0.1M PBS. Three slides for each treatment (FA and untreated control) was prepared. Low melting point agarose (LMPA) was used to make the gels. The 3 layer gel was formed on a frosted microscope slide and comprised of: the first layer - 700µl 2% LMPA, followed by the second layer that contained 0.5µl 5x concentration of gel red dye, 25µl cell suspension and 175µl 1% LMPA and finally a third layer of 200µl 1% LMPA. For each gel layer, coverslips were added and slides were incubated at 4°C for 10 minutes, followed by the removal of the coverslip and addition of the next gel layer. After the third layer solidified, coverslips were removed and slides were submerged in cold cell lysis buffer [2.5M sodium chloride (NaCl), 10mM Tris (pH 10), 100mM ethylenediaminetetraacetic acid (EDTA), 1% Triton X-100 and 10% DMSO] and incubated in the dark for 1 hour at 4°C.

The slides were transferred to an electrophoresis tank filled with electrophoresis buffer [300mM sodium hydroxide (NaOH), 1mM disodium ethylenediaminetetraacetic acid (Na_2EDTA) (pH 13) and allowed to equilibrate for 20 minutes. The tank was then sealed and a constant voltage of 25V was applied for 35 minutes at room temperature, using the Bio-Rad Compact power supply. After electrophoresis was complete, slides were washed thrice with neutralization buffer [0.4M Tris (pH 7.4)] for 5 minutes each. Slides were viewed using an Olympus IX5I inverted fluorescent microscope (510–560nm excitation, 590nm emission filters) (Figure.2.6). Images of approximately 50 comets were taken per treatment (3 replicates) and the comet tail lengths were measured using the analySIS Image Processing Software (Novell; Provo, Utah, United States) and expressed in µm.

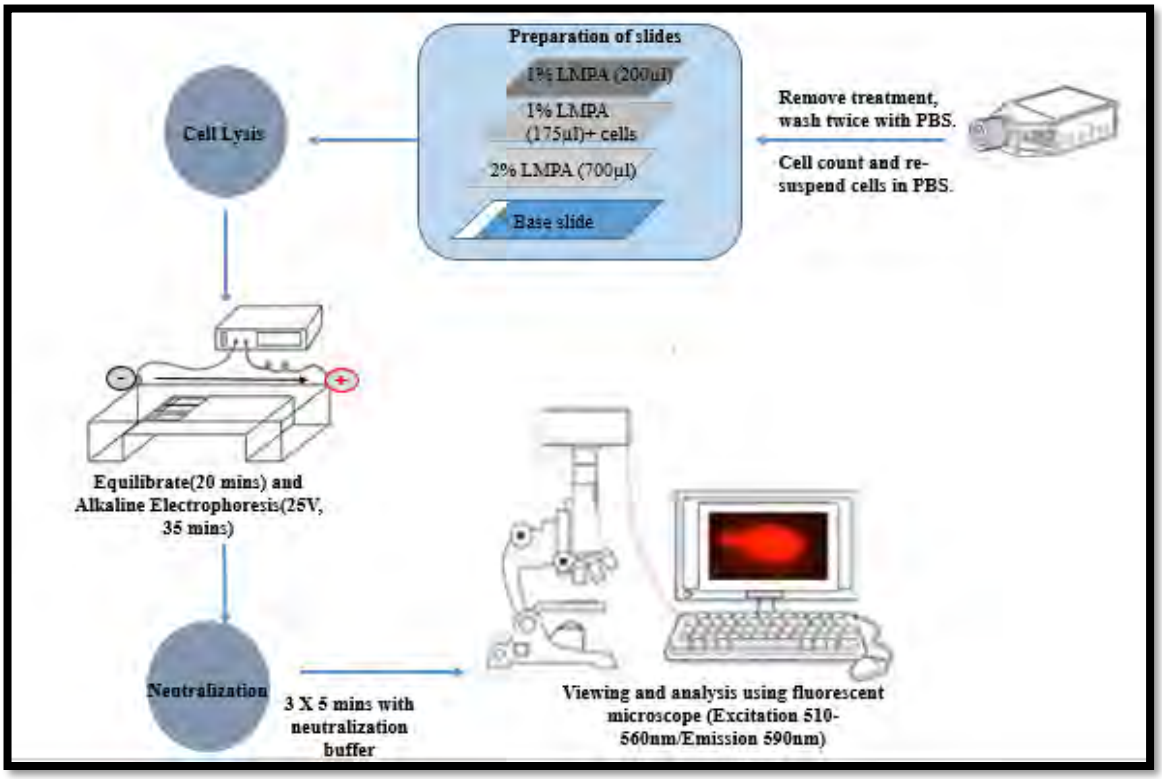

Figure 2.3: The process used in the comet assay.

2.7. Quantitative-polymerase chain reaction

2.7.1. Principle

PCR is a technique used in molecular biology to exponentially amplify a small segment of DNA or RNA. This technique was developed by an American biochemist, Kary Mullis in 1984. PCR simulates the process of DNA replication within the cell whereby a DNA polymerase synthesises a new strand of DNA complementary to the starting template strand [119]. The components required for PCR include: DNA template, DNA polymerase, nucleotides, forward and reverse primers and a buffer system containing Mg^{2+} ions. The primers bind the 3' ends of each DNA template thereby flanking the target region. Thereafter the thermostable DNA polymerase (*Thermus aquaticus* (*Taq*) polymerase) incorporates the deoxynucleotide triphosphates (dNTPs), the building blocks of the new DNA strand, in a stepwise manner to the 3' ends the primers [120]. There are 3 distinct steps in each PCR cycle:

1. Denaturation involves separation of the 2 strands of the target DNA. This step takes place at 90°C, which allows for breakage of weak hydrogen bonds that exist between nucleotides and enables the target sequence to be made accessible.
2. Annealing occurs at a lowered reaction temperature of 50-60°C, which is optimal for the binding of the primers to complementary sites flanking the target region.
3. Extension takes place at an increased reaction temperature of 72°C, which is the optimal temperature for *Taq* Polymerase activity. During this phase of the reaction, the new DNA strand is synthesised by the addition of dNTPS to the 3' end of the primers catalysed by the DNA polymerase.

This process is repeated for 30 to 40 cycles, resulting in an exponential amplification of the template DNA (Figure 2.7).

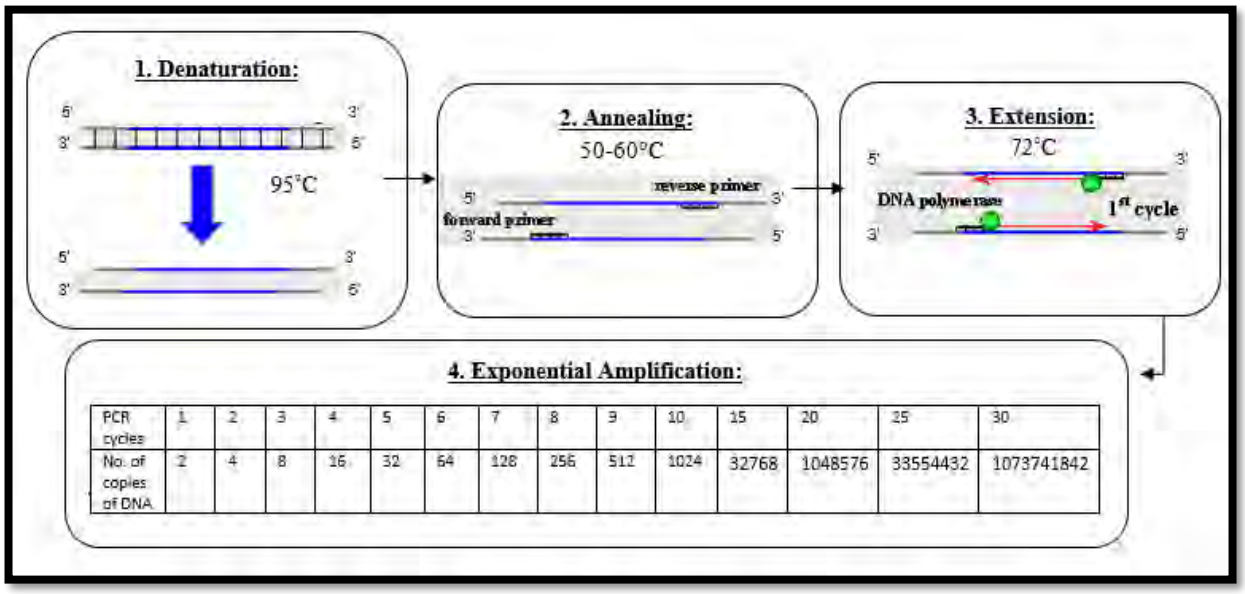

PCR cycles	1	2	3	4	5	6	7	8	9	10	15	20	25	30
No. of copies of DNA	2	4	8	16	32	64	128	256	512	1024	32768	1048576	33554432	1073741842

Figure 2.4: The stepwise procedure used to amplify a gene of interest using PCR (prepared by author).

Conventional PCR is a reliable method for amplifying DNA, and is able to measure the amount of accumulated PCR product at the end of the cycles. One major drawback of conventional PCR is that

it is not able to efficiently and accurately quantify the starting amount of DNA. Real-time PCR, also known as qPCR enables quantification of PCR products as it occurs [121]. Data collection occurs during the exponential growth (log) phase of PCR, when the quantity of the PCR product is directly proportional to the amount of template DNA. The process of qPCR begins with the isolation of RNA from cells, which are subsequently reverse transcribed to single-stranded (ss) complementary DNA (cDNA). Complementary DNA is used as the starting material for qPCR [120].

Quantitative PCR does not differ much from conventional PCR, except for the addition of a fluorescent dye called SYBR green to the reaction mix. SYBR green binds to the minor groove of the double-stranded (ds) DNA amplicons. The unbound dye exhibits very little fluorescence, however, fluorescence is greatly enhanced upon DNA-binding [122]. Progression of PCR allows for product accumulation. The SYBR green binds to all the dsDNA present, therefore the resulting increase in fluorescence is proportional to the amount of PCR product produced which is systematically relayed at the end of each cycle. A curve is plotted with fluorescent emission over time from which the initial amount of DNA present in the sample is obtained. Expression of a house-keeping gene was simultaneously quantified to normalize target gene expression.

2.7.2. Protocol

2.7.2.1. RNA isolation

Following the incubation of the cells with the relevant treatment, cells were washed twice with 0.1M PBS. The total RNA was isolated using an in-house protocol described by Chuturgoon *et al*., (2014) [123]. Briefly, 500µl PBS and 500µl Triazol was added to the flask and incubated at room temperature for 5 minutes. Thereafter the flasks were scraped and the contents were transferred to 1.8ml micro-centrifuge tubes and stored at -80ºC overnight.

Thereafter, 100µl chloroform was added to the thawed samples and mixed vigorously for 15 seconds. The samples were incubated at room temperature for 3 minutes. The micro-centrifuge tubes were then centrifuged (12000 x g, 4˚C for 15 minutes), and the upper aqueous layer was

transferred to a new 1.8ml micro-centrifuge tube, which was placed on ice. Subsequently, 250µl isopropanol was added to each sample and incubated on ice for 2 hours before being returned to -80ºC overnight.

Samples were thawed again and centrifuged (12000 x g, 4ºC for 20 minutes). The resulting pellet contained the total RNA and was washed with 500µl cold 75% ethanol. Samples were then centrifuged again (7400 x g, 4ºC for 15 minutes). All ethanol was discarded and the pellet was left to air-dry, before re-suspending in 15µl RNase-free water. RNA samples were incubated at room temperature (3 minutes) and thoroughly mixed, before being quantified (Figure 2.8).

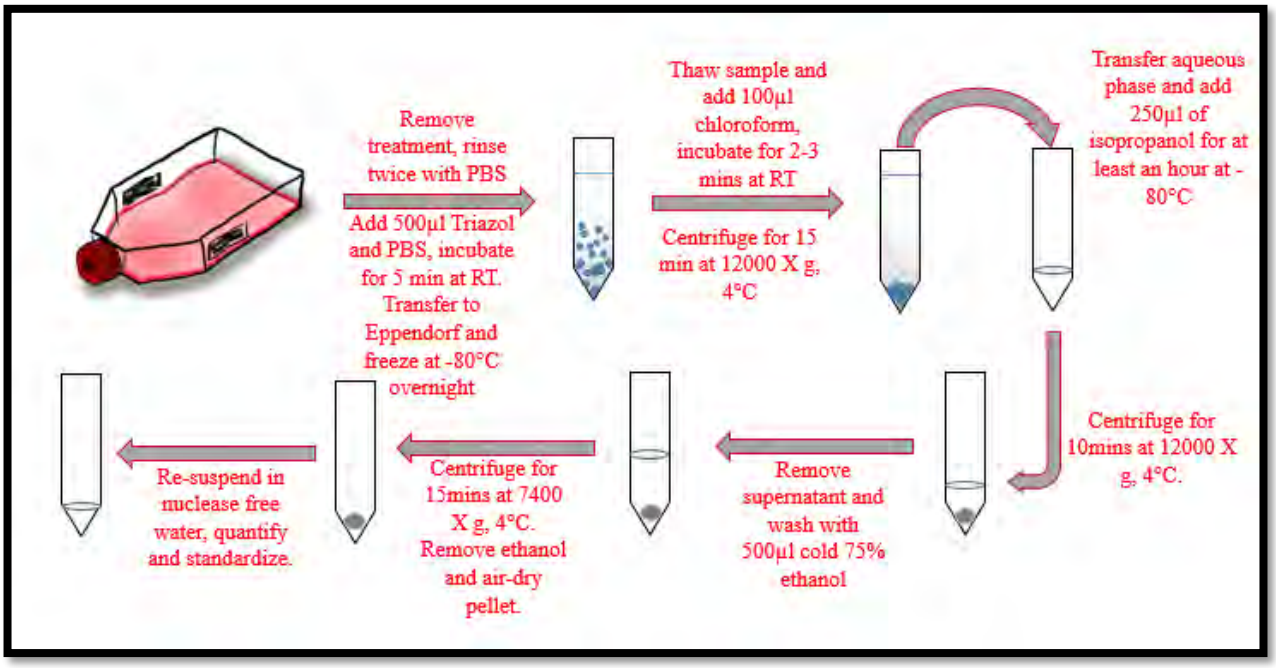

Figure 2.5: The procedure of isolating RNA using the Triazol method (prepared by author).

2.7.2.2. Quantification and standardization

Accurate quantification of nucleic acids remains a critical step prior to performing downstream processes such as qPCR. The use of the Thermo Scientific™ Nanodrop 2000 (Thermo Fisher

Scientific; Johannesburg, South Africa) allowed for the quality and quantity of the isolated RNA to be determined. The absorbance ratio of 260nm/280nm was used to determine purity of samples (~2). RNA samples were standardized to a concentration of 1000ng/µl with RNase-free water and stored at -80°C until required.

2.7.2.3. Complementary DNA synthesis

RNA was reverse transcribed to cDNA as per manufacturers' guidelines using the iScript™ cDNA Synthesis kit (Bio-Rad; 107-8890):- a 20µl reaction volume containing, 1µl iScript™ reverse transcriptase, 4µl 5X iScript™ reaction mix and the RNA template (2000ng) made up in nuclease free water. Thermocycler conditions were set to 25°C for 5 minutes, 42°C for 30 minutes, 85°C for 5 minutes and a final hold at 4°C.

Gene expression was analyzed using the iQ™ SYBR Green Supermix (Bio-Rad; 170-880), according to the manufacturer's instructions. Briefly, 1.5µl cDNA template, 1µl sense primer, 1µl antisense primer, 5x iScript reaction mix and nuclease free water was made up to a reaction volume of 25µl. The genes of interest were *CAT* [forward 5'-TAAGACTGACCAGGGCATC-3'; reverse 5'-CAACCTTGGTGAGATCGAA-3'(58 °C)], *GPx* [forward 5'-GACTACACCCAGATGAACGAGC-3'; reverse 5'-CCCACCAGGAA CTTCTCAAAG-3' (58 °C)] and *OGG1* [forward 5'-GCATCGTACTCTAGCCTCCAC-3'; reverse 5' -AGGACTTTGCTCCCTCCAC-3' (60°C)]. All primers were obtained from Inqaba Biotechnologies (Pretoria, South Africa).

All qPCR experiments were conducted using the CFX Touch™ Real Time PCR Detection System (Bio-Rad; Hercules, California, United States). The assay was run with three replicates per treatment. 18s [forward 5'- ACAGGGACAGGATTGACAGA -3'; reverse 5'-CAAATC GCTCCACCAACCTAA -3'] was used as a housekeeping gene and was amplified simultaneously under the same conditions as the treatment samples. The reaction was subjected to an initial denaturation (95°C, 4 minutes), followed by 37 denaturation cycles (95°C, 15 seconds), an annealing phase (specific to each primer, 40 seconds), and an extension phase (72°C, 30 seconds).

The data obtained was analyzed using the method described by Livak and Schmittgen (2001) [124], which is represented as fold-change in mRNA expression ($2^{-\Delta\Delta CT}$) relative to the control.

2.8. Western blotting

2.8.1. Principle

2.8.1.1. Protein preparation

Cells are treated with a lysing reagent to digest cell membranes and facilitate release of proteins into solution. The BCA protein assay is a quantification method that allows for the colorimetric detection of the total protein present in a sample. The principle of this assay is formulated on the basis that in an alkaline medium, a Cu^{2+}protein complex forms which is then followed by a Cu^{2+} to Cu^{1+} reduction reaction, known as the biuret reaction [125]. The Cu^{1+} ion is then detected by a reaction with BCA in a 1:2 ratio to produce a water-soluble purple coloured product which absorbs maximally at 562nm (Figure 2.9). The intensity of the colour produced is proportional to the protein concentration within the sample [126].

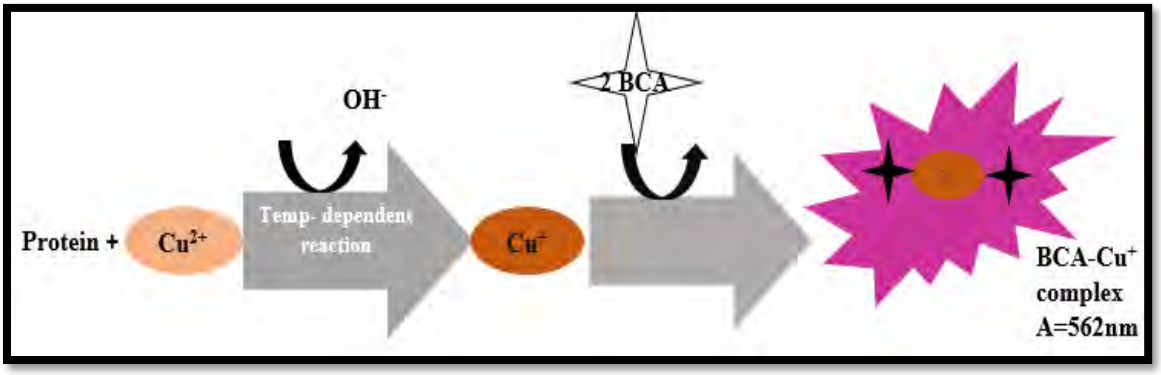

Figure 2.6: The principle of the BCA protein quantification assay (prepared by author).

2.8.1.2. SDS-PAGE and transfer

Sodium dodecyl sulphate - polyacrylamide gel electrophoresis (SDS-PAGE) is a technique that is often utilised to facilitate separation of proteins. Polyacrylamide gels are a crosslinked polymer network composed of monomers of acrylamide and bisacrylamide ("bis," N, N'-methylene

bisacrylamide). The polymerisation reaction requires the addition of the polymerising agent, ammonium persulfate (APS). TEMED (N, N, N, N'-tetramethylethylenediamine) catalyses the polymerisation reaction by promoting the production of free radicals by APS [127]. Polyacrylamide gels are inert in nature and therefore will not interfere with the proteins during migration. Sodium dodecyl sulphate is an anionic detergent that binds to positive charges in the protein, thereby conferring a uniform negative charge. Additionally, SDS aids denaturation of proteins (unfolding) by breaking hydrogen bonds within and between molecules. Removal of intrinsic protein charges and linearizing of proteins allows for separation in SDS-PAGE to be based on molecular weight (Figure. 2.10).

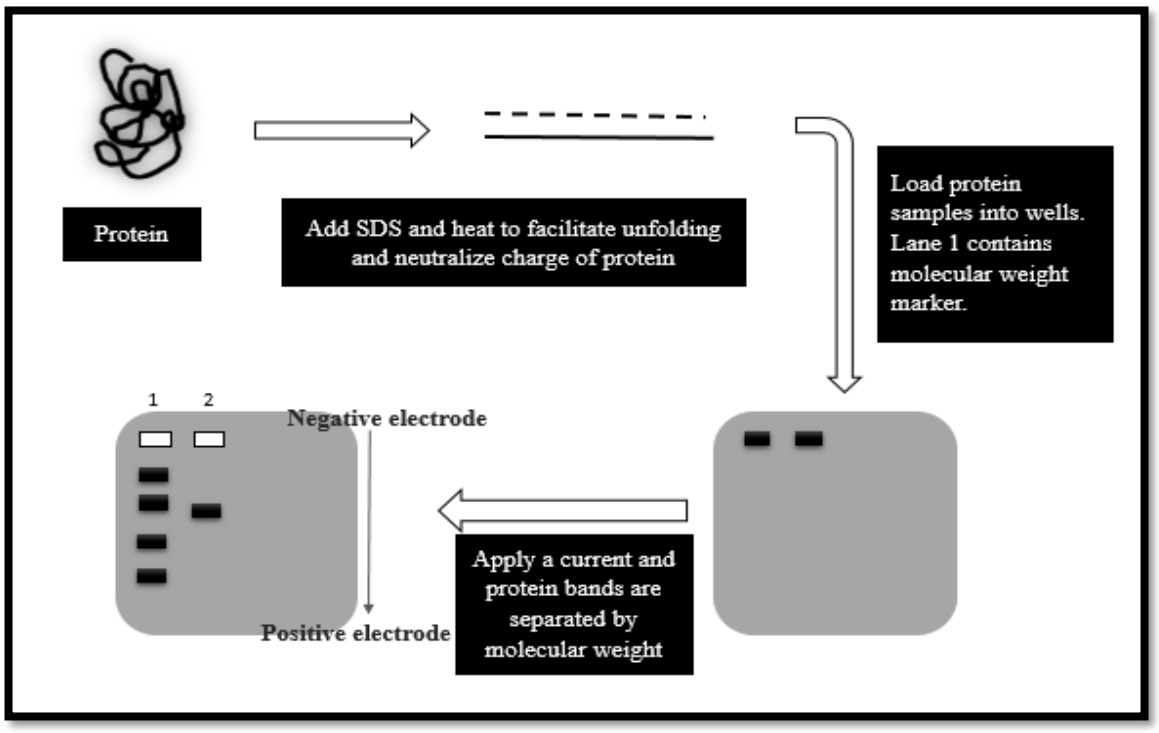

Figure 2.7: An Overview of the protein preparation and SDS-PAGE process (prepared by author).

Following protein standardisation, samples are prepared with sample buffer (Laemmli buffer). The constituents of the buffer include: SDS, bromophenol blue- a tracker dye to visualise the dye front, β-mercaptoethanol- strong reducing agent that cleaves intra -and inter- disulphide bonds to allow unfolding of tertiary protein structures, and glycerol – increase density of the sample and facilitate

migration. Thereafter samples are loaded on SDS-PAGE gels which are subjected to electrophoresis [128]. These gels consist of a stacking and separating (resolving) layer. The stacking gel has a high porosity to enable the stacking of protein at the interface of the 2 gel layers. This allows proteins to begin migrating through the separating gel from the same place. The resolving gel has a lower porosity which has a sieving action and therefore protein samples are separated according to molecular weight (Figure. 2.11). The lower the molecular weight of the protein, the faster it will migrate through the gel matrix [127].

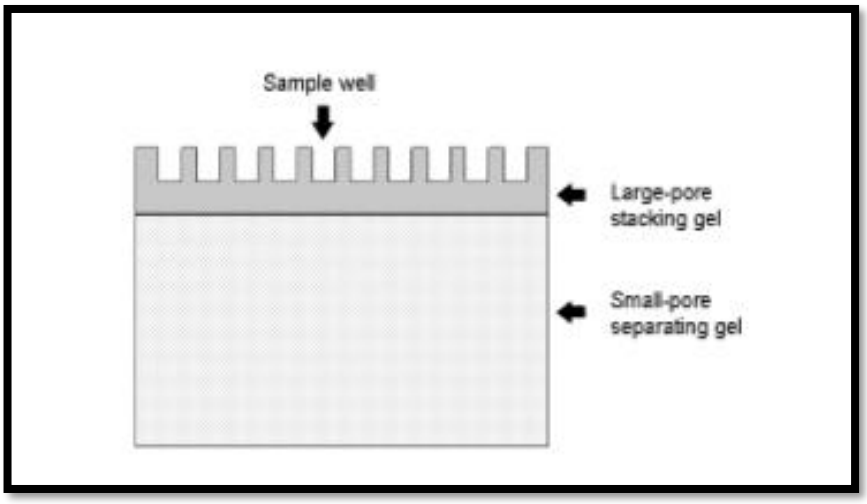

Figure 2.8: An example of an SDS- polyacrylamide gel (prepared by author).

Once electrophoresis is completed, the gel containing protein bands is electro-transferred onto a nitrocellulose membrane. This process involved the sandwiching of the gel and nitrocellulose membrane between fibre pads. Protein transfer from the gel to the membrane is achieved by applying a high intensity electric field produced by electrode plates at a right angle to the sandwich (Figure. 2.12) [128].

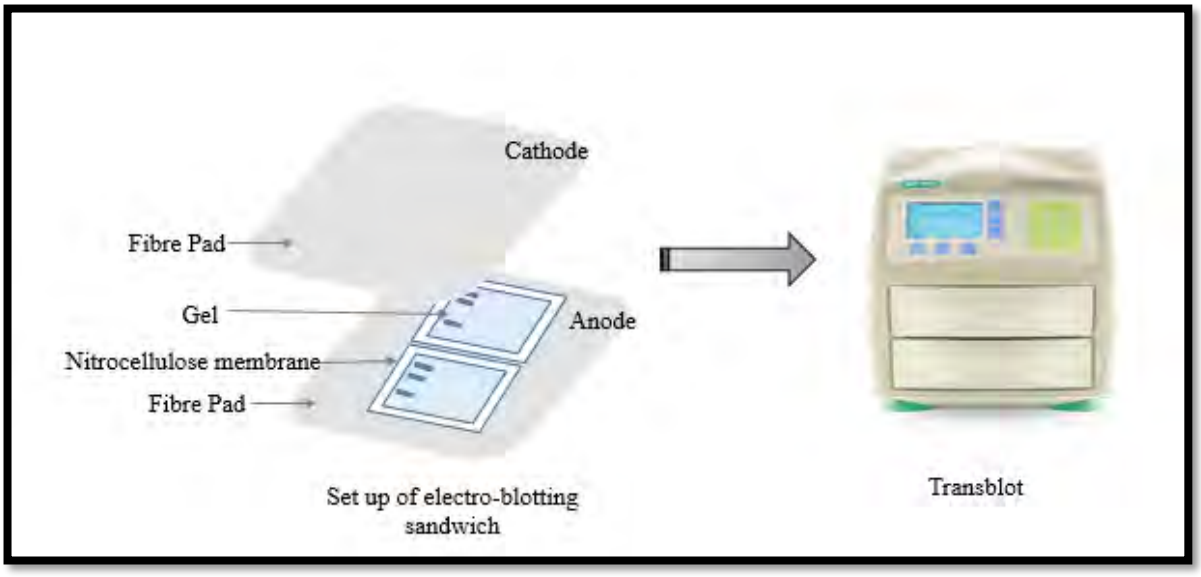

Figure 2.9: The setup of the apparatus for the electro-transfer process (prepared by author).

2.8.1.3. Immunoblotting

The immunoblotting technique exploits the interaction between an antibody and antigen to enable detection of a protein of interest in a mixture of other proteins. Prior to exposure to antibodies, the membranes are first blocked to prevent non-specific binding of the antibody to the hydrophobic binding sites with a protein solution [128]. Membranes are incubated with primary antibody that has been specifically raised against the protein of interest. The secondary antibody is conjugated to a detection enzyme, which binds to the primary antibody that has reacted with target proteins [128]. The detection process involves a substrate reacting with the enzyme that is bound to the secondary antibody leading to the generation of a chemiluminescent signal that can be measured (Figure 2.13). One of the most extensively utilised enzyme detection tags is horseradish peroxidase (HRP), which is used in enhanced chemiluminescent detection. Horseradish peroxidase, in the presence of hydrogen peroxide, oxidises luminol (luminescent substrate) with concomitant generation of light [129]. The use of chemical enhancers results in a 1000-fold increase in the intensity of light, which is detected by a photographic film [130]. The intensity of light produced is proportional to the expression of the protein of interest. Target proteins are evaluated by locating the visible protein band which correlates with the relevant molecular weight on the molecular weight ladder and carrying out densitometric analysis of the respective band.

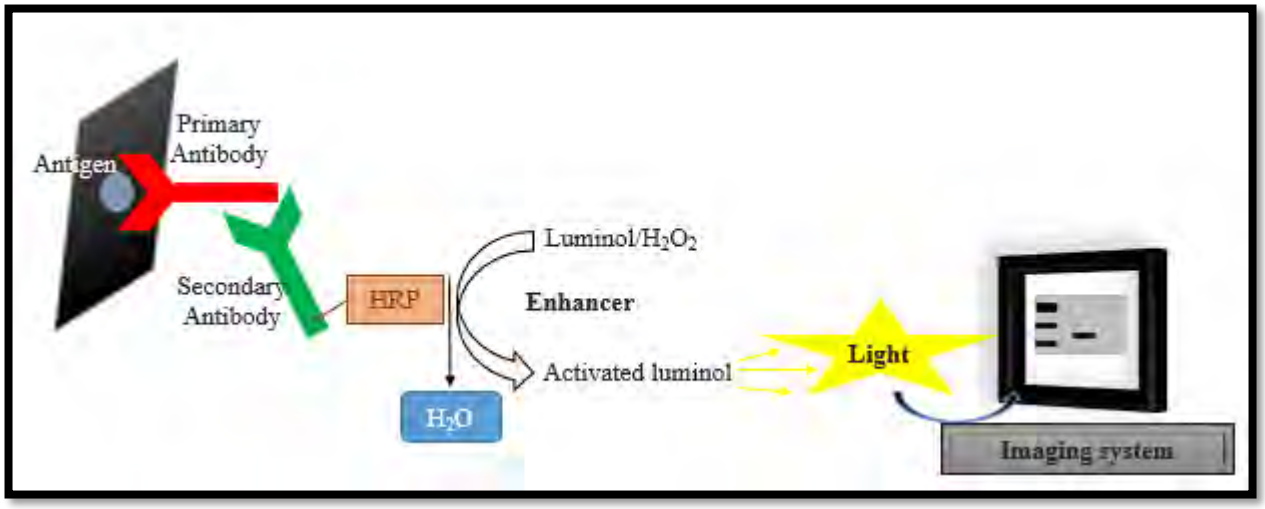

Figure 2.10: An overview of the immunoblotting reactions that allows visualization of protein bands (prepared by author).

2.8.2. Protocol

Protein expression of total Nrf2, phosphorylated Nrf2 (ser40), p53 and Parp1 were evaluated using western blots. Cytobuster™ reagent (Novagen, San Diego, California, United States) supplemented with protease and phosphatase inhibitors (Roche, Mannheim, Germany; 05892791001 and 04906837001) was used for protein isolation. Cytobuster™ (200µl) was added to cell culture flasks following treatment of cells and incubated on ice for 10 minutes. Thereafter flasks were scraped and Cytobuster™ mixture containing lysed cells were transferred to a new 1.8ml micro-centrifuge tube. The cell lysates were centrifuged (10000 x g, 4°C, 10 minutes) to obtain crude protein. All protein samples were quantified using the BCA assay and standardized to 1.5mg/ml (Appendix C). Thereafter, 50µl 5x Laemmli buffer (0.5M Tris-HCl (pH 6.8), glycerol, 10% SDS, β-mercaptoethanol, 1% bromophenol blue) was added to 200µl standardized protein before samples were boiled at 100°C for 5 minutes. The prepared protein was stored at -20°C until required.

Protein samples (25µl) and a molecular weight marker (5µl) (Bio-Rad; Precision Plus Protein Dual Colour Standard) were loaded into the wells of the SDS-PAGE gel (4% stacking, 10% resolving/separating), which was then subjected to electrophoresis (1 hour, 150V) using a Bio-Rad compact power supply. Prior to electrotransfer, membranes, gels and fibre pads were soaked for 10

minutes in transfer buffer (25mM Tris, 192mM glycine and 20% methanol). The protein transfer sandwich was assembled with the gel placed on the nitrocellulose membrane with a fibre pad on either side (Figure.2.13). Separated proteins on SDS-PAGE gel were then transferred onto nitrocellulose membranes using the Trans-Blot® Turbo Transfer system (Bio-Rad, Hercules, California, United States; 170-4155) (30 minutes, 400mA).

The membranes were blocked with 3% bovine serum albumin (BSA) in Tween 20-Tris buffered saline (TTBS; 25mM Tris (pH 7.5), KCl, 150mM NaCl, 0.05% Tween 20) for 2 hours at room temperature on a shaker. Membranes were then incubated with primary antibody (anti-Nrf2 (phospho-ser40) (ab76026, rabbit monoclonal); anti-Nrf2 (cs8882, rabbit monoclonal); anti-p53 (sc6243, rabbit polyclonal); anti-parp1 (sc1561, goat polyclonal); 1:1000 dilution in 1% BSA in TTBS (5µl antibody:4995µl 1% BSA)) for 1 hour at room temperature and then overnight at 4°C. The membranes were washed with TTBS (5 x 10 minutes each) before being incubated in HRP-conjugated secondary antibody (goat anti-rabbit IgG HRP (sc2004) and donkey anti-goat IgG HRP (sc2020); 1:10000 dilution in 1% BSA in TTBS (0.5µl antibody: 4999.5µl 1% BSA)) for 1 hour at room temperature. Membranes were washed again with TTBS (5 x 10 minutes each). Thereafter clarity western enhanced chemiluminescence (ECL) substrate (400µl) (Bio-Rad) was added to the membrane and images were captured using the Chemidoc XRS system (Bio-Rad). The Image Lab™ software (Bio-Rad) was used to analyse protein expression.

Membranes were stripped with 5% hydrogen peroxide (30 minutes, 37°C), rinsed twice in TTBS (10 minutes each), incubated in blocking solution (3% BSA in TTBS; room temperature) for 1 hour, and probed with HRP-conjugated housekeeping antibody, β-actin (A3854, 1:5000 dilution in 1% BSA in TTBS, 30 minutes). The relative band intensity was normalized against house-keeping protein, β-Actin. Results were expressed as relative band density (RBD).

2.9. Assessment of cell death parameters

2.9.1. Caspase activity assay

2.9.1.1. Principle

Caspases are a family of intracellular proteases that are responsible for the organised breakdown of a cell into apoptotic bodies during apoptosis. Caspases exist as inactive pro-enzymes that are activated by proteolytic cleavage which leads to execution of cell death [98]. Luminometry was used to assess caspase activity. This assay consisted of a proluminescent caspase-specific luciferin substrate, which is cleaved by caspases. This facilitates luciferin release, which is processed by the luciferase enzyme, generating a luminescent signal that correlates with caspase activity (Figure 2.14).

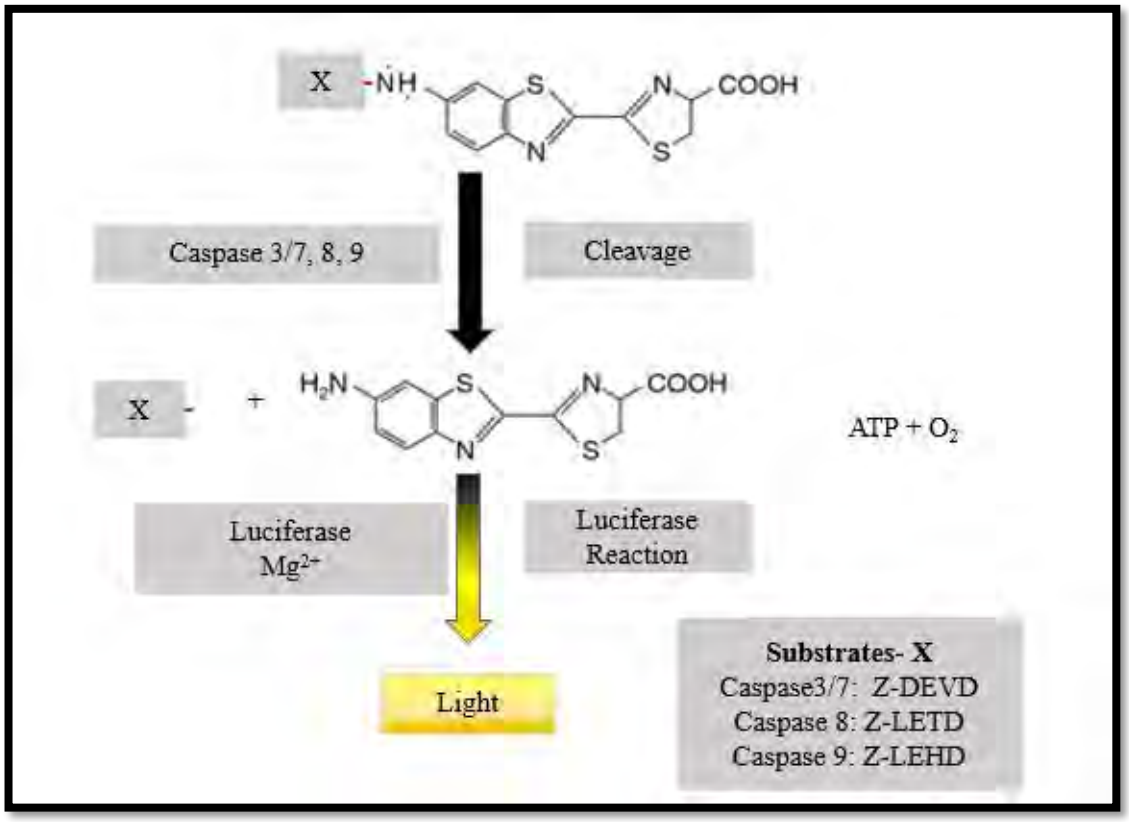

Figure 2.11: The luminometric reaction used to determine caspase activity (prepared by author).

2.9.1.2. Protocol

Caspase-3/-7, -8 and -9 activities were detected with Caspase-Glo® assays (Promega, Madison, Wisconsin, United States). Following treatment of cells, cells were washed twice with 0.1M PBS, counted and adjusted (20000 cells in 50µl 0.1M PBS per well, 3 replicates). As per manufacturer's protocol, Caspase-Glo®-3/-7, -8 and -9 reagents (Peptide-conjugated aminoluciferin were synthesised for each caspase substrate: Z-DEVD-aminoluciferin for caspase 3/7, Z-LETD-aminoluciferin for caspase 8 and Z-LEHD-aminoluciferin for caspase 9) were reconstituted and added to the wells of a white 96-well microtitre plate (20µl caspase reagent per well). The plate was then incubated in the dark for 30 minutes at room temperature. Luminescence was measured using the Modulus™ microplate luminometer (Turner Biosystems; Sunnyvale, California, United States). Caspase-3/-7, -8 and -9 activities were expressed as relative light units (RLU).

2.9.2. **Lactate dehydrogenase cytotoxicity assay**

2.9.2.1. Principle

Necrotic cell death is characterised by swelling of the cell, followed by cell lysis and leakage of intracellular contents. It is the increase in cell membrane permeability in necrotic cells that can be assessed by measuring the extracellular levels of the cytosolic enzyme lactate dehydrogenase (LDH). Measurement of this enzyme in the supernatant of the cells can serve as a measure of cytotoxicity [131]. The principle of this assay is based on the ability of LDH to catalyse the reduction of NAD^+ to NADH by oxidising lactate to pyruvate. In the second step of the reaction, diaphorase reduces a tetrazolium salt (in the presence of NADH) to a coloured formazan product that can be measured with a spectrophotometer (Figure.2.15) [131].

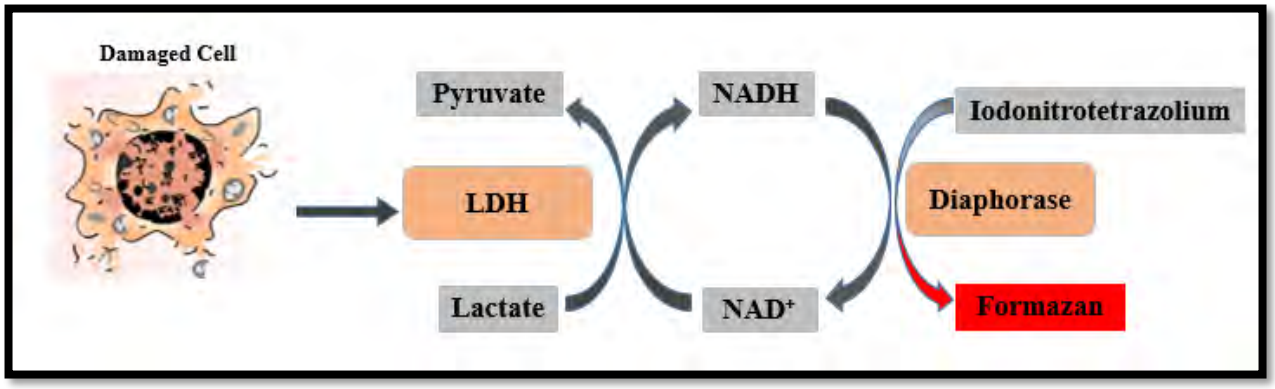

Figure 2.12: The Principle of the Lactate Dehydrogenase Cytotoxicity (adapted from Forest *et al*.,(2015) [132].

2.9.2.2. Protocol

The method used to carry out the LDH cytotoxicity assay was described by Nagiah *et al*.,(2016) [133]. After cells were incubated with the respective treatment for 24 hours, 100µl supernatant was added to each well in triplicate in a 96-well microtiter plate. Thereafter 100µl substrate mix (Roche; Mannheim, Germany), containing the catalyst (diaphorase) and dye solution (sodium lactate/ Iodonitrotetrazolium (INT)), was added to each well. The plate was then incubated at room temperature for 25 minutes in the dark. The OD was measured at 500nm and results were reported as mean OD. The intensity of the coloured product produced is proportional to the amount of the LDH present in the supernatant.

2.10. Statistical analysis

Statistical analysis was performed using the Students' T-test (Nonparametric- Mann-Whitney test) on the GraphPad Prism Version 5.0 Software (GraphPad Software Inc., San Diego, California, United States). All data is expressed as mean ± standard deviation. All experiments were conducted independently with 3 replicates in each test. The level of statistical significance was established at a p value of < 0.05.

Chapter 3

Results

3.1 Cell viability

3.1.1. MTT assay / IC_{50} determination

A dose response curve was determined using a range of FA concentrations (0-500µg/ml) in HEK293 cells over 24 hours (Figure.1). Analysis of the dose-response curve showed that 137.9µg/ml of FA was sufficient to cause 50% reduction in HEK293 cell viability (IC_{50}) (Figure 3.1). This concentration of FA was used in all subsequent assays.

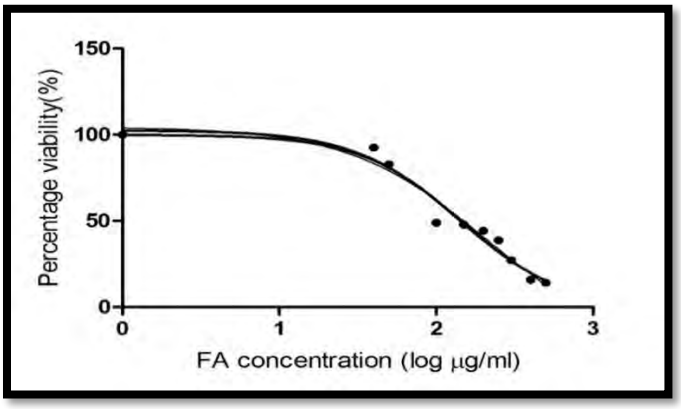

Figure 3.1: A dose-dependent decline in HEK293 cell viability following FA treatment.

3.1.2. ATP assay

Intracellular ATP levels were assessed using the CellTitre Glo™ assay. FA caused a significant reduction ($p = 0.0048$) in ATP levels ($0.74 \pm 0.19 \times 10^6$RLU) compared to the untreated control ($2.96 \pm 0.19 \times 10^6$RLU) (Figure 3.2).

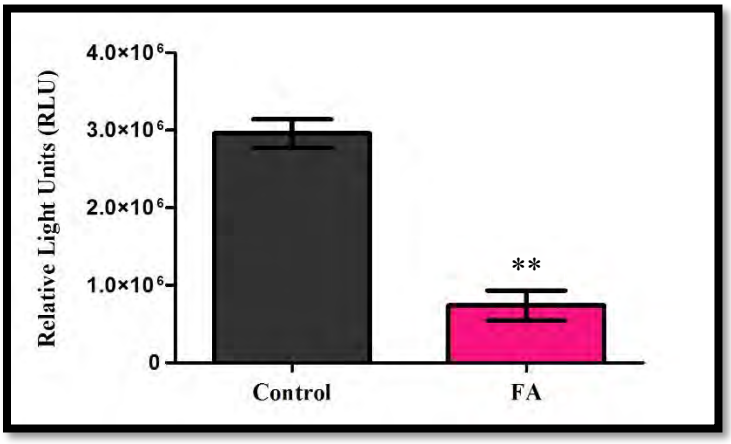

Figure 3.2: Luminometric assessment of ATP levels in HEK293 cells decreased 4-fold after 24 hour exposure to FA (**$p < 0.005$).

3.2. Oxidative status

The GSH-Glo™ Assay was used to assess GSH concentrations, as a marker of intracellular antioxidant capacity. The data illustrated a significant decrease ($p = 0.0136$) in GSH levels in cells treated with FA ($28.33 \pm 3.68\mu M$) relative to the control cells ($51.93 \pm 1.97\mu M$) (Figure.3.3 (A)). Furthermore, levels of MDA, a byproduct of lipid peroxidation, was observed to be higher ($p = 0.0048$) in FA treated cells ($14.07 \pm 0.64 \times 10^{-1}\mu M$) compared to the control cells ($8.98 \pm 0.39 \times 10^{-1}\mu M$) (Figure.3.3 (B)).

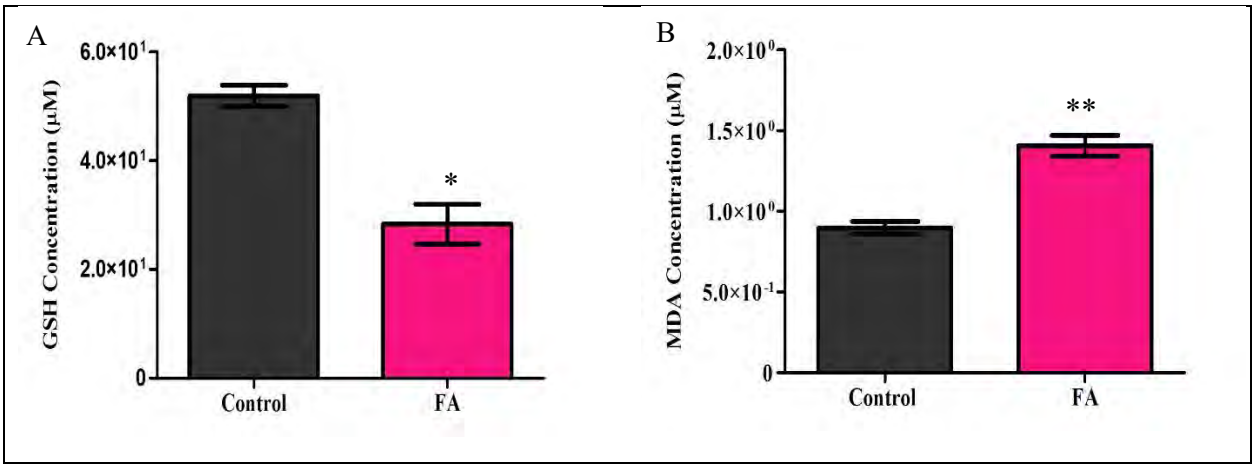

Figure 3.3: Fusaric acid exposure resulted in the induction of oxidative stress as shown by a 1.8-fold decrease in reduced glutathione levels (*$p < 0.05$), with a concomitant 1.5-fold increase in MDA levels (**$p < 0.005$).

3.3. Assessment of DNA damage and repair

3.3.1. **The comet assay**

The genotoxic effects of FA were assessed using the comet assay. Comet tail lengths were measured as an indication of DNA damage. The data showed that FA significantly ($p < 0.0001$) increased DNA damage as noted by the longer comet tail lengths seen in FA treated cells (13.26 ± 1.07µm) compared to the control cells (6.30 ± 1.06µm) (Figure.3.4).

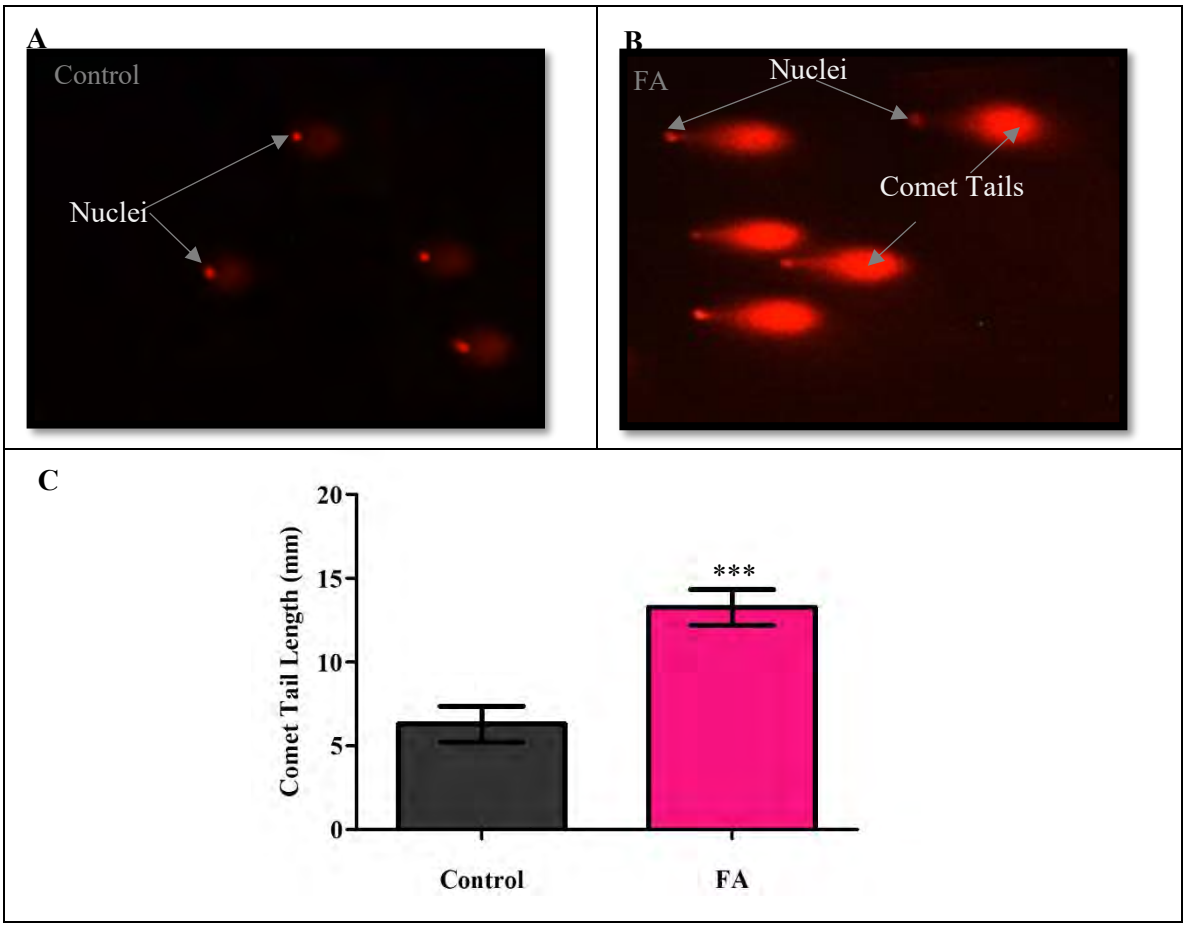

Figure 3.4: FA induced a 2.1-fold increase in DNA comet tail length (C). Comparison of Comet tail length (μm) between FA (B) with the untreated control cells (A) (***$p < 0.0001$) (10x).

3.3.2. **DNA repair**

The effect of FA on DNA damage and the associated base excision repair response was assessed by determining mRNA levels of *OGG1* (qPCR) and protein expression of Parp1 and p53 (western blotting). FA significantly decreased (0.49 ± 0.10; $p = 0.0049$) the mRNA level of *OGG1*, a DNA glycosylase enzyme, in relation to untreated control cells (1.01 ± 0.11) (Figure.3.5 (A)).

Evaluation of Parp1 (FA: 0.15 ± 0.01 vs. control: 0.26 ± 0.03; $p = 0.0079$) (Figure.3.5 (B)) and p53 (FA: 0.05 ± 0.01 vs. control: 0.10 ± 0.02; $p = 0.0136$) (Figure.3.5 (C)) by densitometric analysis

showed reduced expression of these proteins in cells that were exposed to FA compared to untreated cells.

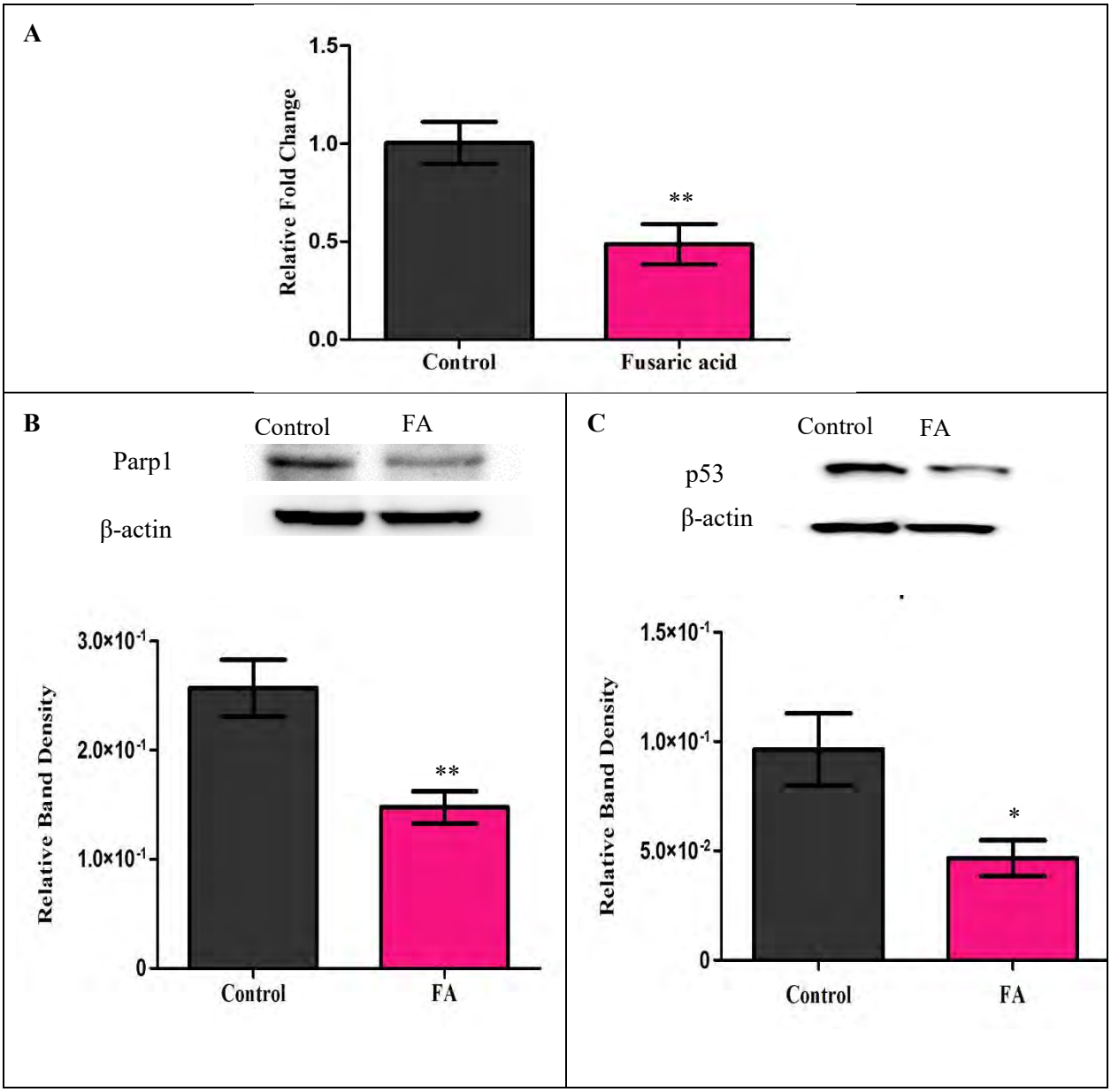

Figure 3.5: FA diminishes DNA repair responses resulting from oxidative damage. (A) The fold change analysis of *OGG1* mRNA expression indicated a 2-fold decrease post FA exposure relative to control cells ($p < 0.005$). Western blot images and protein expression of DNA repair proteins, Parp1 (B) and p53 (C) in HEK293 cells reported as relative band density following exposure to FA (**$p < 0.005$; *$p < 0.05$).

3.4. The antioxidant response

The protein expression of Nrf2, a key regulator of the antioxidant response, and phosphorylated Nrf2 was evaluated using western blotting. The expression of the total Nrf2 protein was significantly decreased ($p = 0.0117$) (2-fold) by FA compared to the untreated control (FA: 0.65 ± 0.21 vs control: 1.31 ± 0.28) (Figure3.6 (A)). Conversely, FA induced a 1.8-fold increase in phosphorylation of Nrf2 relative to the control (FA: 1.41 ± 0.27 vs. control: 0.93 ± 0.09; $p = 0.0136$), indicating increased activation of Nrf2 (Figure3.6 (B)). The associated antioxidant gene expression was significantly reduced with respect to GPx (FA: 0.49 ± 0.03 vs control: 0.82 ± 0.05; $p = 0.0136$) and CAT (FA: 0.18 ± 0.00 vs control: 1.00 ± 0.09; $p < 0.0001$) relative to normalized control (Figure3.6 (C)).

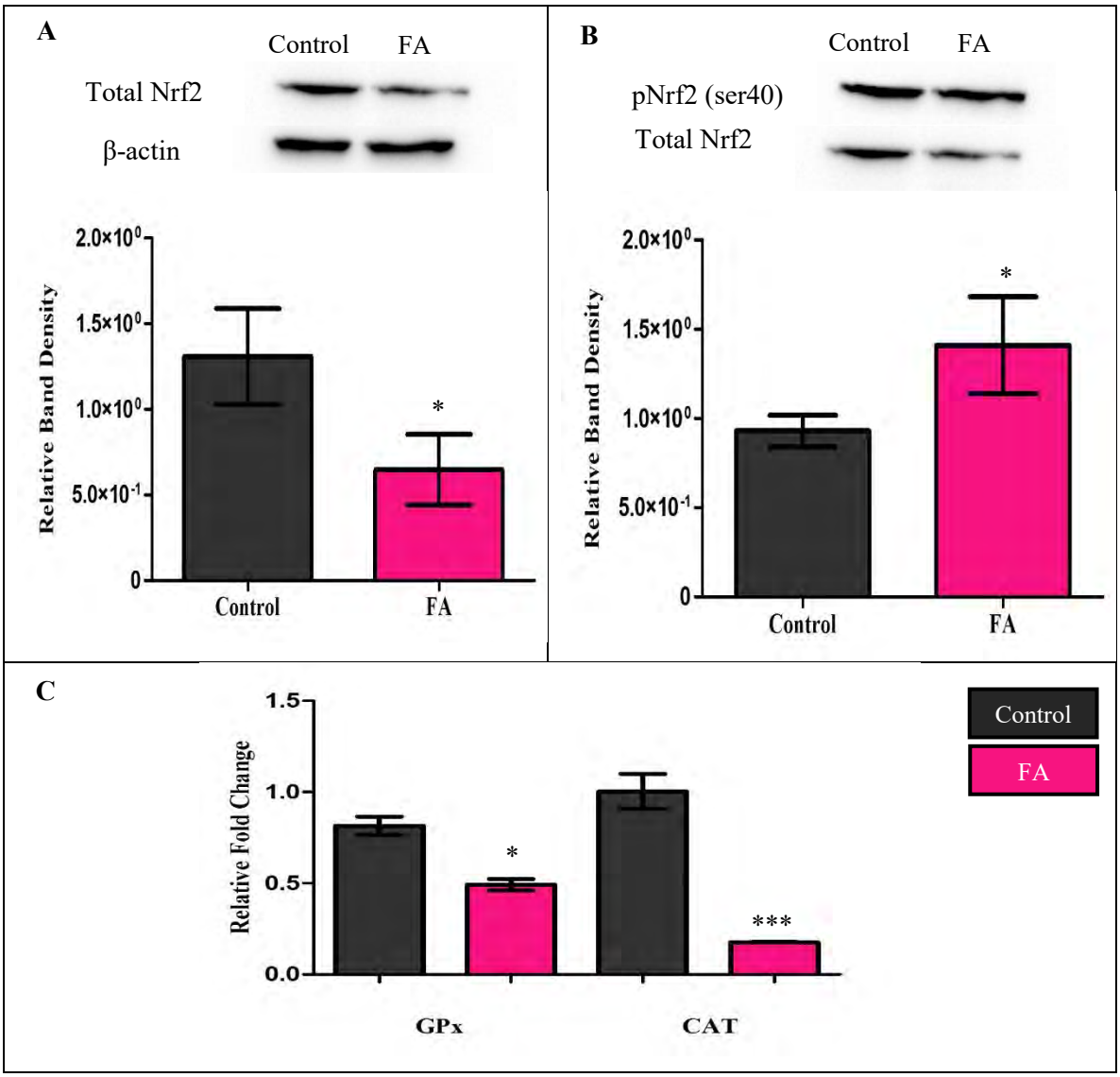

Figure 3.6: FA altered the Antioxidant response in HEK293 cells. Protein expression reported as relative band density and western blot images for Total Nrf2 (A) and phosphorylated Nrf2 (ser40) (B) following acute treatment with FA (**p < 0.005 relative to control). (C) mRNA quantification of antioxidant genes, reported as relative fold change, showed a decrease in GPx (*p < 0.05) and CAT (***p < 0.001) compared to untreated control cells.

3.5. Analysis of cell death parameters

3.5.1. Caspase activity

Caspase-Glo® assays were used to determine caspase activity. FA significantly increased the activity of initiator caspases 8 (control: 4.61 ± 0.26 x 10^5 vs. FA: 5.12 ± 0.39 x 10^5RLU; p = 0.0298) and 9 (control: 2.58 ± 0.49 vs. FA: 3.78 ± 0.34 x 10^5RLU; p = 0.0136) as well as executioner caspases-3/-7 (control: 8.77 ± 0.57 vs. FA: 11.44 ± 1.27 x 10^4RLU; p = 0.0048) compared to the control (Figure.3.7). Therefore, this indicates activation of apoptotic cell death.

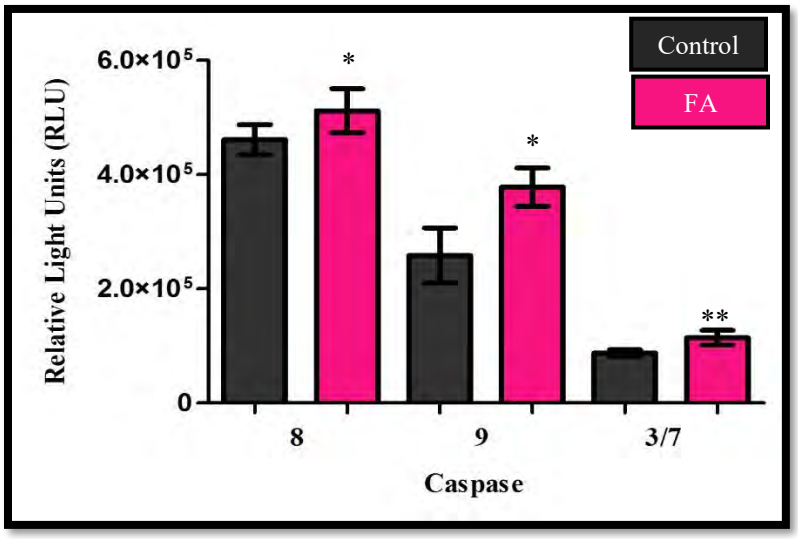

Figure 3.4: Luminometric assessment of the initiator caspases 8 (1.1-fold) and 9 (1.4-fold) and executioner caspases 3/7 (1.3-fold) showed increased activity in response to FA exposure (*p < 0.05; **p < 0.005).

3.5.2. **Lactate dehydrogenase cytotoxicity**

The leakage of the cytosolic enzyme LDH is used as an indicator of cytotoxicity. HEK cells treated with to FA demonstrated significantly increased extracellular LDH compared to control cells (control: 0.77 ± 0.02 vs. FA 1.67 ± 0.10OD; p = 0.0009), which is indicative of loss of membrane integrity and necrotic cell death (Figure.3.8).

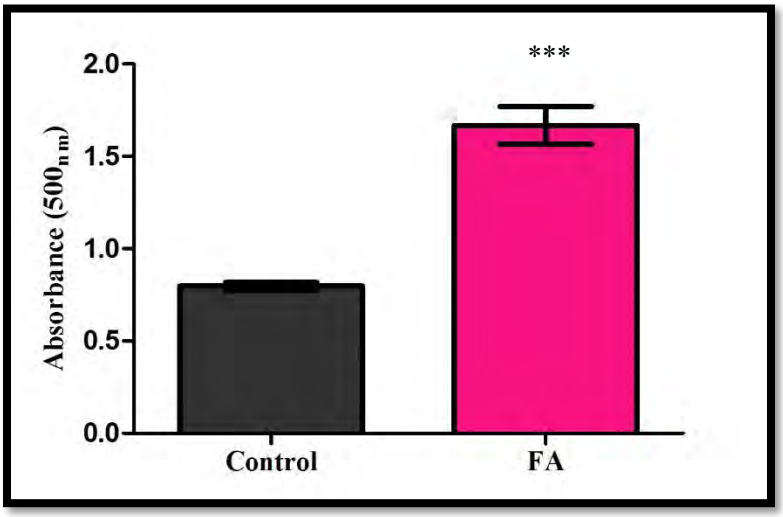

Figure 3.5: Spectrophotometric analysis of LDH leakage in FA treated cells resulted in a 2.1-fold increase compared to control cells (p = 0.0009).

Chapter 4

Discussion

Fusaric acid is a ubiquitous mycotoxin that frequently contaminates cereal grains used for human and animal consumption. Previous studies have identified FA primarily as a potent phytotoxin [55], however FA has been shown to exhibit low to moderate toxic effects in humans and animals [1, 38]. The effects observed following FA exposure has been associated with mitochondrial dysfunction [15, 54, 69, 70], induction of increased ROS generation [14, 54] and activation of cell death [134]; however little is known regarding the effect of FA on cellular stress response mechanisms that mediate these outcomes.

In this study, evidence was presented to demonstrate that FA induces cytotoxicity in human embryonic kidney (HEK) 293 cells by inhibiting cellular antioxidant and DNA repair responses, thereby facilitating cell death. Previous studies have proposed that FA toxicity is linked to 2 biochemical properties, which include FA's ability to act a weak acid and a chelator of divalent cations [45, 46].

Weak acids disrupt mitochondrial function by depolarizing mitochondrial membranes, which can compromise the integrity of the mitochondrial membrane. This mediates changes in permeability and subsequently causes mitochondrial dysfunction. Furthermore, weak acids can interrupt processes that take place within the mitochondria, such as ETC activity by dissipating the proton gradient between the mitochondrial matrix and intermembrane space, which is responsible for ATP synthesis [135]. Fusaric acid can also cause structural and functional alterations to heme structures, iron-sulphur clusters and copper proteins that are present in ETC complexes through its chelating activity. Fusaric acid not only causes mitochondrial dysfunction but compromises metabolic activity by impeding reactions catalysed by oxidoreductases within the Krebs cycle (mitochondrial matrix), that produces reducing equivalents [69, 70]. Fusaric acid acts as a nicotinamide analog, and competitively inhibits NAD^+-requiring reactions. These actions culminate in a compromised metabolic state and a loss of mitochondrial integrity, which is observed following FA exposure [15]. Impaired mitochondrial function was confirmed by the dose dependent decline in cell viability

under increasing concentrations of FA (Figure.3.1), demonstrated as a decrease in formazan production (decrease in reducing potential of mitochondrial oxidoreductases) and the decreased ATP levels (Figure.3.2) post FA exposure.

The induction of ROS generation by FA has been reported previously in both human-derived cancer cell and plant models [14, 15, 24, 136]. It is likely that inhibition of the ETC is associated with the increased production of ROS. Mitochondrial electron transport generates $\bullet O_2^-$ as a by-product at complex I and complex III [12, 137]. Other studies have shown that, under mitochondrial dysfunction, there is increased leakage of electrons to molecular oxygen producing $\bullet O_2^-$ [138-141]. Fusaric acid can also act alone to exacerbate ROS production in the form of hydroxyl radicals by promoting the Fenton reaction [45].

The data strongly suggests that FA exposure results in a change in oxidative status. This claim is supported by the significant decline in cellular GSH concentrations (Figure.3.3 (A)) with an accompanying increase in extracellular MDA levels (Figure.3.3 (B)), a lipid peroxidation by-product indicative of oxidative stress, following treatment with FA. Reduced glutathione is the most abundant endogenous antioxidant and is a critical regulator of redox homeostasis [142, 143]. Upon exposure to external factors such as FA, oxidative challenge to cells is increased resulting in rapid utilization of GSH stores, which reduces the detoxifying capacity of the cell. This creates an imbalance caused by excessive ROS production and limited antioxidant defences, referred to as oxidative stress [144]. Oxidative stress promotes ROS-mediated damage to cellular macromolecules. Due to the abundance of long chain polyunsaturated fatty acids present in kidney cells [145], lipid peroxidation is one of the likely outcomes of oxidative insult. The cell possesses several intrinsic mechanisms that are activated when exposed to increasing levels of stress. The pathway central to mounting a response against oxidative stress is the Nrf2/ARE pathway [13].

Under homeostatic conditions, Nrf2 is sequestered in the cytosol by its repressor, Keap1 which facilitates ubiquitination and proteasomal degradation of Nrf2. Keap1 is a cysteine-rich protein, which undergoes conformation changes in response to oxidative stress, thereby leading to the liberation of Nrf2 [146]. Nrf2 is then available to translocate to the nucleus, where it binds to the

ARE resulting in transcriptional induction of several phase II enzymes and antioxidant proteins [76, 146].

The activation of Nrf2 has also been shown to be regulated through phosphorylation [76]. Protein Kinase C (PKC) phosphorylates unbound Nrf2 in its NEH2 domain at serine 40, which disrupts association between Nrf2 and Keap1 and thus promotes transport of Nrf2 to the nucleus [147]. Fusaric acid appears to exhibit an inhibitory effect on the Nrf2 mediated response to oxidative stress. It is postulated that this could be due to the chelation of zinc ions that are required for Nrf2 expression and transcriptional function [148]. The findings of this study show that FA exposure resulted in a decrease in Nrf2 expression (Figure.3.6 (A)), however phosphorylation at serine 40 was significantly increased (Figure.3.6 (B)). The increased phosphorylation can be attributed to the increased activation of PKC in response to oxidative stress, however phosphorylation of Nrf2 does not influence the stabilization of Nrf2, accumulation in the nucleus or transcriptional activation of ARE-mediated genes in response to Nrf2 interaction [149]. This provides a plausible explanation as to why, despite increased phosphorylation, the overall expression of Nrf2 was diminished. The downstream implications of this, would result in reduced transactivation of the target cytoprotective proteins and antioxidant enzymes, which correlate with our findings of significantly reduced expression of the *GPx* and *CAT* genes (Figure.3.6 (C)). The reduced capacity to mount an antioxidant stress response, would inadvertently have detrimental repercussions for the cell, were it will be subjected to increased oxidative insult that perpetuates DNA damage and cell death.

The data supports a mechanism of genotoxicity induced by FA in cells. The increased level of DNA damage, as observed by the increased comet tail lengths (Figure.3.4), is in agreement with other studies illustrating increased DNA damage following FA treatment [25, 60]. Damage to DNA can be caused by electrophilic and reactive oxygen species. It has been shown that genomic integrity can be severely compromised by ROS which produces a number of DNA lesions. These lesions include base modifications, strand breaks, inter-and intra- strand crosslinks and DNA-protein crosslinks, all of which affect structure and function [150]. Malondialdehyde, an endogenous electrophile, has also been found to react with nucleotide bases in DNA forming adducts, which have mutagenic potential that promote carcinogenesis [151, 152].

ROS accumulation and the concomitant DNA damage activates cell death pathways. Previous studies have shown FA can induce apoptosis by activation of both intrinsic and extrinsic pathways as well as through independent activation of caspase 3 [15, 24, 25, 27, 134]. The data obtained in this study show that FA increases caspase activation in kidney cells (Figure.3.7). The signal transduction of apoptosis involves a cascade of initiator and executioner caspases, which form the machinery that drive apoptosis [153]. The findings of this study support both intrinsic and extrinsic pathway activation, which is shown by the significantly increased the activities of caspases-3/-7, -8 and -9.

This cellular response is possibly linked to ATP depletion, which has been shown to abrogate caspase activation and subsequent apoptotic events in damaged cells [154, 155]. It is known that apoptotic cell death is an ATP-requiring process, and it is suggested that the level of intracellular ATP determines which cell death mechanism is activated [94, 155]. There are multiple early stage events in apoptosis that drastically increase ATP demand, such as the proteolytic cleavage and activation of the caspase cascade and apoptosome formation, resulting in rapid depletion of ATP levels. Apoptosis may be initiated following FA treatment, however as ATP levels are depleted, the cell switches to the passive form of cell death, necrosis. This is validated by the increased presence of the cytosolic enzyme LDH in the extracellular medium (Figure.3.8), indicating loss of cell membrane integrity, which is characteristic of necrosis.

The data also provides evidence of impaired DNA repair in cells exposed to FA. This has been demonstrated previously whereby it was proposed that FA inactivates zinc finger proteins, involved in the DNA repair process by chelation of their zinc ions [46, 156]. In this study, FA caused a significant decrease in PARP-1 and p53 protein expression (Figure.3.5 (B) and (C)). Activation of PARP-1 and p53 represents two of the earliest DNA damage responses that trigger various cellular functions involved in maintaining genome stability [157]. PARP-1 is a nuclear protein, whose catalytic activity is enhanced by binding to DNA strand breaks via either of its two zinc finger motifs (N-terminal), bringing about conformational changes through its third zinc finger to increase catalytic activity(C-terminal). This causes post-translational modification (poly (ADP-ribosyl)ation) of itself and other acceptor proteins using NAD^+, causing its dissociation from the DNA and recruitment of BER enzymes to the repair site [89]. Fusaric acid exhibits structural similarities to

nicotinamide, which is a natural inhibitor of PARP-1 and therefore could act through competitive inhibition to reduce PARP-1 function [73]. It is also probable that FA could alter the zinc finger domains of PARP-1, therefore hindering its ability to carry out its function. However, PARP-1 (116kDa) is a major substrate of activated caspase 3, and thus the reduced levels of PARP-1 is likely due to its cleavage into a 24kDa and 89kDa fragment [158].

The p53 protein acts downstream of PARP-1 in the DNA damage signalling pathway [157], and is responsible for checkpoint control of the cell cycle, in addition to DNA repair and apoptosis induction [159]. PARP-1 and p53 have been shown to work together to promote DNA repair via physical interactions with the BER multiprotein complex [160]. The reduced p53 levels (Figure.3.5 (C)) could have been caused by an altered PARP-1 response to DNA damage mediated by FA or related to chelation of the zinc ion present in the conserved central DNA binding domain of its own structure.

Therefore, it is fair to assume that due to inactivation of the proteins that stimulate the DNA damage response, further downstream events were not initiated. This was confirmed by decreased mRNA expression of *OGG1* (Figure.3.5 (A)), a DNA glycosylase, in cells treated with FA. Other studies have demonstrated that other aspects of this pathway are also inhibited by FA, such as the activity of the DNA polymerase, whereby FA exhibited inhibitory effects on DNA synthesis in both cancer and normal cell models [56, 60].

Chapter 5

Conclusion

This study provides evidence of FA induced cytotoxicity in the HEK293 cell line. Collectively, these results provide insight into the mechanism of action of FA, which shows that FA induces oxidative stress and promotes cellular damage and subsequent cell death by impairing the antioxidant and DNA repair responses.

These findings highlight the need to conduct further studies to ascertain if the effect of FA is consistent in other non-cancer based cell models. These damaging effects were observed after a short term exposure, which brings into question the potential threat posed by this mycotoxin following chronic exposure. In addition, this study emphasizes the need for the implementation of safety standards to regulate FA concentration in commercially produced goods.

One limitation of the study was the use of HEK293 cells which provided an overview of the sensitivity of kidney cells to FA toxicity. However, for future work, it would be beneficial to make use of a specialised kidney cell line or possibly even an *in vivo* model.

References

1. Bacon, C.W., Porter, J.K., Norred, W.P. and Leslie, J.F., *Production of fusaric acid by Fusarium species.* Applied and Environmental Microbiology, 1996. **62**(11): p. 4039-4043.
2. Bankole, S., Schollenberger, M. and Drochner, W., *Mycotoxins in food systems in Sub Saharan Africa: A review.* Mycotoxin research, 2006. **22**(3): p. 163-169.
3. Smith, T.K. and Sousadias, M.G., *Fusaric acid content of swine feedstuffs.* Journal of Agricultural and Food Chemistry, 1993. **41**(12): p. 2296-2298.
4. D'mello, J., Placinta, C. and Macdonald, A., *Fusarium mycotoxins: a review of global implications for animal health, welfare and productivity.* Animal feed science and technology, 1999. **80**(3): p. 183-205.
5. Shimshoni, J., Cuneah, O., Sulyok, M., Krska, R., Galon, N., Sharir, B. and Shlosberg, A., *Mycotoxins in corn and wheat silage in Israel.* Food Additives & Contaminants: Part A, 2013. **30**(9): p. 1614-1625.
6. Nedělník, J., *Damage to corn by fungi of the genus Fusarium and the pressence of fusariotoxins.* Plant Protection Science, 2002. **38**(2): p. 46-54.
7. Matsuzaki, M., Matsumoto, H., Ochiai, K., Tashiro, Y. and Hino, M., *[Absorption, distribution and excretion of 14C-fusaric acid in rat (author's transl)].* The Japanese journal of antibiotics, 1976. **29**(5): p. 456-466.
8. Van Vleet, T.R. and Schnellmann. R.G., *Toxic nephropathy: environmental chemicals*. in *Seminars in nephrology*. 2003. **23**(5): p. 500-508.
9. Perazella, M.A., *Renal vulnerability to drug toxicity.* Clinical Journal of the American Society of Nephrology, 2009. **4**(7): p. 1275-1283.
10. Che, R., Yuan, Y., Huang, S. and Zhang, A., *Mitochondrial dysfunction in the pathophysiology of renal diseases.* American Journal of Physiology-Renal Physiology, 2014. **306**(4): p. 367-378.
11. Pillay, Y., Phulukdaree, A., Nagiah, S. and Chuturgoon, A.A., *Patulin triggers NRF2-mediated survival mechanisms in kidney cells.* Toxicon, 2015. **99**: p. 1-5.
12. Turrens, J.F., *Mitochondrial formation of reactive oxygen species.* The Journal of physiology, 2003. **552**(2): p. 335-344.
13. Ma, Q., *Role of nrf2 in oxidative stress and toxicity.* Annual review of pharmacology and toxicology, 2013. **53**: p. 401.

14. Kuźniak, E., *Effects of fusaric acid on reactive oxygen species and antioxidants in tomato cell cultures.* Journal of Phytopathology, 2001. **149**(10): p. 575-582.
15. Abdul, N.S., Nagiah, S. and Chuturgoon, A.A., *Fusaric acid induces mitochondrial stress in human hepatocellular carcinoma (HepG2) cells.* Toxicon, 2016. **119**: p. 336-344.
16. Fulda, S., Gorman, A.M., Hori, O. and Samali, A., *Cellular stress responses: cell survival and cell death.* International journal of cell biology, 2010. doi. 10.1155/2010/214074.
17. Nguyen, T., Nioi, P. and Pickett, C.B., *The Nrf2-antioxidant response element signaling pathway and its activation by oxidative stress.* Journal of Biological Chemistry, 2009. **284**(20): p. 13291-13295.
18. Baird, L. and Dinkova-Kostova, A.T., *The cytoprotective role of the Keap1–Nrf2 pathway.* Archives of toxicology, 2011. **85**(4): p. 241-272.
19. Li, W. and Kong, A.N., *Molecular mechanisms of Nrf2- mediated antioxidant response.* Molecular carcinogenesis, 2009. **48**(2): p. 91-104.
20. Klaunig, J.E., Kamendulis, L.M. and Hocevar, B.A., *Oxidative stress and oxidative damage in carcinogenesis.* Toxicologic pathology, 2010. **38**(1): p. 96-109.
21. Nowsheen, S. and Yang, E., *The intersection between DNA damage response and cell death pathways.* Experimental oncology, 2012. **34**(3): p. 243-254.
22. Jackson, S.P. and Bartek, J., *The DNA-damage response in human biology and disease.* Nature, 2009. **461**(7267): p. 1071-1078.
23. Kim, Y.J. and Wilson III, D.M., *Overview of base excision repair biochemistry.* Current molecular pharmacology, 2012. **5**(1): p. 3-13.
24. Singh, V.K. and Upadhyay, R.S., *Fusaric acid induced cell death and changes in oxidative metabolism of Solanum lycopersicum L.* Botanical Studies, 2014. **55**(1): p. 1-11.
25. Ye, J., Montero, M. and Stack Jr, B.C., *Effects of fusaric acid treatment on HEp2 and docetaxel-resistant HEp2 laryngeal squamous cell carcinoma.* Chemotherapy, 2013. **59**(2): p. 121-128.
26. Jiao, J., Zhou, B., Zhu, X., Gao, Z. and Liang, Y., *Fusaric acid induction of programmed cell death modulated through nitric oxide signalling in tobacco suspension cells.* Planta, 2013. **238**(4): p. 727-737.
27. Devnarain, N., Tiloke, C., Nagiah, S. and Chuturgoon, A.A., *Fusaric acid induces oxidative stress and apoptosis in human cancerous oesophageal SNO cells.* Toxicon, 2017. **126**: p. 4-11.

28. Bennett, J., *Mycotoxins, mycotoxicoses, mycotoxicology andMycopathologia.* Mycopathologia, 1987. **100**(1): p. 3-5.
29. Ciegler, A. and Bennett, J., *Mycotoxins and mycotoxicoses.* Bioscience, 1980. **30**(8): p. 512-515.
30. Zain, M.E., *Impact of mycotoxins on humans and animals.* Journal of Saudi Chemical Society, 2011. **15**(2): p. 129-144.
31. Blount, W., *Turkey "X" disease.* Turkeys, 1961. **9**(2): p. 52-55.
32. Spensley, P., *Aflatoxin, the active principle in turkey'X'disease.* Endeavour, 1963. **22**: p. 75.
33. Bennett, J. and Klich, M., *Mycotoxins.* Clinical Microbiology Reviews, 2003. **16**(3): p. 497-516.
34. Peraica, M., Radic, B., Lucic, A. and Pavlovic, M., *Toxic effects of mycotoxins in humans.* Bulletin of the World Health Organization, 1999. **77**(9): p. 754-766.
35. Food and Agriculture Organization, *Worldwide regulations for mycotoxins in food and feed in 2003*. Food and Agricultural Organization of the United Nations food and nutrition paper *81,* 2004. Rome, Italy.
36. Omar, H.E.-D.M., *Mycotoxins-induced oxidative stress and disease.* Mycotoxin and Food Safety in Developing Countries, 2013: Chapter 3: p. 63-92. doi.10.5772/51806.
37. El-Masry, E.M. and Abou-Donia, M.B., *Mammalian toxicology*, M.B. Abou-Donia, Editor 2015, Chapter 27: p. 605-640. .John Wiley & Sons Inc.: Hoboken, NJ, USA.
38. Wang, H. and Ng, T., *Pharmacological activities of fusaric acid (5-butylpicolinic acid).* Life sciences, 1999. **65**(9): p. 849-856.
39. Peraica, M. and Domijan, A.-M., *Contamination of food with mycotoxins and human health.* Archives of Industrial Hygiene and Toxicology, 2001. **52**(1): p. 23-35.
40. Yabuta, T., Kobe, K. and Hayashi, T., *Biochemical studies of the'bakanae'fungus of rice. I. Fusarinic acid, a new product of the'Bakanae'fungus.*Journal of Plant Diseases., 1934. **10**: p. 1059-1068.
41. Yin, E.S., Rakhmankulova, M., Kucera, K., de Sena Filho, J.G., Portero, C.E., Narváez-Trujillo, A., Holley, S.A. and Strobel, S.A., *Fusaric acid induces a notochord malformation in zebrafish via copper chelation.* BioMetals, 2015. **28**(4): p. 783-789.
42. Bacon, C.W., Porter, J.K. and Norred, W.P., *Toxic interaction of fumonisin B1 and fusaric acid measured by injection into fertile chicken egg.* Mycopathologia, 1995. **129**(1): p. 29-35.

43. Evans, G. W. and Johnson, P. E., C*haracterization and quantitation of a zinc-binding ligand in human milk.* Pediatric Research, 1980. ***14*****:** p. 876-880.
44. Bochner, B.R., Huang, H.C., Schieven, G.L. and Ames, B.N., *Positive selection for loss of tetracycline resistance.* Journal of bacteriology, 1980. **143**(2): p. 926-933.
45. Iwahashi, H., Kawamori, H. and Fukushima, K., *Quinolinic acid, α-picolinic acid, fusaric acid, and 2, 6-pyridinedicarboxylic acid enhance the Fenton reaction in phosphate buffer.* Chemico-biological interactions, 1999. **118**(3): p. 201-215.
46. Stack, B.C., Hansen, J.P., Ruda, J.M., Jaglowski, J., Shvidler, J. and Hollenbeak, C.S., *Fusaric acid: a novel agent and mechanism to treat HNSCC.* Otolaryngology--Head and Neck Surgery, 2004. **131**(1): p. 54-60.
47. Smith, T.K., McMillan, E.G. and Castillo, J.B., *Effect of feeding blends of Fusarium mycotoxin-contaminated grains containing deoxynivalenol and fusaric acid on growth and feed consumption of immature swine.* Journal of animal science, 1997. **75**(8): p. 2184-2191.
48. Dowd, P.F., *Toxicological and Biochemical Interactions of the Fungal Metabolites Fusaric Acid and Kojic Acid with Xenobiotics in Heliothis zea (F.) and Spodoptera frugiperda (J. E. Smith).* Pesticide biochemistry and physiology, 1988. **3**: p. 123-134.
49. Fairchild, A.S., Grimes, J.L., Porter, J.K., Croom Jr, W.J., Daniel, L.R. and Hagler Jr, W.M., *Effects of diacetoxyscirpenol and fusaric acid on poults: Individual and combined effects of dietary diacetoxyscirpenol and fusaric acid on turkey poult performance.* Int. J. Poult. Sci, 2005. **4**: p. 350-355.
50. Ogunbo, S.O., Broomhead, J.N., Ledoux, D.R., Bermudez, A.J. and Rottinghaus, G.E., *The individual and combined effects of fusaric acid and T-2 toxin in broilers and turkeys.* Int. J. Poult. Sci, 2007. **6**(7): p. 484-488.
51. Voss, K., Porter, J.K., Bacon, C.W., Meredith, F.I. and Norred, W.P., *Fusaric acid and modification of the subchronic toxicity to rats of fumonisins in F. moniliforme culture material.* Food and chemical toxicology, 1999. **37**(8): p. 853-861.
52. Ismaiel, A.A. and Papenbrock, J., *Mycotoxins: producing fungi and mechanisms of phytotoxicity.* Agriculture, 2015. **5**(3): p. 492-537.
53. Gäumann, E., *Fusaric acid as a wilt toxin.* Phytopathology, 1957. **47**: p. 342-357.
54. Jiao, J., Sun, L., Zhou, B., Gao, Z., Hao, Y., Zhu, X. and Liang, Y., *Hydrogen peroxide production and mitochondrial dysfunction contribute to the fusaric acid-induced programmed cell death in tobacco cells.* Journal of plant physiology, 2014. **171**(13): p. 1197-1203.

55. Pavlovkin, J., Mistrik, I. and Prokop, M., *Some aspects of the phytotoxic action of fusaric acid on primary Ricinus roots.* Plant Soil and Environment, 2004. **50**(9): p. 397-401.
56. Fernandez-Pol, J., D. Klos, and Hamilton, P., *Cytotoxic activity of fusaric acid on human adenocarcinoma cells in tissue culture.* Anticancer research, 1993. **13**(1): p. 57-64.
57. Ruda, J.M., Beus, K.S., Hollenbeak, C.S., Wilson, R.P. and Stack Jr, B.C., *The effect of single agent oral fusaric acid (FA) on the growth of subcuta neously xenografted SCC-1 cells in a nude mouse model.* Investigational new drugs, 2006. **24**(5): p. 377-381.
58. Jaglowski, J.R. and Stack, B.C., *Enhanced growth inhibition of squamous cell carcinoma of the head and neck by combination therapy of fusaric acid and paclitaxel or carboplatin.* Cancer letters, 2006. **243**(1): p. 58-63.
59. Nagasaka, A., Hara, I., Imai, Y., Uchikawa, T., Yamauchi, K., Suzuki, S. and Nakagawa, H., *Effect of Fusaric Acid (a dopamine β- hydroxylase inhibitor) on Phaeochromocytoma.* Clinical endocrinology, 1985. **22**(4): p. 437-444.
60. Stack Jr, B.C., Ye, J., Willis, R., Hubbard, M. and Hendrickson, H.P., *Determination of oral bioavailability of fusaric acid in male Sprague-Dawley rats.* Drugs in R&D, 2014. **14**(2): p. 139-145.
61. Porter, J.K., Bacon, C.W., Wray, E.M. and Hagler, W.M., *Fusaric acid in Fusarium moniliforme cultures, corn, and feeds toxic to livestock and the neurochemical effects in the brain and pineal gland of rats.* Natural Toxins, 1995. **3**(2): p. 91-100.
62. Toshiharu, N., Hiroyoshi, H., Hiroshi, K., Kazumi, T., Hamao, U., Tomio, T. and Hiroyuki, S., *Inhibition of dopamine β-hydroxylase by fusaric acid (5-butylpicolinic acid) in vitro and in vivo.* Biochemical pharmacology, 1970. **19**(1): p. 35-44.
63. Hidaka, H., Nagatsu, T., Takeya, K., Takeuchi, T., Suda, H., Kojiri, K. and Umezawa, H., *Fusaric acid, a hypotensive agent produced by fungi.* The Journal of antibiotics, 1969. **22**(5): p. 228-230.
64. Smith, T. and MacDonald E., *Effect of fusaric acid on brain regional neurochemistry and vomiting behavior in swine.* Journal of animal science, 1991. **69**(5): p. 2044-2049.
65. Noori, S., *An Overview of Oxidative stress and Antioxidant Defense system.* Journal of Clinical and Cellular Immunology, 2012. **1**(8). doi. 10.4172/scientificreports.413.
66. Davies, K.J., *Oxidative stress, antioxidant defenses, and damage removal, repair, and replacement systems.* IUBMB life, 2000. **50**(4- 5): p. 279-289.

67. Rahal, A., Kumar, A., Singh, V., Yadav, B., Tiwari, R., Chakraborty, S. and Dhama, K., *Oxidative stress, prooxidants, and antioxidants: the interplay.* BioMed research international, 2014. p. 1-19. doi. 10.1155/2014/761264.
68. Rahman, K., *Studies on free radicals, antioxidants, and co-factors.* Clinical interventions in aging, 2007. **2**(2): p. 219-236.
69. Telles-Pupulin, A.R., Diniz, S.P.S.S., Bracht, A. and Ishii-Iwamoto, E.L., *Effects of fusaric acid on respiration in maize root mitochondria.* Biologia plantarum, 1996. **38**(3): p. 421-429.
70. Telles-Pupulin, A.R., Salgueiro-Pagadigorria, C.L., Bracht, A. and Ishii-Iwamoto, E.L., *Effects of fusaric acid on rat liver mitochondria.* Comparative Biochemistry and Physiology Part C: Pharmacology, Toxicology and Endocrinology, 1998. **120**(1): p. 43-51.
71. McEwen, M.L., Sullivan, P.G., Rabchevsky, A.G. and Springer, J.E., *Targeting mitochondrial function for the treatment of acute spinal cord injury.* Neurotherapeutics, 2011. **8**(2): p. 168-179.
72. Birben, E., Sahiner, U.M., Sackseen, C., Erzurum, S. and Kalayci, O., *Oxidative stress and antioxidant defense.* World Allergy Organization Journal, 2012. **5**(1): p. 1-9. doi. 10.1097/WOX.0b013e3182439613.
73. Surjana, D., G.M. Halliday, and D.L. Damian, *Role of nicotinamide in DNA damage, mutagenesis, and DNA repair.* Journal of nucleic acids, 2010. doi: 10.4061/2010/157591.
74. Sack, M.N. and Finkel, T., *Mitochondrial metabolism, sirtuins, and aging.* Cold Spring Harbor perspectives in biology, 2012. **4**(12): p. 13102.
75. Milisav, I., *Cellular stress responses.* Advances in Regenerative Medicine, 2011: p. 215-232.
76. Bryan, H.K., Olayanju, A., Goldring, C.E. and Park, B.K., *The Nrf2 cell defence pathway: Keap1-dependent and-independent mechanisms of regulation.* Biochemical pharmacology, 2013. **85**(6): p. 705-717.
77. Espinosa-Diez, C., Miguel, V., Mennerich, D., Kietzmann, T., Sánchez-Pérez, P., Cadenas, S. and Lamas, S., *Antioxidant responses and cellular adjustments to oxidative stress.* Redox biology, 2015. **6**: p. 183-197.
78. Lobo, V., Patil, P., Phatak, A. and Chandra, N., *Free radicals, antioxidants and functional foods: Impact on human health.* Pharmacognosy reviews, 2010. **4**(8): p. 118-126.
79. Hermes-Lima, M., *Oxygen in biology and biochemistry: role of free radicals.* Functional metabolism: Regulation and adaptation, 2004. **1**: p. 319-66.

80. Lu, S.C., *Glutathione synthesis.* Biochimica et Biophysica Acta (BBA)-General Subjects, 2013. **1830**(5): p. 3143-3153.
81. Zitka, O., Skalickova, S., Gumulec, J., Masarik, M., Adam, V., Hubalek, J., Trnkova, L., Kruseova, J., Eckschlager, T. and Kizek, R., *Redox status expressed as GSH: GSSG ratio as a marker for oxidative stress in paediatric tumour patients.* Oncology letters, 2012. **4**(6): p. 1247-1253.
82. Couto, N., Wood, J. and Barber, J., *The role of glutathione reductase and related enzymes on cellular redox homoeostasis network.* Free Radical Biology and Medicine, 2016. **95**: p. 27-42.
83. Owen, J.B. and. Butterfield, D.A, *Measurement of oxidized/reduced glutathione ratio.* Protein Misfolding and Cellular Stress in Disease and Aging: Concepts and Protocols, 2010: p. 269-277.
84. Deavall, D.G., Martin, E.A, Horner, J.M. and Roberts, R., *Drug-induced oxidative stress and toxicity.* Journal of toxicology, 2012. doi. 10.1155/2012/645460.
85. Zhang, W., Xiao, S. and Ahn, D.U., *Protein oxidation: basic principles and implications for meat quality.* Critical reviews in food science and nutrition, 2013. **53**(11): p. 1191-1201.
86. Cooke, M.S., Evans, M.D., Dizdaroglu, M. and Lunec, J., *Oxidative DNA damage: mechanisms, mutation, and disease.* The FASEB Journal, 2003. **17**(10): p. 1195-1214.
87. Dunlop, R.A., Brunk, U.T. and Rodgers, K.J., *Oxidized proteins: mechanisms of removal and consequences of accumulation.* IUBMB life, 2009. **61**(5): p. 522-527.
88. Jaiswal, M., LaRusso, N.F., Nishioka, N., Nakabeppu, Y. and Gores, G.J., *Human Ogg1, a protein involved in the repair of 8-oxoguanine, is inhibited by nitric oxide.* Cancer research, 2001. **61**(17): p. 6388-6393.
89. Ko, H.L. and Ren, E.C., *Functional aspects of PARP1 in DNA repair and transcription.* Biomolecules, 2012. **2**(4): p. 524-548.
90. Hooten, N.N., Kompaniez, K., Barnes, J., Lohani, A. and Evans, M.K., *Poly (ADP-ribose) polymerase 1 (PARP-1) binds to 8-oxoguanine-DNA glycosylase (OGG1).* Journal of Biological Chemistry, 2011. **286**(52): p. 44679-44690.
91. Gambino, V., De Michele, G., Venezia, O., Migliaccio, P., Dall'Olio, V., Bernard, L., Minardi, S.P., Fazia, M.A.D., Bartoli, D. and Servillo, G., *Oxidative stress activates a specific p53 transcriptional response that regulates cellular senescence and aging.* Aging Cell, 2013. **12**(3): p. 435-445.

92. Liu, D. and Xu, Y., *p53, oxidative stress, and aging.* Antioxidants & redox signaling, 2011. **15**(6): p. 1669-1678.
93. Achanta, G. and Huang, P., *Role of p53 in sensing oxidative DNA damage in response to reactive oxygen species-generating agents.* Cancer research, 2004. **64**(17): p. 6233-6239.
94. Tsujimoto, Y., *Apoptosis and necrosis: intracellular ATP level as a determinant for cell death modes.* Cell Death & Differentiation, 1997. **4**(6).
95. Van Cruchten, S. and Van Den Broeck, W., *Morphological and biochemical aspects of apoptosis, oncosis and necrosis.* Anatomia, histologia, embryologia, 2002. **31**(4): p. 214-223.
96. Elmore, S., *Apoptosis: a review of programmed cell death.* Toxicologic pathology, 2007. **35**(4): p. 495-516.
97. Chang, H.Y. and Yang, X., *Proteases for cell suicide: functions and regulation of caspases.* Microbiology and molecular biology reviews, 2000. **64**(4): p. 821-846.
98. Alberts, B., Johnson, A., Lewis, J., Raff, M., Roberts, K. and Walter, P., *Programmed cell death (apoptosis).* 2002. 4th edition. Garland Sciences. New York.
99. Hengartner, M.O., *The biochemistry of apoptosis.* Nature, 2000. **407**(6805): p. 770-776.
100. Fulda, S. and Debatin, K., *Extrinsic versus intrinsic apoptosis pathways in anticancer chemotherapy.* Oncogene, 2006. **25**(34): p. 4798-4811.
101. Wang, C. and Youle, R..J., *The role of mitochondria in apoptosis.* Annual review of genetics, 2009. **43**: p. 95-118.
102. Stepanenko, A. and Dmitrenko, V., *HEK293 in cell biology and cancer research: phenotype, karyotype, tumorigenicity, and stress-induced genome-phenotype evolution.* Gene, 2015. **569**(2): p. 182-190.
103. Strober, W., *Trypan blue exclusion test of cell viability.* Current protocols in immunology, 2001: p. A3. B. 1-A3. B. 3.
104. Mosmann, T., *Rapid colorimetric assay for cellular growth and survival: application to proliferation and cytotoxicity assays.* Journal of immunological methods, 1983. **65**(1-2): p. 55-63.
105. Supino, R., *MTT assays.* In vitro toxicity testing protocols, 1995: p. 137-149.
106. Riss, T.L., Moravec, R.A., Niles, A.L., Duellman, S., Benink, H.A., Worzella, T.J. and Minor, L., *Cell viability assays.* Assay Guidance Manual, 2015. Bethesda , USA

107. Barahuie, F., Hussein, M.Z., Fakurazi, S. and Zainal, Z., *Development of drug delivery systems based on layered hydroxides for nanomedicine.* International journal of molecular sciences, 2014. **15**(5): p. 7750-7786.

108. Wilson, T. and Hastings, J.W., *Bioluminescence.* Annual review of cell and developmental biology, 1998. **14**(1): p. 197-230.

109. Held, P., *Luciferase Measurements using the ClarityTM Luminescence Microplate Reader-Luminescence made easy.* Nature Methods| Application Notes, 2006. doi. 10.1038/an1755.

110. Weydert, C.J. and Cullen, J.J., *Measurement of superoxide dismutase, catalase and glutathione peroxidase in cultured cells and tissue.* Nature protocols, 2010. **5**(1): p. 51-66.

111. Ayala, A., Muñoz, M.F. and Argüelles, S., *Lipid peroxidation: production, metabolism, and signaling mechanisms of malondialdehyde and 4-hydroxy-2-nonenal.* Oxidative medicine and cellular longevity, 2014. p. 1-31. doi. 10.1155/2014/360438.

112. Frijhoff, J., Winyard, P.G., Zarkovic, N., Davies, S.S., Stocker, R., Cheng, D., Knight, A.R., Taylor, E.L., Oettrich, J. and Ruskovska, T., *Clinical relevance of biomarkers of oxidative stress.* Antioxidants & redox signaling, 2015. **23**(14): p. 1144-1170.

113. Basu, S., *The enigma of in vivo oxidative stress assessment: isoprostanes as an emerging target.* Scandinavian Journal of Food & Nutrition, 2007. **51**(2): p. 48.

114. Janero, D.R., *Malondialdehyde and thiobarbituric acid-reactivity as diagnostic indices of lipid peroxidation and peroxidative tissue injury.* Free Radical Biology and Medicine, 1990. **9**(6): p. 515-540.

115. Ostling, O. and Johanson, K., *Microelectrophoretic study of radiation-induced DNA damages in individual mammalian cells.* Biochemical and biophysical research communications, 1984. **123**(1): p. 291-298.

116. Singh, N.P., McCoy, M.T., Tice, R.R. and Schneider, E.L., *A simple technique for quantitation of low levels of DNA damage in individual cells.* Experimental cell research, 1988. **175**(1): p. 184-191.

117. Collins, A.R., *The comet assay for DNA damage and repair.* Molecular biotechnology, 2004. **26**(3): p. 249-261.

118. Raghubeer, S., Nagiah, S., Phulukdaree, A. and Chuturgoon, A.A., *The phytoalexin resveratrol ameliorates ochratoxin A toxicity in human embryonic kidney (HEK293) cells.* Journal of cellular biochemistry, 2015. **116**(12): p. 2947-2955.

119. Joshi, M. and Deshpande, J., *Polymerase chain reaction: methods, principles and application.* International Journal of Biomedical Research, 2011. **2**(1): p. 81-97.

120. Hernandez-Rodriguez, P. and Ramirez, A.G., *Polymerase Chain Reaction: Types, Utilities and Limitations*. 2012. Intech Open Access Publisher. doi. 10.5772/37450.

121. Pestana, E.A., Belak, S., Diallo, A., Crowther, J.R. and Viljeon, G.J., *Early, rapid and sensitive veterinary molecular diagnostics - Real time PCR applications*. 2010. Chapter 3: p. 27-46. Dordrecht, South Africa: Springer Science & Business Media. doi. 10.1007/978-90-481-3132-7.

122. Navarro, E., Serrano-Heras, G., Castaño, M.J. and Solera, J., *Real-time PCR detection chemistry.* Clinica chimica acta, 2015. **439**: p. 231-250.

123. Chuturgoon, A.A., Phulukdaree, A. and Moodley, D., *Fumonisin B 1 modulates expression of human cytochrome P450 1b1 in human hepatoma (Hepg2) cells by repressing Mir-27b.* Toxicology letters, 2014. **227**(1): p. 50-55.

124. Livak, K.J. and Schmittgen, T.D., *Analysis of relative gene expression data using real-time quantitative PCR and the* $2^{-\Delta\Delta CT}$ *method.* methods, 2001. **25**(4): p. 402-408.

125. Smith, P.K., Krohn, R., Hermanson, G.T., Mallia, A.K., Gartner, F.H., Provenzano, M.D., Fujimoto, E.K., Goeke, N.M., Olson, B.J. and Klenk, D.C., *Measurement of protein using bicinchoninic acid.* Analytical biochemistry, 1985. **150**(1): p. 76-85.

126. Walker, J.M., *The bicinchoninic acid (BCA) assay for protein quantitation.* The Protein Protocols Handbook, 2009: p. 11-15.

127. Brunelle, J.L. and Green, R., *One-dimensional SDS-polyacrylamide gel electrophoresis (1D SDS-PAGE).* Methods in enzymology, 2014. **541**: p. 151.

128. Mahmood, T. and Yang, P.-C., *Western blot: technique, theory, and trouble shooting.* North American journal of medical sciences, 2012. **4**(9): p. 429.

129. Guy, G.R., *Detection of proteins on blots using chemiluminescent systems.* The protein protocols and book. Totowa: Humana Press Inc, 1996: p. 329-335.

130. Durrant, I., *Enhanced chemiluminescent detection of horseradish peroxidase labeled probes.* Protocols for Gene Analysis, 1994: p. 147-161.

131. Chan, F.K.-M., Moriwaki, K. and De Rosa, M.J., *Detection of necrosis by release of lactate dehydrogenase activity.* Immune Homeostasis: Methods and Protocols, 2013: p. 65-70.

132. Forest, V., Figarol, A., Boudard, D., Cottier, M., Grosseau, P. and Pourchez, J., *Adsorption of Lactate Dehydrogenase Enzyme on Carbon Nanotubes: How to Get Accurate Results for the Cytotoxicity of These Nanomaterials.* Langmuir, 2015. **31**(12): p. 3635-3643.

133. Nagiah, S., Phulukdaree, A. and Chuturgoon, A.A., *Inverse association between microRNA-124a and ABCC4 in HepG2 cells treated with antiretroviral drugs.* Xenobiotica, 2016. **46**(9): p. 825-830.

134. Ogata, S., Inoue, K., Iwata, K., Okumura, K. and Taguchi, H., *Apoptosis induced by picolinic acid-related compounds in HL-60 cells.* Bioscience, biotechnology, and biochemistry, 2001. **65**(10): p. 2337-2339.

135. Komen, J., Distelmaier, F., Koopman, W.J.H., Wanders, R.J.A., Smeitink, J. and Willems, P.H.M.G., *Phytanic acid impairs mitochondrial respiration through protonophoric action.* Cellular and Molecular Life Sciences, 2007. **64**(24): p. 3271-3281.

136. Bouizgarne, B., El- Maarouf- Bouteau, H., Frankart, C., Reboutier, D., Madiona, K., Pennarun, A.M., Monestiez, M., Trouverie, J., Amiar, Z. and Briand, J., *Early physiological responses of Arabidopsis thaliana cells to fusaric acid: toxic and signalling effects.* New Phytologist, 2006. **169**(1): p. 209-218.

137. Raha, S. and Robinson, B.H., *Mitochondria, oxygen free radicals, disease and ageing.* Trends in biochemical sciences, 2000. **25**(10): p. 502-508.

138. Chen, Y., McMillan-Ward, E., Kong, J., Israels, S.J. and Gibson, S.B., *Mitochondrial electron-transport-chain inhibitors of complexes I and II induce autophagic cell death mediated by reactive oxygen species.* Journal of cell science, 2007. **120**(23): p. 4155-4166.

139. Dröse, S. and Brandt, U., *Molecular mechanisms of superoxide production by the mitochondrial respiratory chain*. Advances in experimental medicine and biology, 2012. **748**: p. 145-169. doi. 10.1007/978-1-4614-3573-0-6.

140. Li, N., Cui, W., Tan, Y., Luo, P., Chen, Q., Zhang, C., Qu, W., Miao, L. and Cai, L., *Mitochondrial complex I inhibitor rotenone induces apoptosis through enhancing mitochondrial reactive oxygen species production.* Journal of Biological Chemistry, 2003. **278**(10): p. 8516-8525.

141. Muller, F.L., Liu, Y. and Van Remmen, H., *Complex III releases superoxide to both sides of the inner mitochondrial membrane.* Journal of Biological Chemistry, 2004. **279**(47): p. 49064-49073.

142. Ribas, V., García-Ruiz, C. and Fernández-Checa, J.C., *Glutathione and mitochondria.* 2014.

143. Marí, M., Morales, A., Colell, A., García-Ruiz, C. and Fernández-Checa, J.C., *Mitochondrial glutathione, a key survival antioxidant.* Antioxidants & redox signaling, 2009. **11**(11): p. 2685-2700.

144. Ott, M., Gogvadze, V., Orrenius, S. and Zhivotovsky, B., *Mitochondria, oxidative stress and cell death.* Apoptosis, 2007. **12**(5): p. 913-922.
145. Ozbek, E., *Induction of oxidative stress in kidney.* International journal of nephrology, 2012. p. 1-9. doi. 10.1155/2012/465897.
146. Niture, S.K., Khatri, R. and Jaiswal, A.K., *Regulation of Nrf2—an update.* Free Radical Biology and Medicine, 2014. **66**: p. 36-44.
147. Huang, H.-C., Nguyen, T. and Pickett, C.B., *Phosphorylation of Nrf2 at Ser-40 by protein kinase C regulates antioxidant response element-mediated transcription.* Journal of Biological Chemistry, 2002. **277**(45): p. 42769-42774.
148. Li, B., Cui, W., Tan, Y., Luo, P., Chen, Q., Zhang, C., Qu, W., Miao, L. and Cai, L. , *Zinc is essential for the transcription function of Nrf2 in human renal tubule cells in vitro and mouse kidney in vivo under the diabetic condition.* Journal of cellular and molecular medicine, 2014. **18**(5): p. 895-906.
149. Bloom, D.A. and Jaiswal, A.K., *Phosphorylation of Nrf2 at Ser40 by protein kinase C in response to antioxidants leads to the release of Nrf2 from INrf2, but is not required for Nrf2 stabilization/accumulation in the nucleus and transcriptional activation of antioxidant response element-mediated NAD (P) H: quinone oxidoreductase-1 gene expression.* Journal of Biological Chemistry, 2003. **278**(45): p. 44675-44682.
150. Jena, N., *DNA damage by reactive species: Mechanisms, mutation and repair.* Journal of biosciences, 2012. **37**(3): p. 503-517.
151. Niedernhofer, L.J., Daniels, J.S., Rouzer, C.A., Greene, R.E. and Marnett, L.J., *Malondialdehyde, a product of lipid peroxidation, is mutagenic in human cells.* Journal of Biological Chemistry, 2003. **278**(33): p. 31426-31433.
152. Łuczaj, W. and Skrzydlewska, E., *DNA damage caused by lipid peroxidation products.* Cell Mol Biol Lett, 2003. **8**(2): p. 391-413.
153. Parrish, A.B., Freel, C.D. and Kornbluth, S., *Cellular mechanisms controlling caspase activation and function.* Cold Spring Harbor perspectives in biology, 2013. **5**(6): p. a008672.
154. Eguchi, Y., Shimizu, S. and Tsujimoto, Y., *Intracellular ATP levels determine cell death fate by apoptosis or necrosis.* Cancer research, 1997. **57**(10): p. 1835-1840.
155. Leist, M., Single, B. Castoldi, A.F., Kühnle, S. and Nicotera, P., *Intracellular adenosine triphosphate (ATP) concentration: a switch in the decision between apoptosis and necrosis.* The Journal of experimental medicine, 1997. **185**(8): p. 1481-1486.

156. Fernandez-Pol, J.A., *Conservation of multifunctional ribosomal protein metallopanstimulin-1 (RPS27) through complex evolution demonstrates its key role in growth regulation in Archaea, eukaryotic cells, DNA repair, translation and viral replication.* Cancer Genomics-Proteomics, 2011. **8**(3): p. 105-126.

157. Süsse, S., Scholz, C. J., Burkle, A. and Wiesmuller, L., *Poly (ADP‐ ribose) polymerase (PARP‐ 1) and p53 independently function in regulating double‐ strand break repair in primate cells.* Nucleic acids research, 2004. **32**(2): p. 669-680.

158. Chaitanya, G.V., Alexander, J.S. and Babu, P.P., *PARP-1 cleavage fragments: signatures of cell-death proteases in neurodegeneration.* Cell Communication and Signaling, 2010. **8**(1): p. 1-31.

159. Albrechtsen, N., Dornreiter, I., Grosse, F., Kim, E., Wiesmuller, L. and Deppert, W., *Maintenance of genomic integrity by p53: complementary roles for activated and non-activated p53.* Oncogene, 1999. **18**(53): p. 7706-7717.

160. Valenzuela, M.T., Guerrero, R., Nunez, M.I., Ruiz de Almodovar, J.M., Sarker, M., de Murcia, G. and Oliver, F J., *PARP-1 modifies the effectiveness of p 53-mediated DNA damage response.* Oncogene, 2002. **21**(7): p. 1108-1116.

Appendix A

Table 1: Raw data obtained in calculating FA IC_{50}

Concentration (µg/ml)	Log Concentration	OD1	OD2	OD3	Mean OD	Percentage Viability
0	0.000	0.821	1.067	0.821	0.903	100.000
30	1.477	0.892	0.548	0.666	0.702	77.741
35	1.544	0.769	0.764	0.699	0.744	82.392
40	1.602	0.849	0.900	0.760	0.836	92.617
50	1.699	0.708	0.694	0.840	0.747	82.761
100	2.000	0.512	0.398	0.415	0.442	48.911
150	2.176	0.435	0.399	0.463	0.432	47.877
200	2.301	0.391	0.369	0.439	0.400	44.260
250	2.398	0.364	0.367	0.322	0.351	38.870
300	2.477	0.267	0.24	0.233	0.247	27.316
400	2.602	0.141	0.127	0.164	0.144	15.947
500	2.699	0.127	0.119	0.139	0.128	14.212

Appendix B

Table 2: Raw luminometry data for GSH standards

GSH Standards Concentration (µM)	RLU 1	RLU 2	RLU 3	Mean
10	374279	297727	356326	342777.333
20	514615	497342	458765	490240.667
30	742065	706014	716944	721674.333
40	957788	950115	987295	965066
50	1383410	1037300	1245430	1222046.667
60	1795650	1777780	1625420	1732950

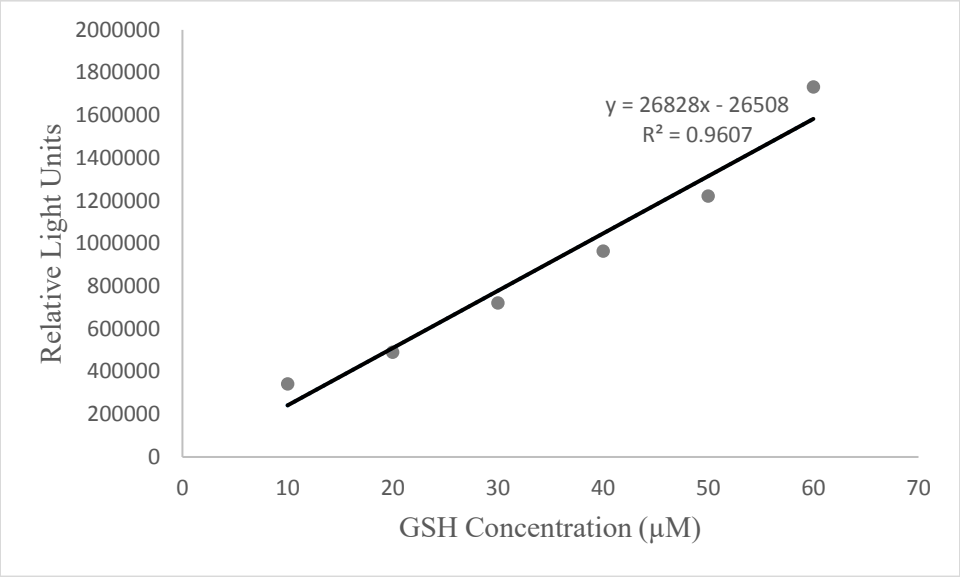

Figure 1: Standard curve generated from GSH standards

Appendix C

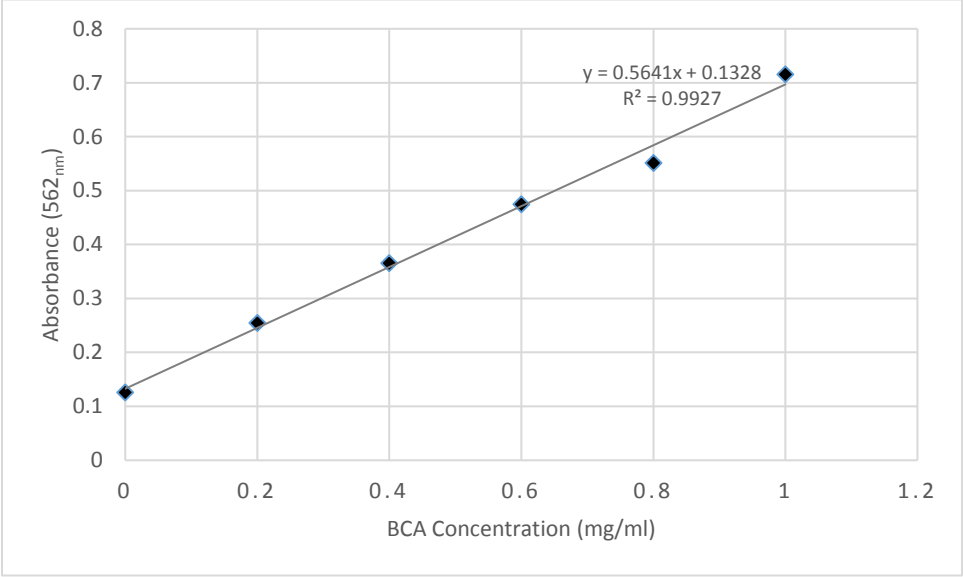

Figure 2: Standard curve using known concentrations of BSA to determine the unknown concentrations of protein samples in the BCA assay.

Table 3: Calculations for protein standardization of samples

Sample	OD1	OD2	Average OD	Protein Concentration (mg/ml)	Protein Volume (µl)	Cytobuster Volume (µl)
Control	1.707	1.859	1.783	2.925	102.564	97.436
FA	1.384	1.368	1.376	2.204	136.116	63.884

Appendix D

Table 4: Raw data obtained for positive and negative control in TBARS assay

	Absorbance (532_{nm})		
Control	3.333	3.358	3.359
FA	0.005	0.003	0.002